



Australia's National  
Science Agency

# Aerosol-formation pathways in a liquid absorption-based CO<sub>2</sub>-capture process

## Case study: MEA-based PCC plant at Vales Point Power Station

EP 21022 [RDE493-19]

Brendan Halliburton\*, Adrian Element, Merched Azzi, Ali  
Pourkhesalian

\*Corresponding Author

11 May 2020

Department of Regional New South Wales

NSW Coal Innovation Fund

Final report

## Copyright

© Commonwealth Scientific and Industrial Research Organisation 2020. To the extent permitted by law, all rights are reserved and no part of this publication covered by copyright may be reproduced or copied in any form or by any means except with the written permission of CSIRO.

## Important disclaimer

CSIRO advises that the information contained in this publication comprises general statements based on scientific research. The reader is advised and needs to be aware that such information may be incomplete or unable to be used in any specific situation. No reliance or actions must therefore be made on that information without seeking prior expert professional, scientific and technical advice. To the extent permitted by law, CSIRO (including its employees and consultants) excludes all liability to any person for any consequences, including but not limited to all losses, damages, costs, expenses and any other compensation, arising directly or indirectly from using this publication (in part or in whole) and any information or material contained in it.

CSIRO is committed to providing web accessible content wherever possible. If you are having difficulties with accessing this document please contact [csiroyenquiries@csiro.au](mailto:csiroyenquiries@csiro.au).

# Contents

Acknowledgments.....	6
Executive summary .....	7
1. Introduction .....	11
1.1 Carbon dioxide capture – A means to control greenhouse gas emissions .....	11
1.2 The challenge of aerosols in the amine-based PCC process: Aerosol characterisation .....	13
2. Project objectives, approach, milestones and performance measures .....	14
2.1 Project objectives .....	14
2.2 Methodology/experimental design.....	14
2.3 Milestones and performance measures.....	16
2.4 Stage 1 – Desktop study .....	20
2.5 Stage 2 – Laboratory-based study .....	21
2.6 Stage 3 – Validation of laboratory-based results .....	22
3. Experimental method: Solvent-degradation rig.....	23
3.1 Overview of the solvent-degradation rig .....	23
3.2 Recommissioning.....	24
3.3 Solvent-degradation rig modifications .....	24
3.4 Results .....	28
3.5 Discussion/conclusion .....	45
4. Vales Point post-combustion capture pilot plant study: Validation of solvent-degradation rig results .....	48
4.1 Introduction.....	48
4.2 Equipment and modification to the post-combustion capture pilot plant.....	49
4.3 Results .....	57
4.4 Discussion/conclusion .....	68
5. Recommendations for future work .....	72
Shortened forms .....	73
Glossary.....	75
References.....	79
Appendices.....	81

Appendix A: Instrumentation – Limitations and challenges.....	82
A.1 Introduction.....	82
A.2 Laser diffraction analyser .....	82
A.3 Aerodynamic particle sizer .....	83
A.4 Engine exhaust particle spectrometer .....	83
A.5 Electrical low-pressure impactor.....	84
A.6 ProCea <sup>SM</sup> SO <sub>2</sub> /SO <sub>3</sub> .....	85
A.7 Conclusion .....	86
Appendix B: Assessment of solvent-degradation rig operation .....	87
B.1 First experiments.....	87
B.2 Second-phase experiments (following solvent degradation rig modifications) .....	88
Appendix C: Extracts from State of Knowledge – Review.....	90
C.1 Aerosol characterisation.....	90
C.2 Particulate matter emissions from a post-combustion capture plant.....	96
C.2.1 Role of SO <sub>2</sub> and SO <sub>3</sub> in new particle formation .....	100
C.2.2 Supersaturation and particle emission.....	104
C.2.3 Predicting particulate matter emissions from post-combustion capture plants..	105
C.2.4 Absorbent management.....	106
C.2.5 Environmental effects .....	107
C.2.6 Aerosol emission management .....	109
Appendix D: List of Key Personnel .....	117

# Figures

Figure 1 Schematic diagram displaying the primary processes involved in amine-based carbon dioxide capture from a flue gas .....	12
Figure 2 Solvent-degradation rig – standard configuration used for undertaking degradation studies .....	23
Figure 3 Solvent degradation rig with particle-measuring instruments installed .....	27
Figure 4 The laser diffraction analyser (Malvern™ Insittec) assembly-ready for installation into the solvent degradation rig.....	28
Figure 5 Aerodynamic particle sizer-particle size distribution baseline prior to each target experiment.....	29
Figure 6 Aerodynamic particle sizer-mode particle concentration for each baseline as a function of experiment run time.....	30
Figure 7 Aerodynamic particle sizer- <0.5 µm particle concentration for each baseline as a function of experiment run time .....	30
Figure 8 Laser diffraction analyser transmission 97 ppm NO, 7% O <sub>2</sub> and 17 % CO <sub>2</sub> with a nitrogen balance, CAL008 example .....	32
Figure 9 Laser diffraction analyser transmission 91 ppm SO <sub>2</sub> , 13% O <sub>2</sub> and 15 % CO <sub>2</sub> with a nitrogen balance, CAL008 example .....	33
Figure 10 Laser diffraction analyser number distribution 91 ppm SO <sub>2</sub> , 13% O <sub>2</sub> and 15 % CO <sub>2</sub> with a nitrogen balance, CAL008 example (LDA reports particle concentration as particles/m. Volume concentration can be calculated using the diameter of the duct and flowrate).....	34
Figure 11 Laser diffraction analyser transmission at 0, 10 and 100 ppm NO <sub>2</sub> , 13% O <sub>2</sub> and 15 % CO <sub>2</sub> with a nitrogen balance, CAL008 example .....	35
Figure 12 Laser diffraction analyser transmission at 30, 50, 70 and 100 ppm NO <sub>2</sub> , 13% O <sub>2</sub> and 15 % CO <sub>2</sub> with a nitrogen balance, CAL008 example.....	36
Figure 13 Laser diffraction analyser transmission data at 64 ppm NO .....	37
Figure 14 Aerodynamic particle sizer particle size distribution baseline example prior to experiments .....	38
Figure 15 Aerodynamic particle sizer particle size distribution low concentration NO shows removal of particles .....	38
Figure 16 Laser diffraction analyser transmission data showing the transition as NO <sub>2</sub> flow commences and is terminated.....	40
Figure 17 Laser diffraction analyser transmission data showing the transition as NO <sub>2</sub> flow commences and is terminated at 9 ppm .....	41
Figure 18 Aerodynamic particle sizer particle size distribution at 9 ppm NO <sub>2</sub> .....	42
Figure 19 Laser diffraction analyser transmission data 8 ppm SO <sub>3</sub> – MEA .....	43

Figure 20 Averaged aerodynamic particle sizer particle size distribution 8 ppm SO <sub>3</sub> – MEA .....	44
Figure 21 Laser diffraction analyser transmission data 8 ppm SO <sub>3</sub> – CAL008 .....	44
Figure 22 Absorber inlet and outlet flue gas pipes .....	50
Figure 23 Schematic diagram of sampling ports and locations .....	50
Figure 24 Optics sampling port section for the laser diffraction analyser .....	51
Figure 25 Aerosol sampling ports being installed .....	52
Figure 26 Laser diffraction analyser average aerosol background particle distribution .....	58
Figure 27 Laser diffraction analyser transmission – 60 ppm SO <sub>2</sub> in flue gas .....	59
Figure 28 Laser diffraction analyser aerosol distribution – 60 ppm SO <sub>2</sub> in flue gas .....	59
Figure 29 Laser diffraction analyser transmission – 1200 ppm SO <sub>2</sub> in flue gas .....	60
Figure 30 Laser diffraction analyser transmission – 1200 ppm SO <sub>3</sub> in flue gas .....	61
Figure 31 Laser diffraction analyser aerosol distribution – 1200 ppm SO <sub>3</sub> in flue gas .....	61
Figure 32 Flue gas venting from the outlet of the absorber during SO <sub>3</sub> experiments .....	62
Figure 33 Laser diffraction analyser transmission with addition of NO <sub>2</sub> to the absorber at a concentration of 325 ppm .....	63
Figure 34 Laser diffraction analyser particle distribution with addition of NO <sub>2</sub> to the absorber at a concentration of 325 ppm .....	64
Figure 35 Laser diffraction analyser transmission – 160 ppm NO <sub>2</sub> with 60 ppm SO <sub>2</sub> in flue gas ..	65
Figure 36 Laser diffraction analyser particle size distribution – 160 ppm NO <sub>2</sub> with 60 ppm SO <sub>2</sub> in flue gas .....	66
Figure 37 Laser diffraction analyser transmission – 600 ppm NO with 60 ppm SO <sub>2</sub> in flue gas ..	66
Figure 38 Laser diffraction analyser particle size distribution – 600 ppm NO with 60 ppm SO <sub>2</sub> in flue gas .....	67
Figure 39 Temperature profile along the packed height of the Tarong post-combustion capture absorber (Cousins, 2012) .....	68

## Tables

Table 1 Source of each of the gases used to prepare the inlet flue gas of the solvent degradation rig .....	25
---	----

# Acknowledgments

CSIRO thankfully acknowledged the support from Department of Regional NSW through the Coal Innovation NSW Fund, which is administered by the Minister for Regional NSW, Industry and Trade under project number RDE493-19.

Any views expressed herein do not necessarily reflect the views of Coal Innovation NSW or the Department of Regional NSW.

The authors also thank Delta Electricity for the use of their PCC pilot plant at Vales Point power station.

Our colleagues Dan Maher and Phillip Green operated the PCC pilot plant at Vales Point and without their support and dedication the experimental work described here would not have been possible.

# Executive summary

The scientific community has demonstrated that anthropogenic production of CO<sub>2</sub> emissions is leading to a rise in average global temperatures, resulting in climate change. One pathway to limit the increase of these emissions is carbon dioxide (CO<sub>2</sub>) capture and storage in geological formations.

Amine-based CO<sub>2</sub>-capture technologies are mature and ready for commercial application in coal-fired power stations. However, these technologies can release both the amine absorbent and by-products of the process into the atmosphere through the power station's exhaust stacks. One of the pathways for pollutant release is via aerosols, which, depending on size, may pass through conventional water wash and demister equipment. The finer aerosols have the greatest potential for release, due to their reduced capture efficiencies. Liquid-phase aerosols are concentrated transport modes for solvent losses to the atmosphere because they contain a greater density of pollutant molecules than gaseous aerosols.

## Core findings

Each of the following findings has been demonstrated at either the laboratory scale using the CSIRO solvent-degradation rig, or at the Vales Point PCC pilot plant with monoethanolamine (MEA) solvent, or at both facilities.

1. Sulfur trioxide (SO<sub>3</sub>) is the most critical initiator of aerosols. The dominant pathways for mist production are those that produce sulphuric acid (H<sub>2</sub>SO<sub>4</sub>) as a final product. Aerosol formation is independent of the sulphuric acid formation pathway, with aerosol yields being additive when more than one pathway exists. H<sub>2</sub>SO<sub>4</sub> mist forms from the reaction of SO<sub>3</sub> with water or nitrogen dioxide (NO<sub>2</sub>) reacting with sulphur dioxide (SO<sub>2</sub>). Once generated, these fine acid aerosols penetrate the CO<sub>2</sub> absorber and water-wash section of a normal CO<sub>2</sub> post-combustion capture (PCC) process with little resistance. The aerosol formed is a fine mist with particle diameters of normally less than 1 µm.
2. NO<sub>2</sub> has a strong propensity to form aerosols in the presence of SO<sub>2</sub>. This is because it efficiently oxidises SO<sub>2</sub> to form SO<sub>3</sub>. Once produced, the SO<sub>3</sub> initiates a rapid onset of aerosol as H<sub>2</sub>SO<sub>4</sub> is formed.
3. One control method for minimising aerosol is maintaining low SO<sub>x</sub> and low NO<sub>2</sub> in the flue gas supplied to the amine PCC absorber. Even at low concentrations, these gases can produce large quantities of aerosol under appropriate conditions. The chemical properties of the solvent have a measurable, significant impact on the likelihood of aerosol formation and the amount of aerosol produced. The results suggest the existence of a threshold value in acid gas concentration, below which aerosol formation is suppressed. This potential critical concentration could be related to the ability of the solvent to absorb and remove either SO<sub>3</sub> or H<sub>2</sub>SO<sub>4</sub> from the flue gas. It is also likely to be a function of the absorption plant design.

Exposure to acid gases ages PCC solvents, resulting in residual or background aerosol concentrations that can increase over time. While initially reversible, these reactions become irreversible as exposure time increases. This indicates that for the absorber designs examined, aerosol formation is dominated by chemical aerosol pathways rather than physical pathways. Comparative experiments between MEA and CSIRO's absorption liquid CAL008 show that aerosol formation can be suppressed by appropriate solvent chemistry.

4. The small background aerosol concentrations observed for new solvents indicate that aerosol formation arising from the temperature bulge in the absorber may not be as significant as reported in literature. This suggests that aerosol genesis may be suppressed by appropriate absorber design.
5. The differences in residual background aerosol concentrations due to ageing may arise from different solvent-degradation rates, and consequently, different ammonia production rates. The solvent-degradation rig reported large quantities of aerosol during ammonia absorption experiments, which supports this hypothesis. Ammonia has varying degrees of solubility in amines and can produce ammonium aerosols under certain conditions, including ammonium sulphate with  $H_2SO_4$ . It is plausible that the increasing residual aerosol observed during MEA experiments originates from ammonia formation. Much lower residual aerosol concentrations were observed for CAL008. These data may be a function of that solvent's reduced degradation rate and consequently, reduced ammonia formation rates.
6.  $NO_2$  addition at pilot plant scale displayed a strong propensity to form aerosols in aged MEA at concentrations above 160 ppm. Unfortunately,  $NO_2$  concentrations below this value were not evaluated during pilot plant experiments due to time limitations.
7. Nitric oxide (NO) addition at pilot plant scale displayed a strong propensity to form aerosols in aged MEA in the presence of  $SO_2$ , in contrast to the corresponding solvent-degradation rig results. Further work is necessary to identify the origins of this discrepancy.
8.  $SO_2$  addition at pilot plant scale and using real flue gas displayed little propensity to form aerosols in isolation, but rapidly formed aerosols with  $NO_2$  and NO, especially with aged solvents. The lack of aerosol genesis when added to a PCC absorber in isolation also contrasts with the corresponding solvent-degradation rig results.

## Lay Summary

The global scientific community has demonstrated that increasing amounts of greenhouse gas in the atmosphere are leading to a rise in average global temperatures, resulting in climate change.

The dominant greenhouse gas is carbon dioxide (CO<sub>2</sub>), with emissions from human activities being by far the largest source. One pathway to limit emissions is to capture CO<sub>2</sub> from the gas stream of a power station before it is released to the atmosphere, and then re-use or store it.

A class of chemicals called amines can combine with CO<sub>2</sub> allowing it to be removed relatively easily from a flowing gas stream. Amine-based CO<sub>2</sub> capture is a well-developed technology that has been used in several industries over many years and is suited for use in coal-fired power stations. However, it has the potential to release the parent amine chemical, and any by-product chemicals that are formed during the capture process, as pollutants, through the power station's exhaust stacks.

Depending on their toxicity and amount, the release of such chemical pollutants can harm humans and the environment. It is thus of critical importance to understand how much of each pollutant is released by the process and how this occurs, so that we can develop controls that can be deployed on a large scale.

One pathway by which pollutants can be released to the stack in the CO<sub>2</sub> capture process is through aerosols, which are tiny particles of material suspended in the air. Aerosols can be liquid, known as mists, or solid, such as fly ash. Mists release more amines into the atmosphere than gases do, as they contain a greater concentration of pollutant molecules. Depending upon the size of the mist particles, they have a strong potential to pass pollutants through the entire CO<sub>2</sub>-capture process. Finer mists have the greatest potential for releasing pollutants.

In this project, we investigated how mist forms during CO<sub>2</sub> capture. We found that the main way is through two different chemical reactions that produce sulphuric acid. The main reaction involves sulphur trioxide gas combining with water vapour. A second reaction occurs when sulphur dioxide gas reacts with nitrogen dioxide gas to initially form sulphur trioxide. The sulphur trioxide then further reacts with water to form sulphuric acid mist. Our results showed that sulphuric acid mist formed regardless of which reaction occurred, and that when it is formed by more than one type of reaction, the amount of mist is additive.

The heat that is released during CO<sub>2</sub> capture normally increases the temperature within the absorber unit, which is where the CO<sub>2</sub> is removed from the gas stream. Publicly available literature suggests that the temperature rise could be a potential source of mist during CO<sub>2</sub> capture, but we found that it had almost no influence on the amount of mist produced. Barely any aerosol was measured during CO<sub>2</sub> capture when we used fresh amine solvents in the absence of acid gases, such as sulphur dioxide, or particles, such as fly ash. However, when acidic gases were present, a fine mist formed and travelled through both the CO<sub>2</sub> absorber and the wash section, where some of the amine solvent is removed by water.

Our results indicate that the chemical characteristics of the solvent used to capture CO<sub>2</sub> can potentially limit the conditions under which aerosols may form, and therefore reduce the amount

of aerosol produced. We also suspect that there might be a threshold value of acid gas concentration, and that aerosols will not form below this level. The threshold concentration may be related to the ability of the solvent to absorb and remove either SO<sub>3</sub> or sulphuric acid from the flue gas flow. This is likely to occur at specific gas concentrations and be related to the design of the absorption equipment. We found that as the conventional absorbent known as monoethanolamine (MEA) ages during the capture process, residual or background aerosol concentrations increase accordingly.

Some evidence suggests that this increase in residual aerosol formation properties of the solvent is a result of increased ammonia as the solvent degrades. Ammonia dissolves to different degrees in different amines and can produce ammonium-based aerosols under certain conditions. Our laboratory-based, small-scale experiments reported very large quantities of aerosol formation during ammonia absorption experiments, which provides some support for this idea. The increasing residual aerosol we observed during MEA experiments certainly originated from ammonia formation. Much lower residual aerosol concentrations were observed for a new CSIRO absorption liquid known as CAL008. We suspect that this is because the CAL008 solvent degrades much more slowly than MEA, and therefore produces less ammonia.

Overall, our results show that the formation of aerosols during CO<sub>2</sub> capture is influenced far more by the presence of acid gases than by the temperature rise in the absorber. The type of solvent can also significantly affect the amount of aerosol formed and the amount of residual aerosol produced as the solvent degrades. Our experiments provide evidence that the choice of solvent and absorber design can strongly influence the amount of aerosol produced, as well as the sensitivity of aerosol formation to acid gas concentration.

# 1. Introduction

## 1.1 Carbon dioxide capture – A means to control greenhouse gas emissions

It is commonly accepted by the scientific community that anthropogenic CO<sub>2</sub> emissions are leading to a rise in average global temperatures and resulting in climate change. Based on the extensive scientific data supporting global warming, 195 countries adopted the legally binding global climate deal at the Paris climate conference (COP21) in December 2015, to limit global warming to no more than 2°C above pre-industrial levels. Since the global transition to zero-carbon or low-carbon emissions energy sources has not kept pace with global energy demands, global CO<sub>2</sub> emissions have continued to steadily increase. As the impacts from global warming become more pronounced, the urgency to stabilise or decrease the amount of CO<sub>2</sub> emitted to the atmosphere escalates.

Amine-based CO<sub>2</sub>-capture processes have historically been used for gas processing and purification and are considered established and mature in the oil and gas industry. The capture process is mostly confined from the atmosphere and operates in a closed system. This segregation results in few pollutants being directly released to the atmosphere during the process.

Post-combustion capture of CO<sub>2</sub> (PCC) processes a flue gas stream that is subsequently released to the atmosphere. Fundamentally, this technology has the potential to produce near-zero greenhouse gas emissions from fossil fuels. The technology is arguably the most commercially ready technology available to control greenhouse gas emissions from current from fossil-fuel burning energy technologies.

A generic overview of the amine-based PCC process is shown in schematic form in Figure 1.

## Generic Amine Carbon Dioxide Capture Plant Process

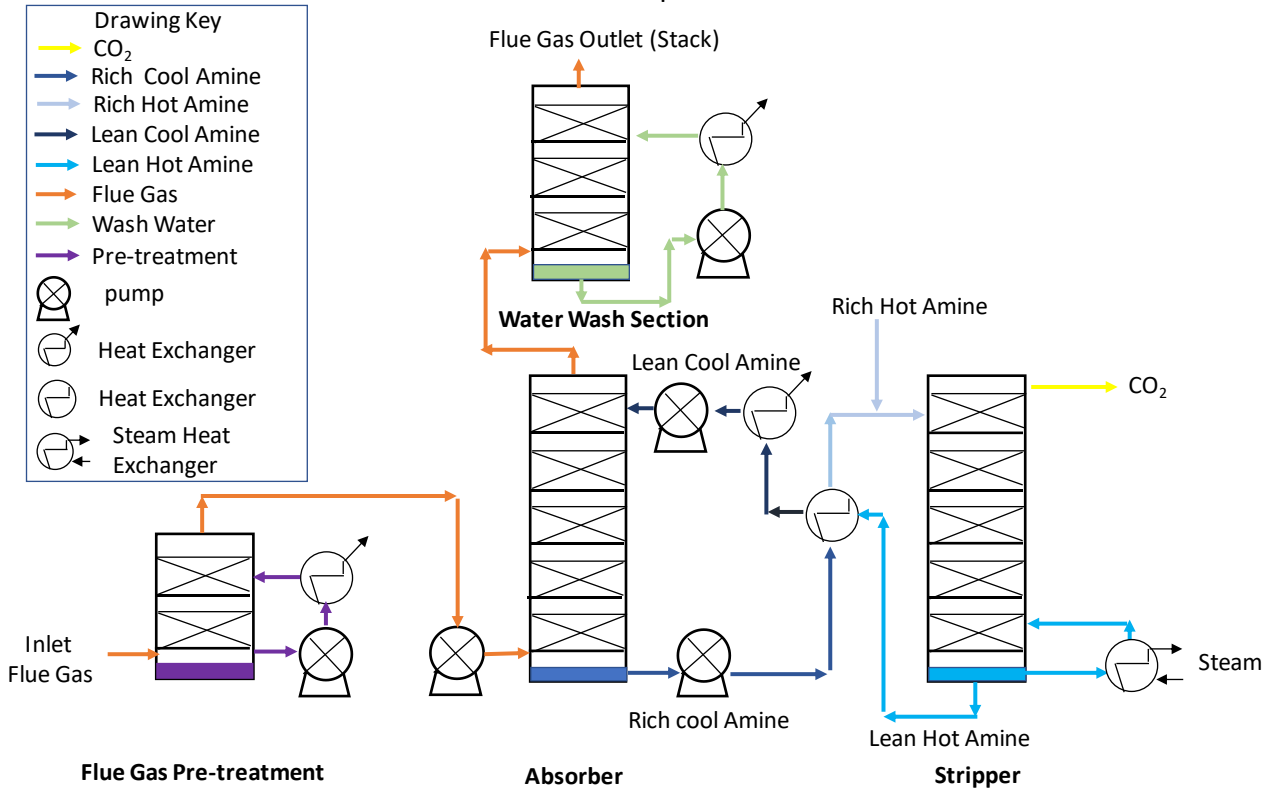


Figure 1 Schematic diagram displaying the primary processes involved in amine-based carbon dioxide capture from a flue gas

When an amine-based CO<sub>2</sub>-capture process is used in industry, for instance for gas treatment, the final product is ultimately combusted, resulting in any contaminants entrained into the gas stream from the treatment process being destroyed. In the amine-based PCC process this is not the case, as after the PCC process, large quantities of flue gas are released into the atmosphere. This raises environmental and human health concerns regarding PCC contaminant emissions.

Much research has been undertaken into the viability of amine-based PCC technology and its requirements for retrofits to existing CO<sub>2</sub> sources. PCC has also been the topic of many reviews, and these provide extensive and detailed descriptions of PCC operations. The most appropriate reviews to PCC operations are identified in the reference list [1-12].

Environmental concerns associated with aerosol emissions from amine-based PCC processes appear to be first raised during the Electric Power Research Institute amine workshop held on 16 August 2011 [13]. A range of operational issues and environmental concerns relating to aerosol formation and aerosol release to the atmosphere were presented. Kamijo (Mitsubishi Heavy Industries, MHI) noted difficulties in amine mist control at MHI PCC plants using conventional demister technologies and highlighted the need for a special (MHI proprietary) demister. In addition, Kamijo raised concerns regarding the high sensitivity of aerosols to SO<sub>3</sub> concentrations in the flue gas.

Two full-scale amine-based PCC plants are now operational. The Boundary Dam Project [14] operated by SaskPower is a 160 MW coal-fired base-load power station located near Estevan Canada. It became the first power station to successfully use amine-based PCC technology in 2014 capturing 90% of CO<sub>2</sub> produced. The captured CO<sub>2</sub> is transported 66 km by pipeline to the

Weyburn oilfields where it is used for enhanced oil recovery. The Petra Nova carbon capture and storage (CCS) project [15] is the second full-scale PCC process and is operated by NRG Energy at the WA Parish coal-fired power station. This project commenced operation in 2016 and captures a 240 MW portion of CO<sub>2</sub> from a 610 MW coal-fired generator. The captured CO<sub>2</sub> is also transported by pipeline (137 km) to oilfields for enhanced oil recovery (West Ranch Oil Field, located near Vanderbilt, Texas). Both projects demonstrate the viability of the overall CCS process. Consequently, it is possible that amine-based PCC technology will be deployed with existing fossil-fuel power plants and in industry in a future low-carbon economy. Thus, there is potential for large-scale release of pollutants to the environment even if these pollutants are at low concentrations. As larger-scale deployment becomes more imminent, research into PCC technology has therefore increasingly focused on the environmental issues arising from stack emissions.

## 1.2 The challenge of aerosols in the amine-based PCC process: Aerosol characterisation

The stack emissions from a PCC plant can be in the form of vapours or gases and aerosols, with aerosols being potentially multiphase with both liquid and solid-phase fractions present.

As noted in Section 1.1, Kamijo [13] first reported difficulties in amine aerosol control at MHI PCC plants and a high sensitivity of aerosol formation to SO<sub>3</sub> concentrations in the flue gas. This work also highlighted that particulate matter (PM) generated by PCC plants can impose a major cost factor on the plant due to potentially large increased loss of the normally expensive absorption liquid, as well as bringing about a number of environmental issues and costs from pollutants released from the stack emission stacks.

The primary problem is that liquid-phase aerosols can contain a larger concentration of pollutants than the corresponding gaseous phase, and thus have the potential to transfer larger quantities of pollutants within the same fluid system. Aerosols can form from both chemical and physical processes. Physically, aerosols form whenever there are temperature or pressure changes occurring that causes a species to be cooled to below its dew point. This normally occurs within the absorber and the pre-treatment process.

Chemical aerosol formation occurs when two suspended species, usually gases for the PCC process, react to form a product with a dew point below that for the prevailing operational conditions. In this case the product species will condense to form an aerosol. Depending upon the chemistry of the condensed species and the moisture loading, additional moisture can further condense onto the formed aerosol, increasing the aerosol volume. This additional moisture may also contain additional solvent and degradation pollutants present in the PCC process. Consequently, it is important to understand how the aerosol forms and what factors can influence this formation.

Aerosol formation and characterisation fundamentals were discussed in detail within the stage gate 1 report, 'Aerosol Formation Pathways in Liquid Absorption-based CO<sub>2</sub> Capture Process: State of Knowledge – Review'. The report sections that discuss aerosol formation are included in Appendix C for reference.

## 2. Project objectives, approach, milestones and performance measures

This document is the final report for the Coal Innovation NSW funded project entitled “Aerosol formation pathways in liquid absorption-based CO<sub>2</sub> capture process. Case study: MEA-based PCC plant at Vales Point Power Station” [RDE493-19]. The objectives, key findings, outcomes and conclusions from the project are summarised in this section.

### 2.1 Project objectives

The project had the following objectives:

- Review the current state of knowledge of aerosol genesis and solvent loss pathways that arise from aerosol transport modes in PCC processes. The effectiveness and limitations of aerosol sampling methodologies will also be reviewed, and the most appropriate approaches identified and incorporated into objective 3.
- Map, using a laboratory-scale PCC process, the physical and chemical parameters that are important for aerosol formation within a PCC process and for a range of solvents.
- Evaluate the representativeness of the laboratory-scale data sets to those of a larger PCC plant using real flue gas.

### 2.2 Methodology/experimental design

The project was completed as three separate, but interrelated stages.

The first stage comprised a technology review of aerosol formation within PCC systems and was focused on gathering the most up-to-date understanding of aerosol formation from SO<sub>2</sub>, SO<sub>3</sub> and NO<sub>x</sub> in an amine-based PCC process. The report from this initial review is included in Appendix C.

The second stage involved laboratory-scale experiments using the CSIRO solvent-degradation rig (SDR). This comprises a small-scale PCC apparatus that can simulate the PCC process using a simulated flue gas stream. The simulated flue gas was formulated by mixing pure gases and gas mixtures that were supplied by commercially available cylinders. Being of small liquid capacity and small size, it provided the advantage of being able to produce a large number of PCC experiments within a relatively short time. It was proposed to undertake laboratory-scale measurements for solutions containing monoethanolamine, ammonia, the amino-acid salt of alanine and CSIRO’s absorption liquid CAL008. Initially, the composition of the gas stream was monitored for a range of permanent gases, including, but not limited to, NO<sub>x</sub>, O<sub>2</sub>, CO<sub>2</sub> as well as SO<sub>2</sub> and SO<sub>3</sub> components. However, instrument failures and delays restricted independent gas monitoring and consequently concentrations of target gases were determined by volumetric mixing. Aerosol concentrations were monitored by a range of size-selective and total-particle-concentration measurement devices to assess the conditions whereby aerosol onset occurs or aerosol penetration through the PCC process is observed.

For gases other than SO<sub>2</sub> and SO<sub>3</sub>, the simulated flue gas components were maintained at constant concentrations for the duration of experiment and in line within the range of gas compositions present in the flue gas fed to the Vales Point PCC pilot plant. The SO<sub>2</sub>, SO<sub>3</sub> and NO<sub>x</sub> concentrations of the simulated flue gas were independently varied according to the condition necessary to precipitate aerosols. It was initially conceived that four concentrations for each gas component would be initially used. However, over the duration of the program, a greater number of separate gas concentrations were used for the target gases.

The third stage involved undertaking experiments at the Vales Point PCC pilot plant to evaluate the representativeness of the laboratory-based data sets. To complete this work, regulatory-compliant sampling planes were installed into the pilot plant pipework using appropriately designed, stainless-steel interface pieces. The installation required replacement and modification of the existing pilot plant ductwork to accommodate the new ductwork sections that supported the sampling planes. Following installation of particle analyses instrumentation, target gases SO<sub>2</sub>, SO<sub>3</sub>, NO and NO<sub>x</sub> were individually, and as mixtures, metered into the inlet gas stream just after the pre-treatment section.

## 2.3 Milestones and performance measures

Milestone ID (% completion)	Milestone title/Description as per contract	Performance measures as per contract	Relevance to project and achievement
Stage 1 100%	<p>M1 Literature study and review of the current state of knowledge of aerosol science arising from SO<sub>2</sub> and SO<sub>3</sub> &amp; NO<sub>x</sub> in an aqueous solvent PCC system that:</p> <ul style="list-style-type: none"> <li>- proves there is a problem with aerosol formation from solvent-based PCC processes</li> <li>- provides information for NSW emission regulators</li> </ul> <p>Literature study and review of the effectiveness and limitations of aerosol sampling methodologies to identify the most appropriate approaches for inclusion into Objective 3</p>	<p>State-of-the-art review based on the available literature and expert opinion generated</p> <p>Review includes a section with information in a format readily accessible to regulator</p> <p>Results and opinion presented in the report will inform CINSW decisions on advancement, or otherwise, to Stage 2</p> <p>Most appropriate approaches for aerosol sampling identified and expert opinion generated</p> <p>Recommendations structured for inclusion into objective three</p>	<p>Review is supplied as Appendix C</p> <p>Review reports the state of the art based on the available literature and expert opinion at the time of creation</p> <p>Results and opinion presented in the report were presented to CINSW with the project advancing to Stage 2</p> <p>The outcome of this review was to reveal that at the time of writing, a deficit in scientific knowledge in this area existed</p>
Stage 2 100%  ~2000 individual experiments completed	<p>Laboratory-scale experiments using CSIRO micro PCC and simulated flue gas</p> <ul style="list-style-type: none"> <li>- M2 Experimental investigation of the drivers for aerosol formation within a range of solvent-based PCC process</li> <li>- M3 Measurement of aerosol movement through the PCC process after genesis</li> </ul>	<p>SO<sub>2</sub>/SO<sub>3</sub> and diffraction aerosol analysers procured. SO<sub>2</sub>/SO<sub>3</sub> analyser interfaced to CSIRO micro PCC</p> <p>Catalytic oxidiser constructed for oxidation of SO<sub>2</sub> to SO<sub>3</sub> for use as the SO<sub>3</sub> source. Oxidiser performance experimentally validated</p> <p>CSIRO micro PCC gas mixing system modified to include independent injection of SO<sub>2</sub> and SO<sub>3</sub>. Validation and calibration using SO<sub>2</sub>/SO<sub>3</sub> analyser and calibration gases</p>	<p>SO<sub>2</sub>/SO<sub>3</sub> and diffraction aerosol analysers were procured, and these were interfaced to CSIRO micro PCC. The laser diffraction analyser (Malvern™ 'Insitex') operated flawlessly and provide high-quality aerosol data sets during both SDR and Vales Point measurements (purchase cost \$130k). High-resolution SO<sub>2</sub>/SO<sub>3</sub> analyser failed during initial testing. Manufacturer revealed that the instrument was not physically tested using MEA. Manufacturer failed to admit liability for the instrument being not fit for purpose and would not repair under warranty. CSIRO funded repairs and development of a new sampling system for the instruments that would remove aerosols prior to sampling. Operational temperature of the</p>

		<p>CSIRO micro PCC stripper reconfigured to simulate a conventional PCC CO<sub>2</sub> stripping process. Stripper operation experimentally validated</p> <p>Aerosol monitors interfaced to CSIRO Micro PCC. Aerosol monitors validated using nebulised polystyrene latex spheres (PSL)</p> <p>CSIRO micro PCC stripper operational performance validated with the above inclusions. Experimental program commenced</p> <p>Experimental program for aerosol genesis completed for SO<sub>2</sub>, SO<sub>3</sub>, NO<sub>2</sub> and NO. Aerosol sensitivity experiments at a minimum of four gas concentrations spanning from zero to the normal range expected for Vales Point PCC pilot plant completed for each of the component gases</p> <p>Completion of the minimum total of 256 experiments to identify gas combinations where aerosol genesis is most sensitive to the concentration of the above gases. Gas combinations where aerosol formation is most sensitive identified, and a more detailed investigative program developed for completion within the available remaining timeframe</p> <p>Targeted and more experiments completed for the most sensitive combinations for aerosol genesis</p> <p>Experiments completed for three solvents: monoethanolamine, ammonia and CAL008</p> <p>The minimum work program to achieve the objectives of Stage 3 formulated based on the findings of Stage 2</p> <p>The earliest results from this work will indicate the need, or otherwise, to advance to Stage 3. These results will be presented in the technical annex to be peer reviewed and these will inform CINSW decision on advancement to Stage 3</p> <p>Environmental approval of MEA gained for use at Vales Point site</p>	<p>instrument was also increased. Initially, the manufacturer advised of a relatively short turnaround for repairs to and return of the instrument. However, the repaired and modified instrument was not returned to CSIRO Newcastle until March 2019. Total cost of instrument ProCeas™ SO<sub>2</sub>/SO<sub>3</sub> including original purchase and subsequent modifications \$180k. Following the ProCeas™ SO<sub>2</sub>/SO<sub>3</sub> failure, the availability of suitable replacement instruments was investigated. No comparable instruments to the ProCeas™ SO<sub>2</sub>/SO<sub>3</sub> were available at that time of the SDR experiments. However, an complementary instrument was identified that would supplement the ProCeas™ SO<sub>2</sub>/SO<sub>3</sub> analyser, an Environment SA MIR 9000H at a cost of \$60k. Note at the time of this selection it was expected that the ProCeas™ SO<sub>2</sub>/SO<sub>3</sub> would be repaired and returned well before the end of the project. The Environment SA MIR 9000H had the capability to measure NO, NO<sub>2</sub>, NH<sub>3</sub>, SO<sub>2</sub> at ppm resolution and was ordered mid-2018. It was expected that both instruments would be available during 2018 to monitor all the target gases with the addition of ammonia, since ammonia was suspected to be a factor in initiating aerosol genesis. However, continued manufacture delays saw the arrival of these instrument during March 2019 at the completion of the project</p> <p>The catalytic oxidiser was constructed for oxidation of SO<sub>2</sub> to SO<sub>3</sub> for use as the SO<sub>3</sub> source. Oxidiser performance experimentally validated and found to have a conversion efficiency of 100%. Production of the SO<sub>3</sub> from ozone was also explored and it was determined that the ozone method was most appropriate for the SDR dur to the small scale of the apparatus and the catalytic method was more appropriate at the larges production scale at Vales Point Power Station</p> <p>The CSIRO micro PCC gas mixing system was modified to include independent injection of SO<sub>2</sub> and SO<sub>3</sub>. Validation and calibration using SO<sub>2</sub>/SO<sub>3</sub> analyser and calibration gases was not possible due to analyser issues noted above. Accurate metering of gases using precision mass flow controllers and volumetric monitoring of flows was considered an appropriate alternative</p>
--	--	---	--

			<p>CSIRO micro PCC stripper was reconfigured, and stripper operation experimentally validated at 95%</p> <p>Aerosol monitors were interfaced to CSIRO Micro PCC and validated initially using PSL</p> <p>CSIRO micro PCC stripper operational performance validated with the above inclusions. Experimental program commenced during 2017</p> <p>2000 standardised experiments undertaken using the CSIRO solvent-degradation rig and 40 experiments completed at the Vales Point PCC pilot plant. Of the 2000 experiments undertaken using the CSIRO apparatus, 550 experiments were completed using monoethanolamine, 870 using CSIRO's CAL008 solvent, 132 using ammonia and 460 using the amino acid alanine. All the experiments undertaken at Vales Point were completed using MEA solvent. Concentration ranges covered those expected at the Vales Point PCC pilot plant. Small-scale measurements were completed in triplicate with background measurements undertaken between each target experiment</p> <p>Targeted and more experiments completed for the most sensitive combinations for aerosol genesis</p> <p>Experiments completed for four solvents: monoethanolamine, ammonia, and CAL008 and alanine</p> <p>Since experiments were not completed at Vales Point PCC pilot plant until the completion of all SDR experiments, repeat SDR experiments to validate differences in between SDR and pilot plant results could not be undertaken</p> <p>Environmental approval of MEA was gained for use at Vales Point site</p>
<p>Stage 3</p> <p>90%</p>	<p>Stage 3 – Pilot-scale experiments at Vales Point PCC pilot plant</p>	<p>M5 Prepare and undertake pilot-scale measurements</p> <p>M6 Evaluate and adjust upscaling relationships of laboratory-scale data</p>	<p>M5 completed as achievable within the availability constraints of Vales Point PCC pilot plant. Preparatory stage could not be completed due to the invalidity of the pilot plant, which significantly impacted the experimental program</p>

		<p>M7 Evaluate and review SOx, NOx and aerosol relationships</p> <p>M8 Analyses include gas analyses for SO<sub>2</sub>, SO<sub>3</sub>, CO<sub>2</sub>, NO NO<sub>2</sub> and other gases. Aerosols will be size selectively analysed</p>	<p>M6 upscaling issues were evaluated. However, due to operational constraints of the Vales Point PCC pilot plant the number and range of experiments were severely limited. Thus, a suitable number of correlation experiments could not be completed within the operational timeframe. Since the planned preparatory stage could not be completed due to the invalidity of the pilot plant, preliminary experimentation was also completed at the time of the final experiments. This limitation significantly impacted on the scope of the final pilot-scale experimental program.</p> <p>M7 SOx, NOx and aerosol relationships have been reviewed and reported for the available number of experiments that were able to complete within the experimental allocation of 2018/2019</p> <p>M8 The gas analyses of SO<sub>2</sub>, SO<sub>3</sub>, NO NO<sub>2</sub> were limited because of instrument failures and time to complete the associated repairs</p>
--	--	--	---

## 2.4 Stage 1 – Desktop study

The desktop study investigating aerosol formation within PCC systems specially focused on aerosol formation arising from SO<sub>2</sub>, SO<sub>3</sub> and NO<sub>x</sub> and defining the current state of knowledge prior to the experimental work being undertaken. The detailed results of the desktop study are contained in Appendix C. The key findings were:

- To meet internationally agreed CO<sub>2</sub> emission reductions, it is highly likely that PCC deployment will be necessary in NSW and more widely across Australia due to the strong dependence of the Australian power industry upon coal.
- International research into PCC processes in the European Union and in the United States over approximately the last seven years have consistently reported problems with aerosol penetration through PCC process, conventional water-wash and demister systems, with potential environmental ramifications.
- There is international scientific consensus that aerosol release from stack emissions of PCC plants will be a significant challenge for the large-scale deployment of PCC technology. These emissions will have direct economic costs from absorbent loss, and may have both direct health implications and secondary effects arising from atmospheric chemical changes, which may include photochemical changes. Any chemical changes to the atmospheric reservoir will be of significant concern to regulators, as such changes to atmospheric chemistry may have undesirable and as-yet unknown impacts.
- Previous CSIRO research using simulated flue gas has shown similar findings to other international research and has shown that without aerosol present, there is little deposition through the PCC process except for volatile species such as mercury.
- The importance of control of aerosols in PCC emissions has been clearly demonstrated by the recent awarding of a significant research program into aerosol generation and control by the Norwegian CLIMIT program.
- The sensitivity of aerosol formation to the composition of real flue gas and PCC process parameters means that an Australian PCC deployment to the power industry will pose unique problems for stack aerosol emissions. The different composition of NSW coal and the impact of particle control devices such as fabric filters means that the findings from non-Australian coals may not be directly applicable to the Australian PCC deployment. Consequently, findings of the CLIMIT aerosol study may not be directly applicable to a NSW PCC deployment.
- The oxides of sulphur, specifically sulphur trioxide, were shown to be a strong drivers for aerosol formation. Understanding how the oxides of sulphur drive aerosol-forming chemistry will be critical for NSW as currently no desulphurisation technology is used at NSW power stations.
- Simulated flue gas measurements are cost effective for evaluating fundamental questions about PCC processes. However, they can overly simplify the complexity of real flue gas. Consequently, it is essential to supplement simulated flue gas experiments with experiments using real flue gas.

- Real flue gas is an essential for any research into aerosol science, because aerosol genesis is highly sensitive to the inlet conditions of the PCC plant.
- It will essential that NSW undertake a robust research program into the origins of aerosol emissions and PCC emissions in general for NSW and Australian coals. Such research will place the PCC industry in a good position to mitigate new pollutants as they arise. This includes development of robust analytical techniques to routinely quantify the degradation products from new PCC absorbents as well as the atmospheric secondary pollutants. Such higher-level understanding will be essential for future PCC deployment.

## 2.5 Stage 2 – Laboratory-based study

During the laboratory program, in excess of 2000 standardised experiments were undertaken using the CSIRO SDR and 40 experiments completed at the Vales Point PCC pilot plant. Of the 2000 experiments undertaken using the CSIRO apparatus, 550 experiments were completed using monoethanolamine, 870 using CSIRO Cal008 solvent, 132 using ammonia and 460 using the amino acid alanine. All the experiments undertaken at Vales Point were completed using MEA solvent. Small-scale measurements were completed in triplicate with background measurements undertaken between each target experiment.

The Stage 2 research component was aimed at identifying the primary drivers for aerosol genesis in the PCC process. However, examining the sensitivity of aerosol genesis for all possible PCC operational conditions, as well as the range of chemical and physical combinations of parameters that can occur under all possible PCC conditions, is clearly challenging. Thus, to confine the measurement parameter space to a manageable size, target gases were limited to NO, NO<sub>2</sub>, SO<sub>2</sub> and SO<sub>3</sub>, while the absorbents were confined to monoethanolamine, CAL008, ammonia and alanine amino acid.

The SDR was identified as a suitable instrument for small-scale laboratory work. This apparatus was specifically created for assessing the degradation behaviour of solvents over longer-term operation. This rig essentially consisted of a miniature PCC absorber/stripper system operating in a closed-loop mode that allowed continuous long-term operation during solvent-degradation trials. In the closed-loop mode, the outlet gas was returned to reform the inlet gas stream with target gases monitored and 'topped up' as necessary. A surrogate flue gas is used, with this gas being prepared from pure target gases sourced from gas cylinders.

The closed-loop recycle mode of the SDR was considered non-representative of a 'normal' PCC processes from an aerosol perspective. Thus, the flow arrangement was changed to reflect the normal, single-pass gas flow arrangement of an amine-based PCC process. Other physical conditions, such as absorber temperature, were, within the constraints of the system, maintained constant and as representative as possible of the normal operating conditions of Vales Point PCC pilot plant. Modifications to the SDR as well as operation conditions are discussed in more detail in Section 4.

## 2.6 Stage 3 – Validation of laboratory-based results

Considering the small size of the SDR, and the use of a surrogate flue gas, it was considered essential to compare the SDR results to comparable experiments at larger scale and with real flue gas. Consequently, Stage 3 involved completing an experimental program designed to evaluate the representativeness of the laboratory-based data sets through undertaking cognate experiments at the Vales Point PCC pilot plant. The number of experiments was determined according to the PCC operation time available and the available supply of target gases. Significant modification and construction was required to complete this work. These modifications, pilot plant operating conditions and results are discussed in more detail in Section 3.

## 3. Experimental method: Solvent-degradation rig

### 3.1 Overview of the solvent-degradation rig

The solvent degradation rig (SDR) was originally conceived by SINTEF (Trondheim, Norway) and donated to CSIRO Energy by Statoil. Previously used with success to investigate the complex degradation chemistry of PCC solvents, the rig has now been enhanced to undertake aerosol-formation studies.

The rig, in the configuration used for studying solvent decomposition, is shown in Figure 2.



Figure 2 Solvent-degradation rig – standard configuration used for undertaking degradation studies

The SDR is essentially a small-scale CO<sub>2</sub> capture system that can broadly simulate the conditions of much larger-scale PCC plants. Many of the components that are used are common to larger-scale PCC pilot plants.

The 'wetted' surfaces of the SDR are considered inert to amines and predominantly comprise 316 grade stainless steel, Teflon™ and some Viton™ surfaces. Viton™ surfaces are mainly associated with seals within sensors and control devices.

A LabVIEW control platform oversees and monitors a wide range of operational parameters, including temperature, pressure, electrical power of heating elements, gas flows, etc., and provides the ability to continuously operate.

Statoil aimed to operate the SDR continuously over many weeks. Consequently, to minimise inlet gas consumption and solvent loss, a flue gas recycling configuration was employed where the outlet gas from the absorber was redirected back into the inlet gas stream. Gases consumed in the process were 'topped up' as necessary to maintain an overall stable gas composition. While such configuration has advantages for longer-term operation, it is unsuitable for aerosol studies. This is because entrained aerosols in the recycled gas stream would behave as additional nucleating sites for aerosol formation. Thus, it is likely that erroneous data sets will be produced. Consequently, this gas recycle system was disconnected and a 'single-pass' process employed with outlet or waste gases being vented to the atmosphere.

## 3.2 Recommissioning

The SDR was designed and previously had been used for identifying decomposition pathways of amine solutions, but with a special focus towards understanding the formation pathways of nitrosamines. Consequently, due to the health and safety implications of nitrosamines, a significant amount of cleaning and decontamination was necessary at the commencement of this study. In addition, the SDR had not been operated since delivery from Statoil and thus considerable operational testing of individual components was also necessary. Recommissioning tasks included:

- completing a full safety audit
- cleaning internal surfaces and clearing and/or replacing all line filters. Some of these components required acid wash of wetted surfaces to decontaminate internal surfaces
- testing the operation of and calibration where necessary associated control and monitoring hardware
- updating LabVIEW software
- acquiring additional mass flow controllers for separate flow control of the additional target gases
- completing a test operation with water.

## 3.3 Solvent-degradation rig modifications

### 3.3.1 Gas composition and flow

The SDR original design included a limited number of the original mass flow controllers (MFCs). In addition, the original MFCs would not be of sufficient flow capacity to complete the experiments

using the new ‘open flow’ configuration. To solve this problem, a number of Environics 6100 multi-gas calibrators were added for metering as well as different MFCs (Brooks) and diluting additional target gases (NO, SO<sub>2</sub> and NO<sub>2</sub>). These calibrators are intelligent units with an on-board computer that enable accurately programmed blending of the target gas with the selected diluent. The installation of these calibrators has had minimal impact on the timeline of the current experimental program.

Concentrations of target gas species during each experiment were prepared by mixing individual target gas components into either nitrogen gas and/or air diluent. The target gases of interest include NO, NO<sub>2</sub>, CO<sub>2</sub>, SO<sub>2</sub> and SO<sub>3</sub>. Oxygen and nitrogen gases can also be independently injected as needed to maintain the correct concentration balance of each gas. This system has the capacity to maintain stable inlet gas compositions within wide concentration bounds. In addition, ‘pure’ gas experiments, which cannot be easily or economically completed at larger pilot-scale plants, can also be undertaken using this apparatus. Precision MFCs are used for accurately metering the individual target gas (Brooks SLA5800 series or Environics 6100 precision MFC mixer/calibrators). The sourcing of each gas and gas mixture is shown in Table 1.

**Table 1** Source of each of the gases used to prepare the inlet flue gas of the solvent degradation rig

GAS SPECIES OR MIXTURE	SOURCE OF GAS OR MIXTURE
Air	Supplied from the filtered reticulated laboratory compressed air system
Nitrogen	Supplied from reticulated laboratory nitrogen gas. This gas is derived from a liquid nitrogen bulk storage vessel
SO <sub>2</sub>	1 – Supplied in cylinders as a dilute mixture in nitrogen gas. Supplied by Coregas 2 – Supplied as liquid SO <sub>2</sub> in cylinders from BOC
SO <sub>3</sub>	1 – Bulk SO <sub>3</sub> is prepared by oxidising SO <sub>2</sub> to SO <sub>3</sub> . Sulphur dioxide is passed through a heated catalyst in the presence of oxygen. 2 – Low level concentrations (<1ppm) of SO <sub>3</sub> are precisely produced by titrating SO <sub>2</sub> with excess ozone. Ozone is generated by an Environics gas mixer/calibrator 3 – SO <sub>3</sub> is also prepared through the titration of SO <sub>2</sub> with NO <sub>2</sub>
NO	Supplied in cylinders as a dilute mixture in nitrogen gas. Supplied by Coregas
NO <sub>2</sub>	Supplied in cylinders as a dilute mixture in nitrogen gas. Supplied by Coregas*
CO <sub>2</sub>	1 – Supplied in cylinders as a dilute mixture in nitrogen gas. Supplied by Coregas 2 – Supplied as liquid CO <sub>2</sub> in cylinder. Supplied by Coregas

\* NO<sub>2</sub> concentrations are regularly re-calibrated/analyses to compensate for NO<sub>2</sub> decomposition

The use of a ‘pure’ surrogate inlet gas mixtures reduces some of the complexities associated with impurities that would be present in the flue gas from a coal fossil-fuel power station. These conditions are advantageous for identifying the primary mechanisms of aerosol genesis, but also require validation by real-world comparisons using real flue gas. Validation of the primary mechanisms of aerosol genesis will occur using flue gas from Vales Point Power Station.

### 3.3.2 SO<sub>3</sub> synthesis

Significant difficulty has been encountered in sourcing bulk SO<sub>3</sub>. Consequently, in situ SO<sub>3</sub> generation methods have been favoured that oxidise SO<sub>2</sub> to SO<sub>3</sub> either in the presence of ozone or through the use of a catalyst.

- Sulphur dioxide oxidation with ozone

Sulphur dioxide is readily oxidised to  $\text{SO}_3$  in the presence of ozone. Since ozone is relatively easily produced in the laboratory using either ultraviolet irradiation (wavelengths of around 185 nm) or during corona discharge of oxygen, these reaction pathways are being used to produce relatively modest, but accurately prepared concentrations of  $\text{SO}_3$ .

- Sulphur dioxide oxidation via sulphuric acid catalyst

The second pathway for producing  $\text{SO}_3$  uses a proprietary catalyst compound (MECS – XLP110 sulphuric acid catalyst). This catalyst is bound to a silica substrate and heated to approximately  $450^\circ\text{C}$  in the presence of oxygen. The catalyst has a large efficiency for oxidising  $\text{SO}_2$  to  $\text{SO}_3$  once operation temperature has been reached. However, it has been found that the catalyst has the disadvantage of retaining significant residual quantities  $\text{SO}_3$  during operation and requires several hours of purging to desorb. While this is not a problem during longer-term experiments where constant  $\text{SO}_3$  concentrations are required, this delayed response is a problem for SDR experiments. Thus, the catalysts, at this stage, have limited use for SDR experiments and especially those experiments for small  $\text{SO}_3$  concentrations.

### 3.3.3 Particle monitors

Due to the limited gas volume flowing through the SDR absorber ( $200\text{ cm}^3/\text{min}$ ), it is not possible to operate all aerosol instruments concurrently. Thus, individual instruments must be combined or operated separately according to the combined flow demand of the monitors. Monitors that are not directly sampling are 'switched out' of the sampling loop and purged with to filtered laboratory supplied air. The laser diffraction analyser (LDA) was continuously operated during experiments to allow comparisons to be made between different monitors while also validating SDR stability and performance.

Heated sampling lines have been installed between the sampling port on the SDR and the inlet of each monitor to minimise thermophoresis and reduce evaporation/condensation artefacts during experiments. The temperature of the heated lines was maintained a few degrees above the temperature of the gas sample at the sampling location.

Figure 3 shows the SDR with several particle monitors installed.

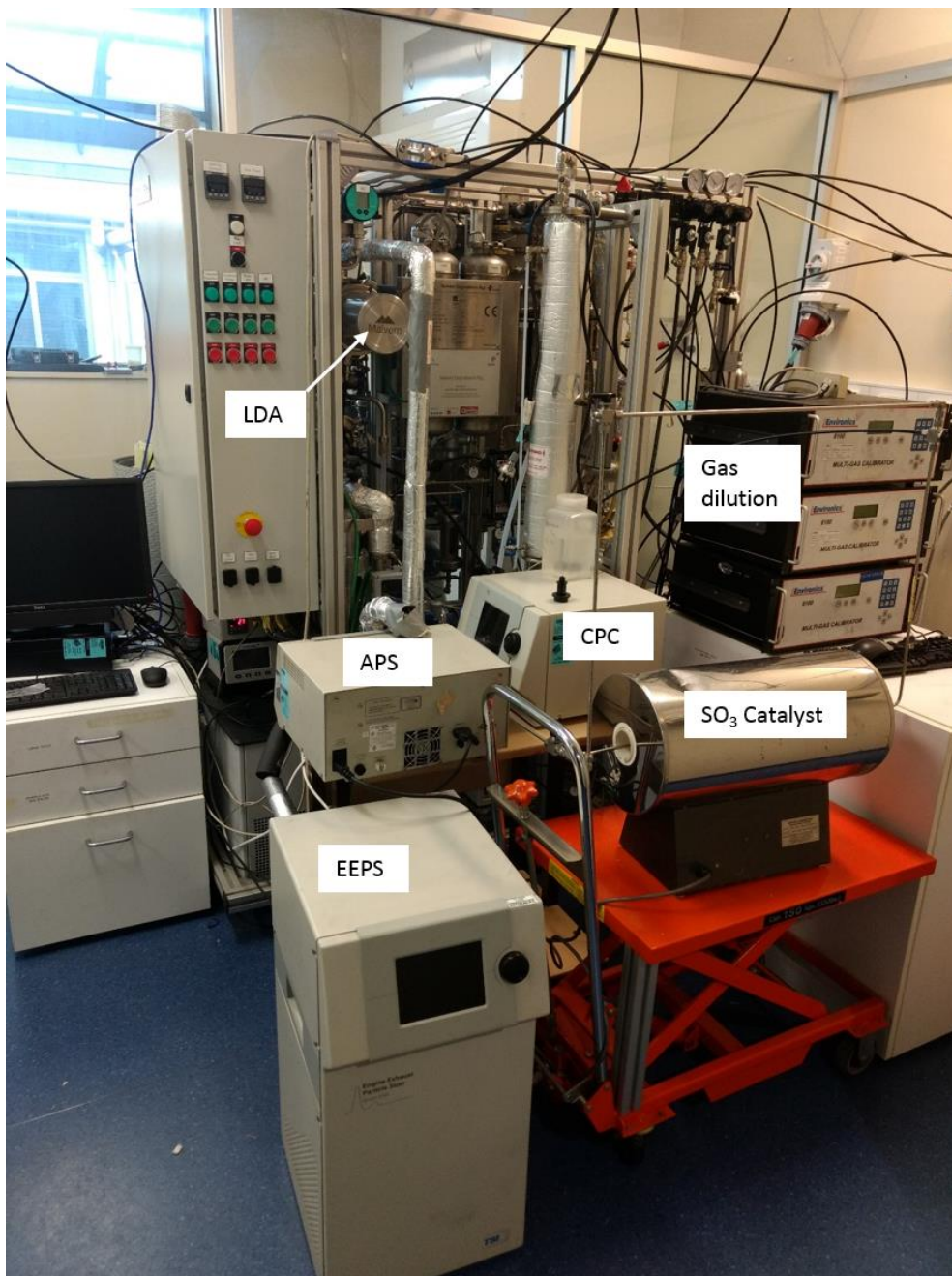


Figure 3 Solvent degradation rig with particle-measuring instruments installed

As is shown in Figure 3, the LDA is installed directly across the ductwork of the gas stream using a stainless-steel alignment/flow assembly shown with greater detail in Figure 4. The relative locations of the laser, detector and position of the optical windows and the direction of the laser beam relative to the gas flow are also shown in Figure 4.

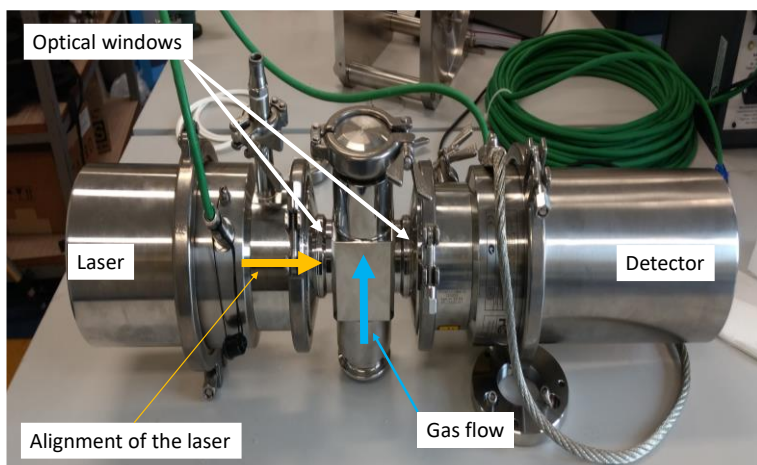


Figure 4 The laser diffraction analyser (Malvern™ Insitac) assembly-ready for installation into the solvent degradation rig

Experimental conditions were maintained by the newly developed computer software platform allowing reproducible experimental conditions to be set and maintained over the duration of the experiment. Experiments were undertaken with  $\text{NO}_2$ ,  $\text{SO}_2$ ,  $\text{NO}$  and  $\text{SO}_3$  as separate individual gases and as a combination of these gases within a makeup gas of  $\text{N}_2$ ,  $\text{Ar}$ ,  $\text{CO}_2$  and  $\text{O}_2$  with concentration representative of a coal-fired power station.

At the start of the experiment, the initial base composition of the surrogate flue gas was delivered to the absorber. This was then altered by adding the target gas(es) in appropriate combinations and concentrations to achieve a final mixture. The duration of individual experiments was normally assigned to be 1 hour. This time was initially considered as a reasonable compromise between the time necessary for the SDR reaching steady-state conditions and a reasonable time period to demonstrate stable aerosol concentrations.

Each target gas mix was repeated in triplicate with each 'target' gas experiment separated by a baseline experiment of at least 1 hour. The baseline experiments consisted of passing the mixture of non-target gases through the absorber. Using this protocol, each experimental combination required a minimum of 6 hours SDR run time. Normally, the SDR required between 2 to 5 minutes to reach steady state after target gas flow commenced. The dataset while at steady state is presented in this section.

After the final automation modification were completed, a total of 550 experiments were undertaken using MEA, 870 experiments completed using CAL008, 132 experiments completed using ammonia and 463 experiments completed using the amino acid alanine.

### 3.4 Results

A large portion of this work was repetitious, with the same experimental matrix generally applied to each of the four solvents. Consequently, for brevity of reporting, only a selection of results is used to demonstrate the primary core findings with other interesting findings discussed in the text as appropriate. Laser scattering is used as a core measurement metric to quantify changes in particle concentration within this work, as it was the instrument that operated throughout all

experiments. Examples of particle distributions are presented as necessary to highlight the aerosol size range.

### 3.4.1 Increasing background aerosol concentrations with MEA solvent

During both the initial studies (Appendix B) and the experiments discussed in this section, it became apparent that using the combination of  $\text{NO}_2/\text{SO}_2$  and/or  $\text{SO}_3$  'conditioned' the solvent during the experiment, resulting in large numbers of residual aerosol being observed after the conclusion of the experiments. This resulted in progressively increasing background aerosol concentrations until the solvent was replaced.

Figure 5 displays a time series of average aerosol size distribution over 1-hour duration for each of 23 baseline experiments that were spaced before and after each experiment test experiment. These data are on a number concentration basis and averaged from 1 Hz data. The MEA was exposed to a mixture 15%  $\text{CO}_2$ , 100 ppm  $\text{SO}_2$ , 13%  $\text{O}_2$  and  $\text{NO}$  increasing from 0 to 75 ppm in 10 ppm increments. The experimental series commences with baseline 1 increasing to baseline 23. These data show very similar modal distributions and a progressive increase in background aerosol as the number of experiments increases.

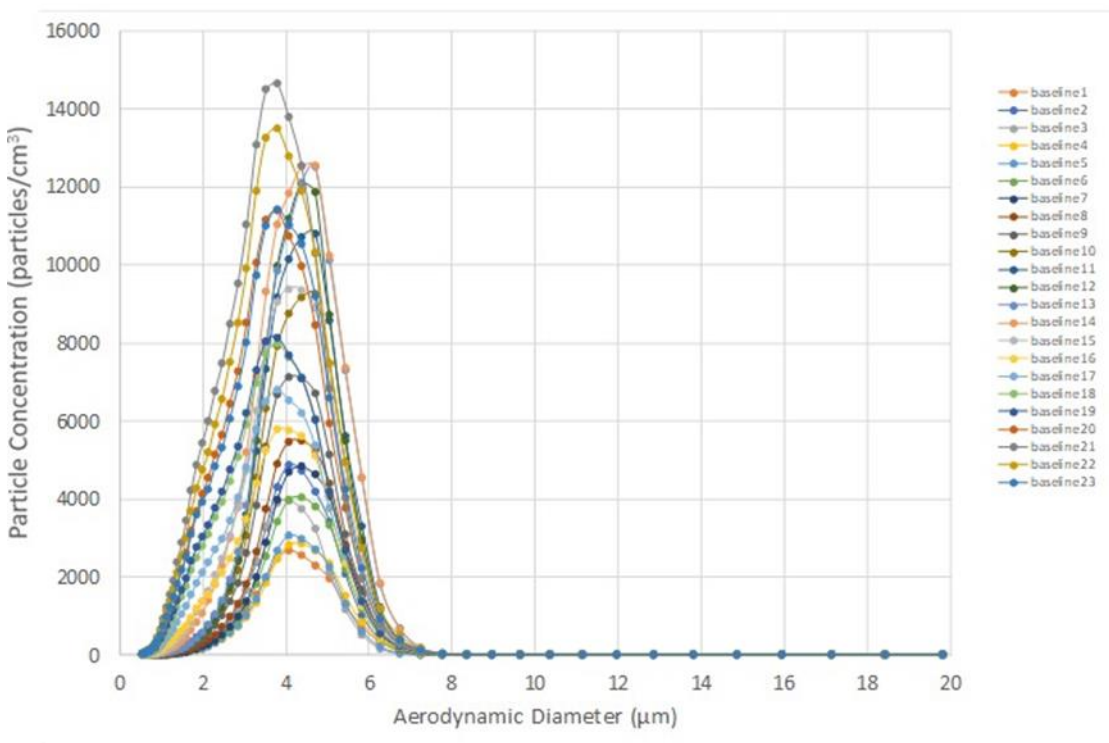


Figure 5 Aerodynamic particle sizer-particle size distribution baseline prior to each target experiment

Figure 6 displays the particle number concentration at the mode for each of the distributions shown in Figure 5, but as a time series with respect to experimental run time. While these data show some variation in number concentration around the 30-hour mark, the overall increasing trend in aerosol numbers as the number of experiments increases is clear.

Figure 7 shows similar data to Figure 6, but for the  $<0.5 \mu\text{m}$  particle fraction. A similar trend with increasing particle numbers can be observed in the dataset.

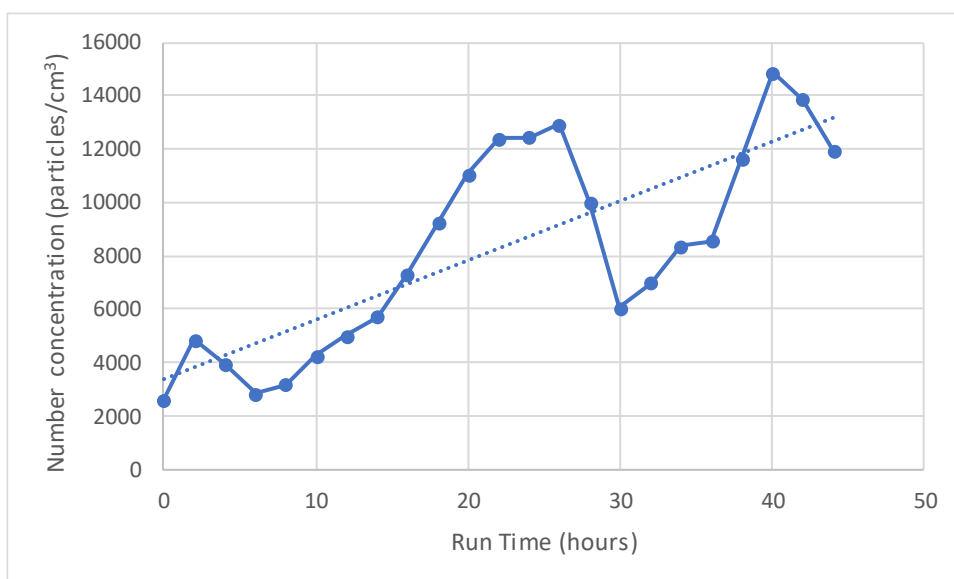


Figure 6 Aerodynamic particle sizer-mode particle concentration for each baseline as a function of experiment run time

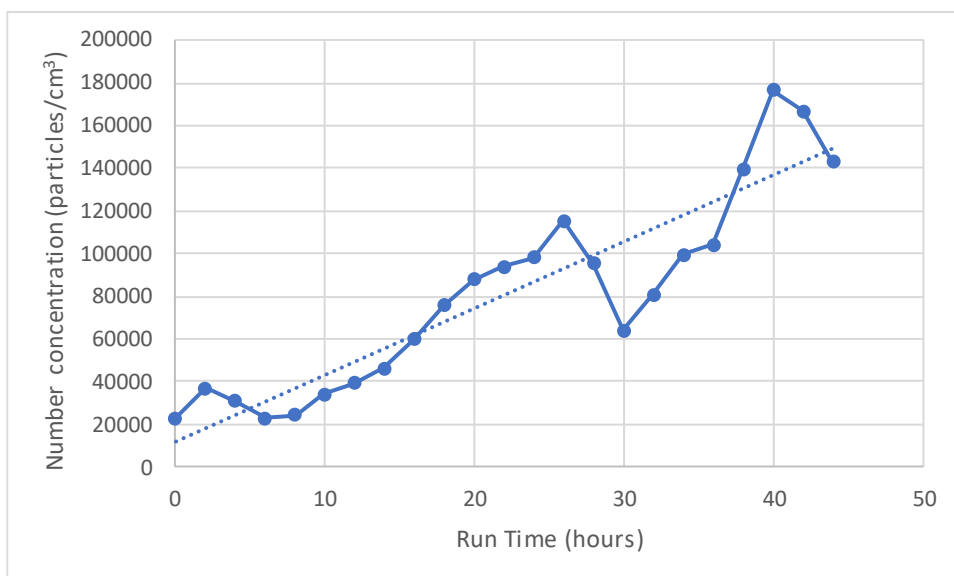


Figure 7 Aerodynamic particle sizer-  $<0.5 \mu\text{m}$  particle concentration for each baseline as a function of experiment run time

The generally increasing aerosol as a function experiment time displayed in Figure 6 and Figure 7 indicates that the characteristics of the solvent are changing as the solvent is exposed to  $\text{SO}_2$ ,  $\text{NO}$  or the combination of these. This increase was observed when the solvent was exposed to  $\text{SO}_3$  or a combination of  $\text{NO}_2$  and  $\text{SO}_2$ . Experiments using  $\text{SO}_3$  produced the strongest increase in aerosol background and necessitated longer background times to 're-condition' the solvent to conditions similar to those at the beginning of the experiment. However, for some experiments, and generally those involving moderate to higher concentrations of  $\text{SO}_3$ , the solvent did not revert to the original conditions even with extended background run time of 20 hours. For some experiments, a continuous partial replacement of aged solvent with new solvent over the duration

of the experiments was explored. This proved useful for SO<sub>3</sub> experiments to reduce the rate of increase in background aerosol concentration.

These data demonstrate that aerosol can be produced with MEA from the residual changes in the chemistry of the solvent after exposure to SO<sub>3</sub> or SO<sub>3</sub> precursor gases. The amount of aerosol formed increases in relation to both SO<sub>3</sub> concentrations and exposure time. It was also apparent that over time the solvent becomes non-reversibly altered, and that this change in solvent behaviour limited the ultimate concentrations of the target gases. Similar observations were found in the preliminary experiments discussed in Appendix B and were the origin of the variable data sets observed. Aerosol concentrations observed for CAL008 were reduced compared to MEA.

The increasing residual aerosol background has significant impacts for the PCC pilot plant trials at Vales Point Station. Given that the current work has been completed using a relatively reproducible background from new MEA, it would be preferential to undertake those experiments that age the solvent the least to be undertaken first, with those that degrade more quickly being undertaken later in the experimental program. Consequently, during the pilot plant study, experiments using NO were completed initially and experiments exposing the solvent to SO<sub>3</sub> were completed later.

Operating engineers at Vales Point PCC pilot plant advised that the flue gas pre-treatment (FPT) process would be highly efficient at removing acid gases from the flue gas reaching the absorber and could achieve close to 100% removal of these gases. Unlike the SDR, solvent within the pilot plant could not be replaced regularly or during experiments due to the cost of the MEA solvent and logistical issues incurred with handling large volumes of solvent. Consequently, these current SDR data direct that the Vales Point PCC pilot plant experiments that use the FPT must be completed initially and before the planned experiments that bypass the FPT and use untreated flue gas.

### 3.4.2 Influence of NO: constant O<sub>2</sub> and CO<sub>2</sub> – CAL008 example

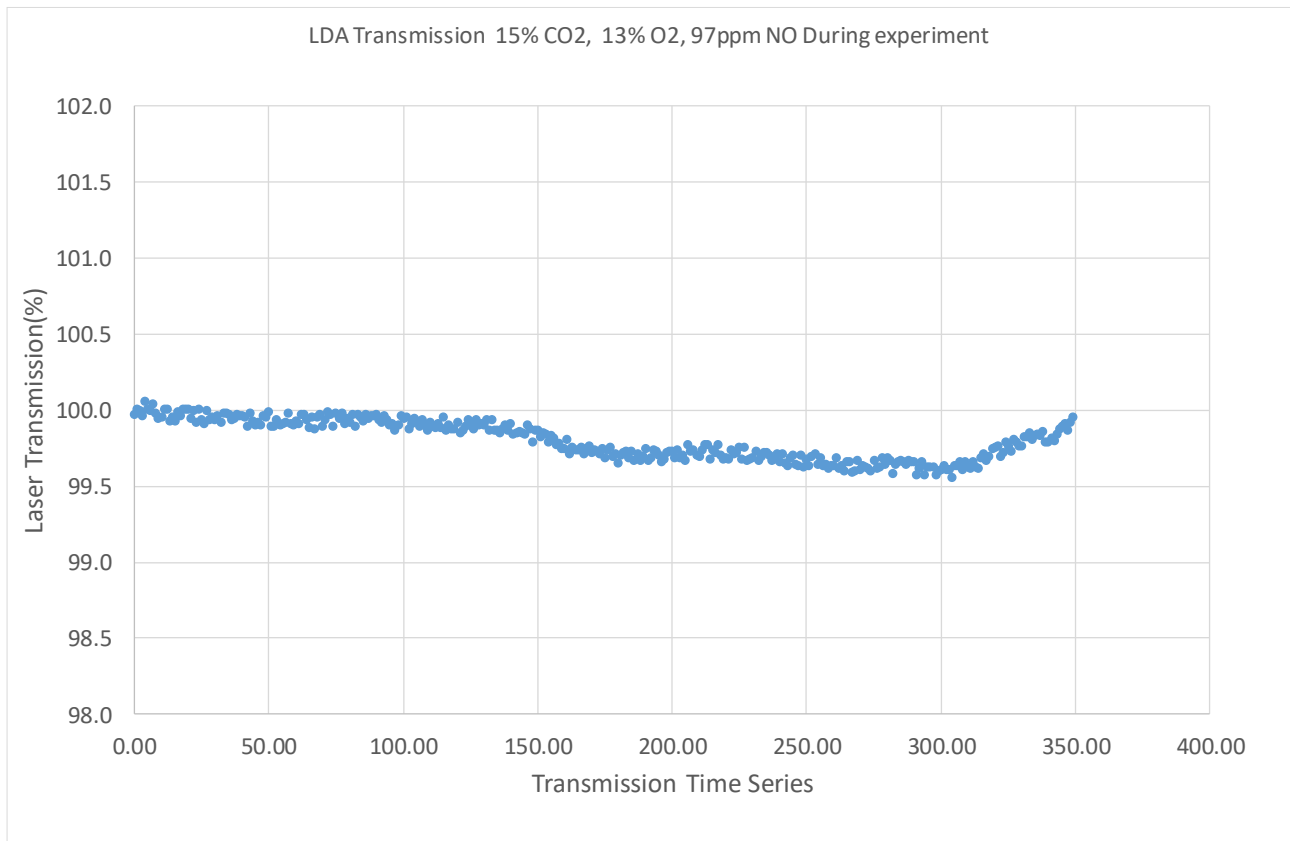
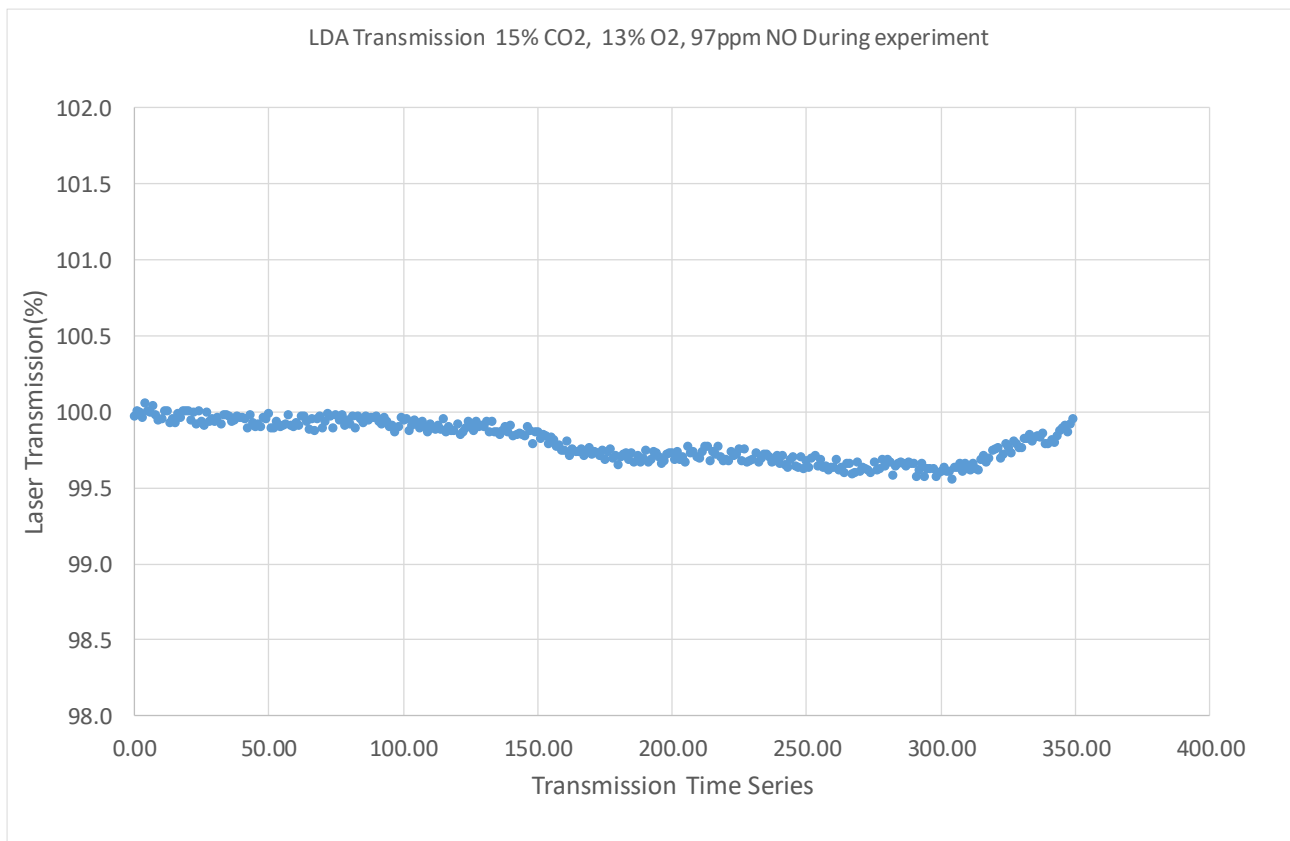


Figure 8 shows a typical time series dataset for an experiment where NO at 97 ppm is added to the gas mixture of 13% O<sub>2</sub> and 15% CO<sub>2</sub> with a nitrogen balance. The gas change occurs at time zero in the presented dataset. Laser transmission reveals no change during or after this addition. Data in Figure 8 are typical of comparable data sets for MEA, ammonia and alanine, with aerosol generation being less than the limit of resolution of the LDA.



**Figure 8 Laser diffraction analyser transmission 97 ppm NO, 7% O<sub>2</sub> and 17 % CO<sub>2</sub> with a nitrogen balance, CAL008 example**

The overall observation from NO experiments indicates that in isolation, NO has minimal potential to generate aerosols. However, these data tend to be in contrast with the Vales Point PCC pilot plant data. While the origin of this significant difference is unknown, it possibly lies in the different designs and scale of the systems.

### **3.4.3 Influence of SO<sub>2</sub>: constant O<sub>2</sub> and CO<sub>2</sub> – CAL008 example**

Figure 9 shows a typical time series dataset from an experiment where SO<sub>2</sub> at 91 ppm is added to gas mixture of 13% O<sub>2</sub> and 15% CO<sub>2</sub> with a nitrogen balance. The gas change occurs just after time zero in the presented data. A change in laser transmission can be observed after the SO<sub>2</sub> addition with laser power reducing from 97.9 to 90.5% as a result of aerosol formation. Data in Figure 9 are again also typical of comparable experiments for the other solvents investigated.

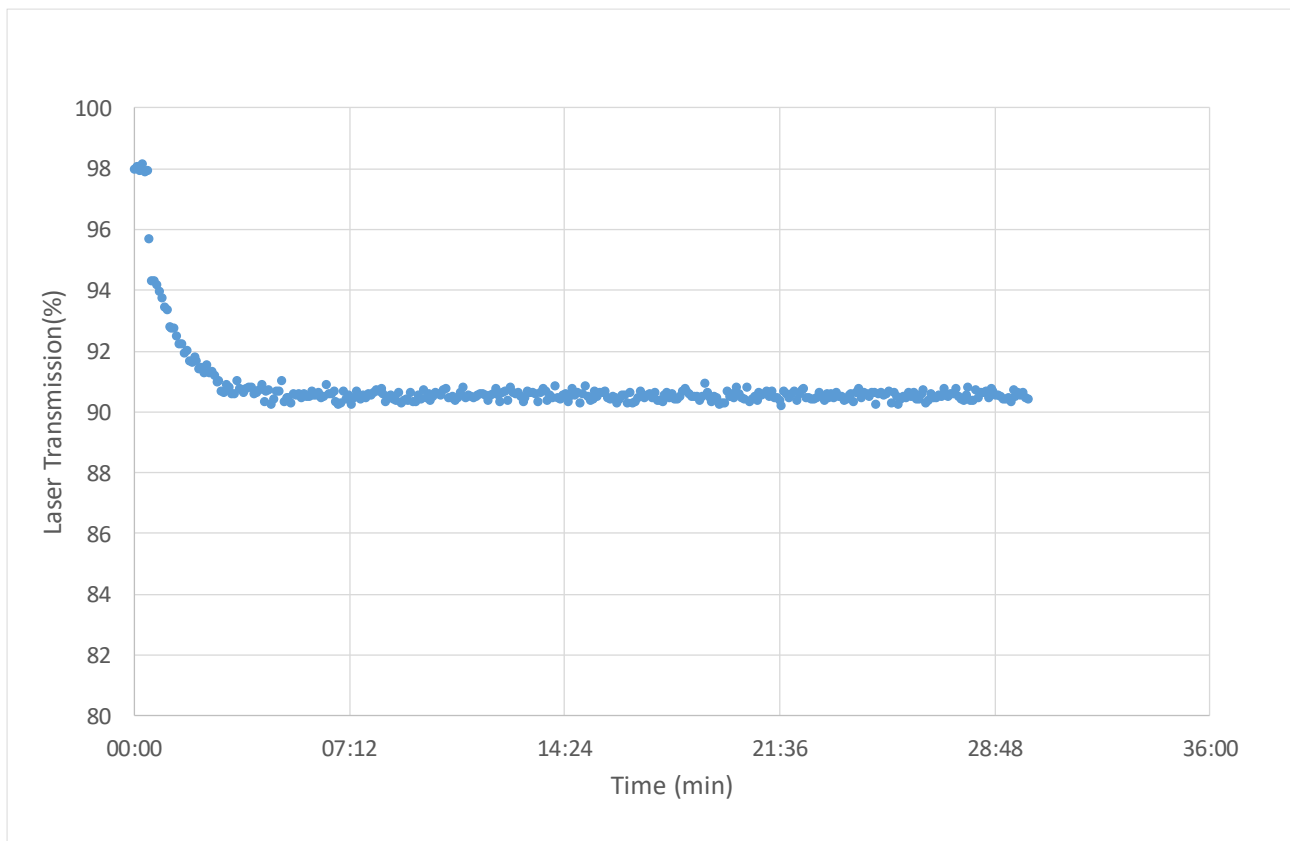


Figure 9 Laser diffraction analyser transmission 91 ppm SO<sub>2</sub>, 13% O<sub>2</sub> and 15 % CO<sub>2</sub> with a nitrogen balance, CAL008 example

Figure 10 shows the number distribution reported by the LDA, which shows a very fine particle distribution of less than 1 µm with a large number of particles of 0.1 µm diameter and less. Such fine aerosol suggests that only a small degree of agglomeration has occurred within the absorber and that the origins of these aerosol is through homogeneous condensation of acid nuclei. Unfortunately, the electrical engine particle spectrometer (EEPS) was not available during these experiments to improve the size resolution, since its increased small size range, down to 0.05 µm diameter, would have provided much information regarding the mode of aerosol formation and the diameter range at aerosol genesis.

It is noted that these SDR data tend to contrast with comparable data measured at Vales Point pilot plants where little aerosol was observed (Figure 27 and Figure 29). However, while the absolute number concentrations differ, the dominant small size fraction tends to be generally similar for both Vales Point PCC pilot plant (Figure 28) and these current data.

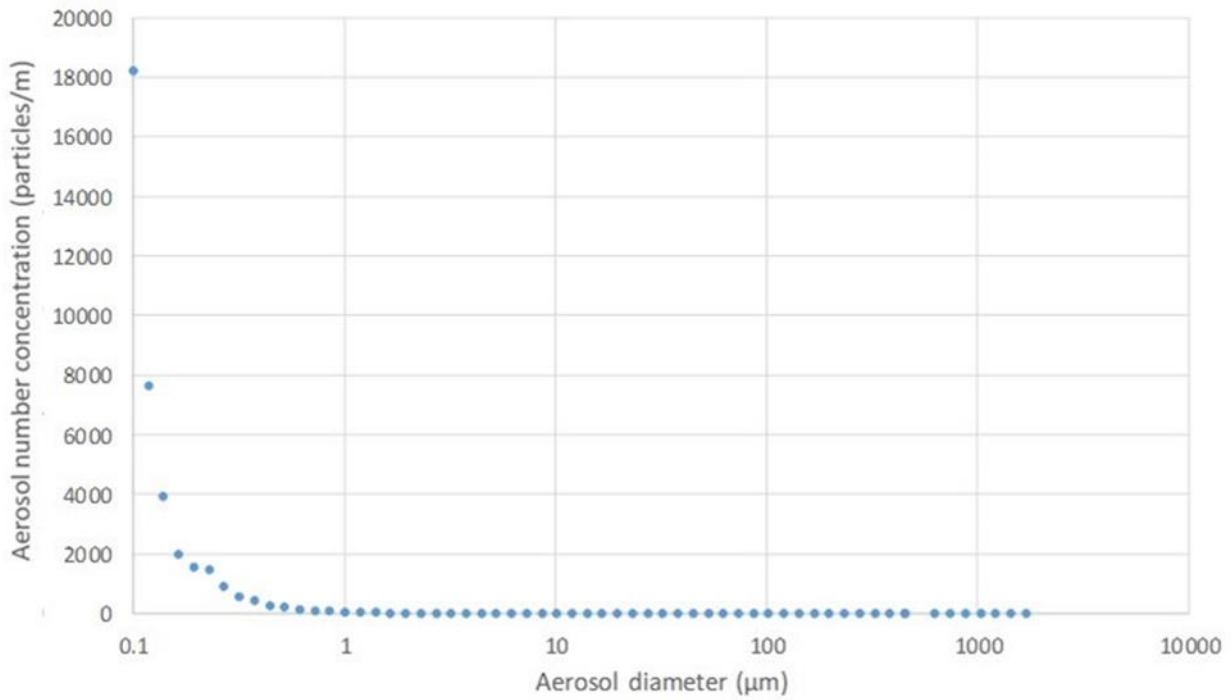


Figure 10 Laser diffraction analyser number distribution 91 ppm SO<sub>2</sub>, 13% O<sub>2</sub> and 15 % CO<sub>2</sub> with a nitrogen balance, CAL008 example (LDA reports particle concentration as particles/m. Volume concentration can be calculated using the diameter of the duct and flowrate)

The overall observation of SO<sub>2</sub> experiments is that, in isolation, SO<sub>2</sub> has a moderate potential to generate aerosols and produces aerosols of very fine diameter. It is likely that the short path length of the SDR absorber limits aerosol growth, reducing the size of the aerosol measured.

### 3.4.4 Influence of NO<sub>2</sub>: constant O<sub>2</sub> and CO<sub>2</sub> – CAL008 example

Figure 11 shows a typical time series dataset from an experiment where NO<sub>2</sub> at 100 ppm is added to a gas mixture of 13% O<sub>2</sub> and 15% CO<sub>2</sub> with a nitrogen balance. The gas change occurs at time zero in the presented data.

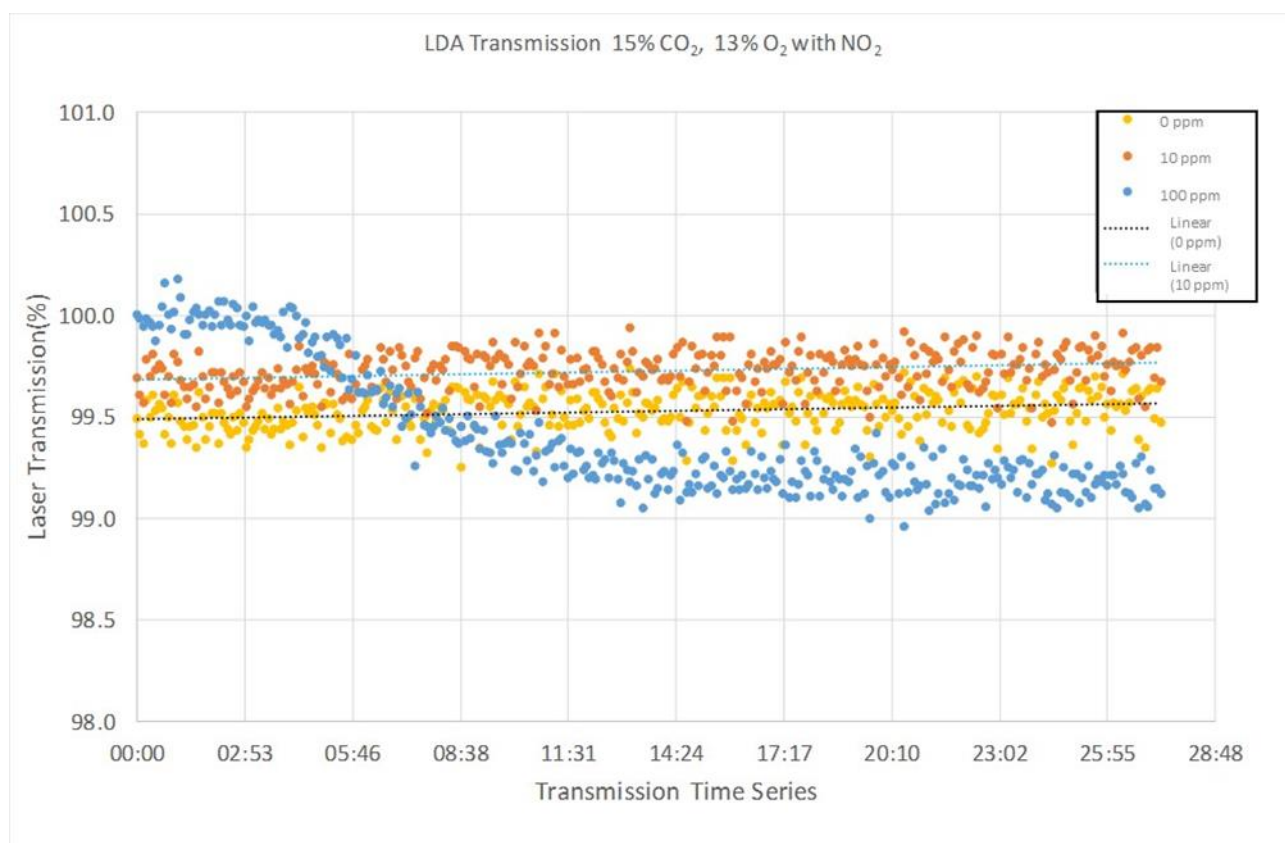


Figure 11 Laser diffraction analyser transmission at 0, 10 and 100 ppm NO<sub>2</sub>, 13% O<sub>2</sub> and 15 % CO<sub>2</sub> with a nitrogen balance, CAL008 example

The concentration axis in this figure has been enlarged to reveal the small changes in transmission that are produced due to NO<sub>2</sub> addition. In addition, the limit of resolution of the LDA data can be observed from the scatter in these data, which is ~0.2%. This figure also contains a dataset for NO<sub>2</sub> addition at 10 ppm, shown by the orange markers, and a background dataset that preceded the 10-ppm experiment, shown by the yellow markers. In this example, the NO<sub>2</sub> experiments were incorrectly programmed to follow, but after a 12-hour solvent recovery period, a series of SO<sub>3</sub> experiments where the solvent was exposed to SO<sub>3</sub> concentrations up to 100 ppm. The yellow trace in this figure has a transmission of 99.5% at the commencement of the experiment background, due to residual aerosol from solvent artefacts. Over the duration of the background experiment, transmission continues to increase as aerosol concentration reduces. At the commencement of the 10 ppm NO<sub>2</sub> addition, LDA transmission continues to increase, showing that the residual aerosol from the SO<sub>3</sub> experiments is larger than the aerosol produced from the NO<sub>2</sub> at a concentration of 10 ppm. Trend lines showing the increase in transmission for the 0 and 10 ppm data sets, shown as blue and black lines, respectively, are also included on Figure 11.

Figure 12 displays similar data to Figure 11, but at concentrations of 30, 50, 70 and 100 ppm, with these data shown as grey, green, orange and blue markers, respectively. By the time the experiment has progressed to the 30 ppm experiment, the residual SO<sub>3</sub>-derived background aerosol had reduced to below the resolution of the LDA. Data in Figure 12 are typical of comparable data sets with MEA showing the largest background aerosols, but still of similar order magnitude as the limit of resolution of the LDA.

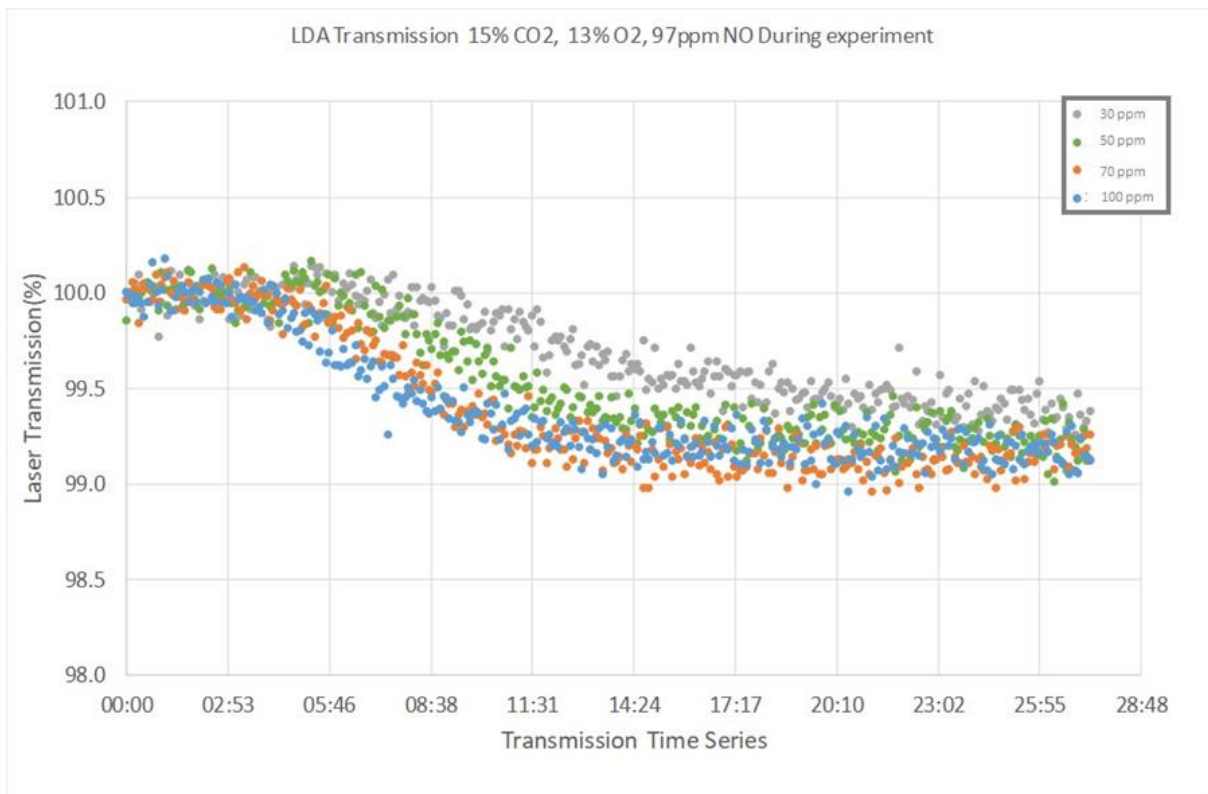


Figure 12 Laser diffraction analyser transmission at 30, 50, 70 and 100 ppm NO<sub>2</sub>, 13% O<sub>2</sub> and 15 % CO<sub>2</sub> with a nitrogen balance, CAL008 example

### 3.4.5 Influence of NO: constant O<sub>2</sub>, SO<sub>2</sub>, CO<sub>2</sub> – MEA example

For this experimental series, MEA was challenged with a gas mixture of 15% CO<sub>2</sub>, 100 ppm (0.01%) SO<sub>2</sub> and 13% O<sub>2</sub>. The target gas NO was varied in concentration from 8 ppm up to 65 ppm in ~8 ppm increments. Similar experiments were completed for the other solvents.

Figure 13 shows an example of the LDA transmission data and includes the transition time period between the preceding baseline measurement and the commencement of a constant addition of 65 ppm NO. The time at which NO addition commences is indicated by the blue arrow, while the insert image shows a magnified view of the gas transition period. These data show that the SDR required approximately 2 minutes to regain constant steady-state conditions following a gas change.

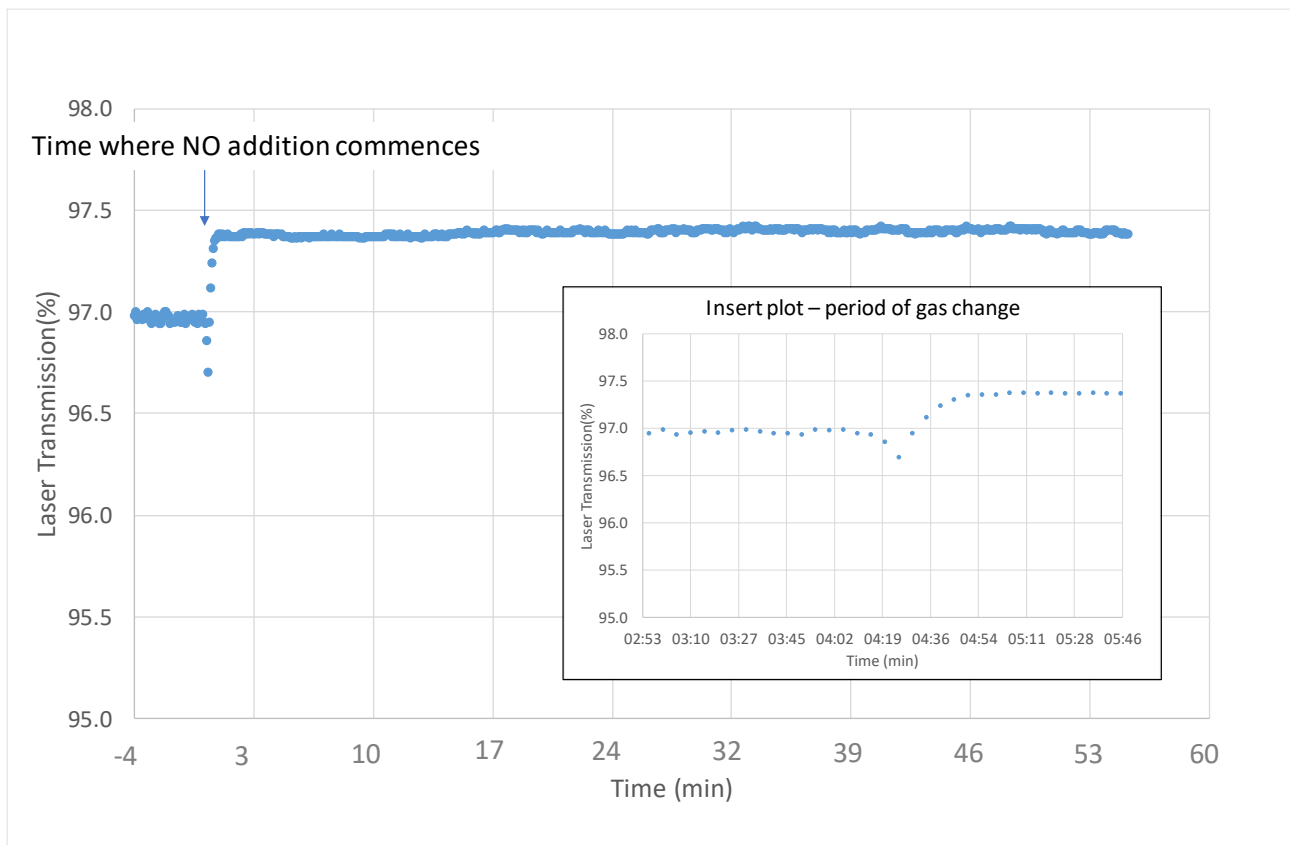


Figure 13 Laser diffraction analyser transmission data at 64 ppm NO

Figure 14 shows the baseline aerodynamic particle sizer (APS) size distribution prior to commencing these measurements<sup>1</sup>.

Residual particles are present in the baseline dataset. These APS data suggest a bi-modal distribution, with one mode with a concentration of 2600 particles/cm<sup>3</sup> at ~4 µm and a second mode with a concentration of 5400 particles/cm<sup>3</sup> at <0.5 µm. The specific origins of these aerosols are unknown and will be a combination of physical and chemical factors.

---

<sup>1</sup> APS measures fine particles (<0.5µm) through light scattering techniques and provides only an indicative measure of ultrafine particles rather than the direct count of particle number as is the case for particles >0.5 µm

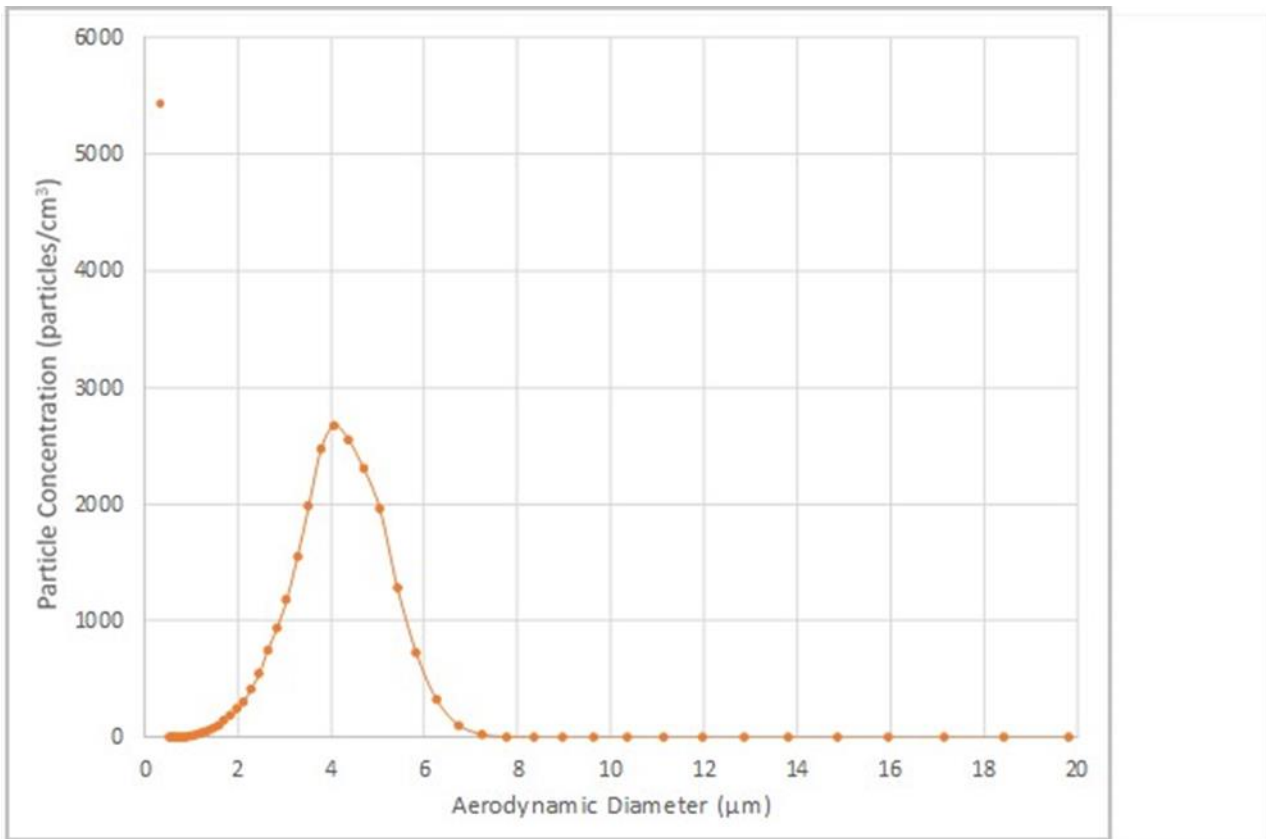


Figure 14 Aerodynamic particle sizer particle size distribution baseline example prior to experiments

Upon injection of NO at 8 ppm, the APS reported reduced aerosol concentrations compared to the background, indicating that the NO was suppressing aerosol. Data for the 8 ppm NO addition (blue traces) and the 64 ppm NO addition (green traces) are shown in Figure 15.

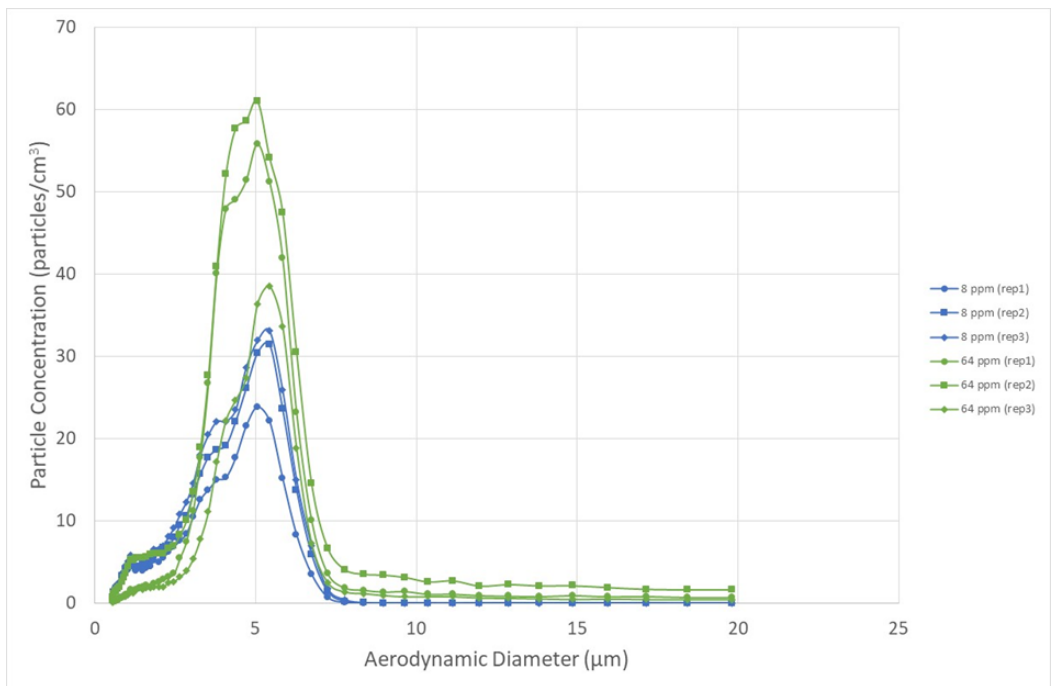


Figure 15 Aerodynamic particle sizer particle size distribution low concentration NO shows removal of particles

The baseline experiments for the 8 ppm and 64 ppm additions are shown in Figure 5 baseline 1 to 4 and baseline 20 to 23, respectively. It can be observed that number concentrations reduce by approximately two orders of magnitude in each case. Similar data was observed for similar NO experiments at concentrations of 16, 24, 32, 40, 48 and 56 ppm. These results are supported by the LDA data, which revealed a small increase in transmission: 0.1% for the 8 ppm experiments and 0.4% increase for the 64 ppm experiments. Reductions in particle number ultrafine particle numbers commensurate to APS data were also observed.

This observation was not seen in the CAL008, ammonia and alanine results where NO addition produced negligible aerosol. These results add additional weight to support a hypothesis that the chemical properties, and thus composition of the solvent, can play a large role in the amount of aerosol produced by a solvent. It is plausible that the NO in this example is influencing an equilibrium reaction that suppresses aerosol formation for species such as SO<sub>3</sub>, i.e. NO drives the removal reaction further to completion. If such a process exists, this may provide the opportunity to design low-aerosol-forming solvents that contain a chemical pathway to reduce aerosol potential. This may need to be developed in conjunction with optimal PCC designs to enhance aerosol suppression. The results for the case for CAL008 suggest this as this solvent displayed reduced aerosol concentration for comparable experiments with MEA. CAL008 also has a more complex chemical structure, which is quite different to the simple structure of MEA. This complexity allows for a number of chemical pathways that could increase SO<sub>3</sub> capacity and suppress aerosol formation.

#### **3.4.6 Influence of NO<sub>2</sub>: constant O<sub>2</sub> (7%), NO (0%), SO<sub>2</sub> (100 ppm), SO<sub>3</sub> (0 ppm), CO<sub>2</sub> (0%), aged MEA example**

In this experimental series, a NO<sub>2</sub> target gas was added to a baseline gas mixture of 0% CO<sub>2</sub>, 100 ppm SO<sub>2</sub> and 5% O<sub>2</sub>. The target gas NO<sub>2</sub> was varied in concentration from 1 ppm up to 9 ppm in ~1 ppm increments.

Figure 16 shows an example of LDA transmission results for an experiment with the addition of NO<sub>2</sub> at 1 ppm. These data include the transition time periods between the preceding and succeeding baseline measurements. The time at which NO<sub>2</sub> addition commenced is indicated by the blue arrow, while the green arrow indicates the time when NO<sub>2</sub> flow terminated. At an NO<sub>2</sub> concentration of 1 ppm these data show that the SDR required approximately 3 minutes to reach constant steady-state conditions after NO<sub>2</sub> flow commenced and nearly 22 minutes after NO<sub>2</sub> ceased.

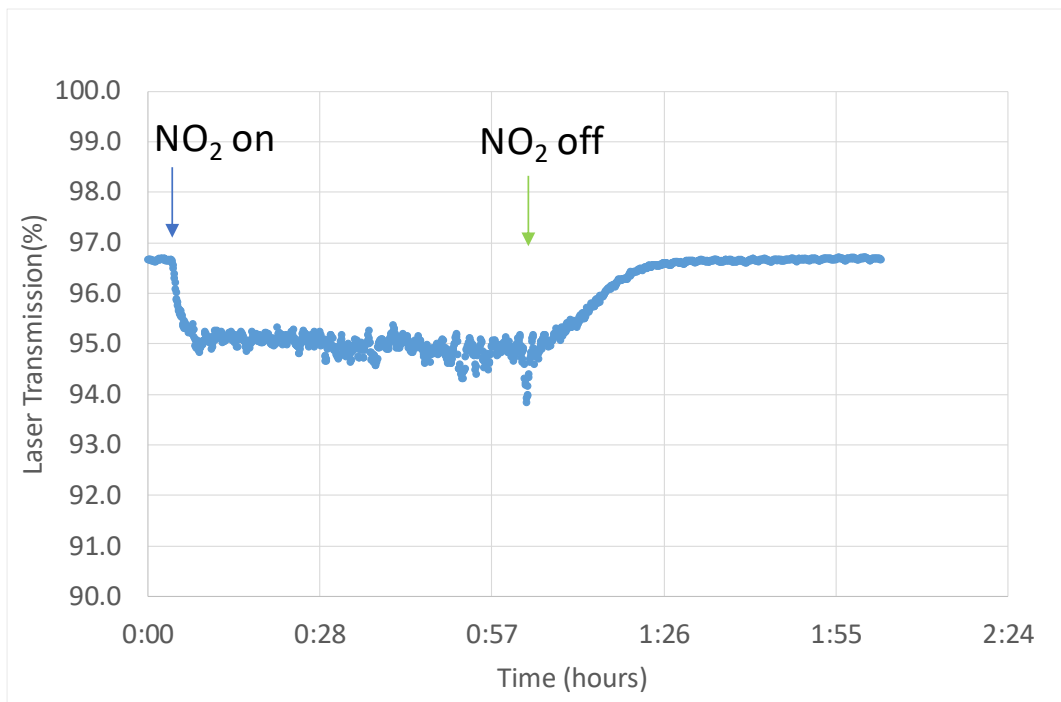


Figure 16 Laser diffraction analyser transmission data showing the transition as NO<sub>2</sub> flow commences and is terminated

Note that the NO<sub>2</sub> data display increased lag times compared to those data displayed for NO in Figure 13. This is especially the case with respect to significantly longer times required for system recovery after NO<sub>2</sub> exposure. This increased lag time after NO<sub>2</sub> exposure is important and suggests the 'ageing', or residual accumulation, of a yet-unknown aerosol-forming species or intermediate species in the solvent over the period of NO<sub>2</sub> addition. It is highly likely this is a result of SO<sub>3</sub> formation. This hypothesis is also supported by the reduction in transmission over the duration of the experiment. An average reduction in transmission of ~0.3% over the experiment is displayed, indicating that increased aerosol is forming.

These data suggest that at 1 ppm NO<sub>2</sub>, this accumulation is reversible, as the aerosol concentrations reduce to approximately those observed before the experiment. This is possibly a reversible equilibrium with aerosol formed from one or more species 'outgassing' or being released from the solvent as the NO<sub>2</sub> in the flue gas reduces. Note this artefact was also observed in preliminary results and was the root cause of the non-reproducibility of aerosols in this work.

Experimentally, this is a significant finding, as these data clearly indicate that a long period of time is required for the system to restabilise before further target experiments can proceed, and that the aerosol-forming potential of the solvent is variable and dependent upon the history of the solvent. However, as noted in Section 3.4.4, these artefacts depend upon the chemistry of the solvent and most likely the conditions of the process.

Figure 16 shows that as the concentration of NO<sub>2</sub> addition was incrementally increased from 1 ppm to 9 ppm over the experiments, the time to form aerosol remained relatively constant and fast. However, the recovery time to return to the initial baseline aerosol concentrations after the experiment progressively increased, until eventually the system ceased to revert to initial baseline values, even after 22 hours of baseline monitoring. Consequently, for these highest concentration experiments, stable background concentrations could not be achieved without a continuous partial replenishment of the solvent. This was a much smaller problem for CAL008 than MEA. It is

suspected that this reduction for CAL008 is a result of a reduced degradation rate from exposure to acid gases, and that this arises from the different chemistry and increased absorption capacity for aerosol nuclei species such as sulphuric acid. An example of this is shown in Figure 17, where the first 6 hours of the LDA transmission during a 9 ppm NO<sub>2</sub> experiment is displayed. In this case, the laser transmission at the time when NO<sub>2</sub> flow commenced remained reduced to 96% after reconditioning compared to the initial transmission at the commencement of the 1 ppm experiment (Figure 16).

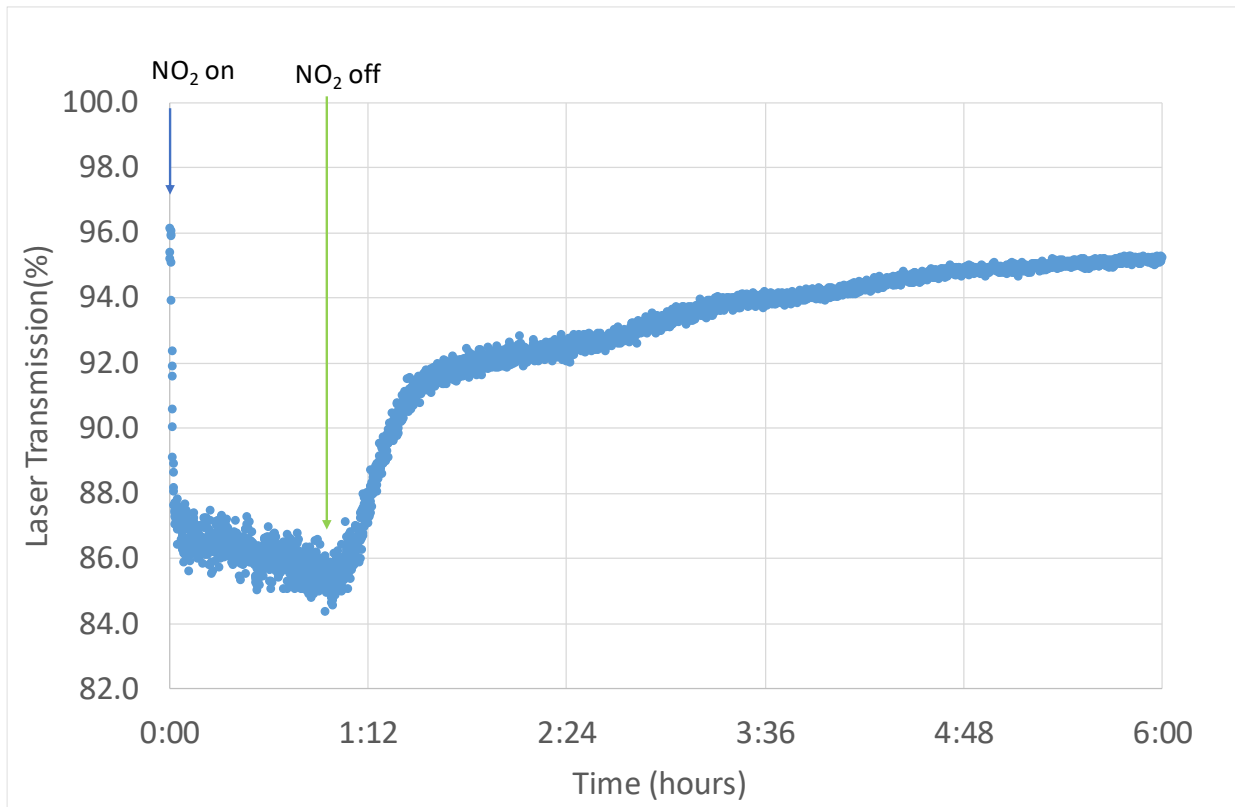


Figure 17 Laser diffraction analyser transmission data showing the transition as NO<sub>2</sub> flow commences and is terminated at 9 ppm

Figure 17 shows an initial reduction in transmission from 96 to 87% as NO<sub>2</sub> flow commences. After the initial reduction, transmission continues to reduce at about 2% per hour. This increased rate of reduction compared to that observed for 1 ppm (Figure 16) clearly indicates an increased solvent ageing rate at higher NO<sub>2</sub> concentrations. These data also reveal that once NO<sub>2</sub> flow ceases, there is a long delay period for the ageing to reverse. For this example, only 6 hours of the 22-hour experiment is displayed; however, it was observed that even after 22 hours of background flow, the aerosol concentration had not reverted to the original aerosol concentration values.

During the NO<sub>2</sub> experiments in this section, large quantities of aerosol were produced at 9 ppm. These aerosol number concentrations approached the maximum resolution of the APS as shown in Figure 18, and thus increased concentrations were not possible without dilution.

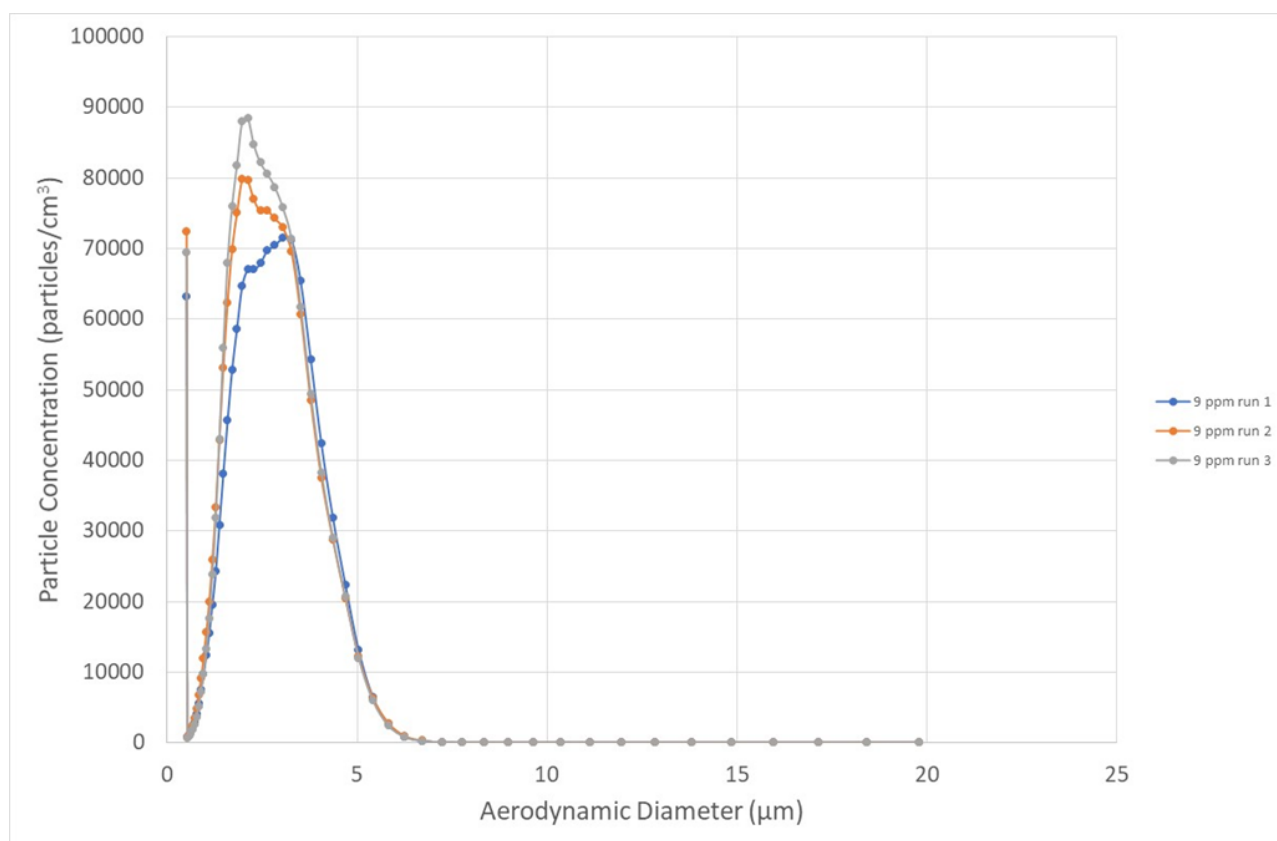


Figure 18 Aerodynamic particle sizer particle size distribution at 9 ppm NO<sub>2</sub>

Consequently, due to the long aerosol recovery times of the solvent, NO<sub>2</sub> addition was limited to 9 ppm. This limits the range over which these data can be applied to PCC processes. The use of dilution will be required to extend this range.

It is well known that SO<sub>2</sub> is oxidised by NO<sub>2</sub> to form SO<sub>3</sub> and consequently increased aerosol formation occurs. Thus, it is not surprising that NO<sub>2</sub> and SO<sub>2</sub> in isolation produce limited aerosol, but in combination produce significant quantities of fine aerosol. It has also been demonstrated that the sulphuric-acid-forming aerosol pathway is independent of the formation pathway, and will form sulphuric acid from SO<sub>3</sub> directly and/or from NO<sub>2</sub> and SO<sub>2</sub> mixtures or mixtures from all three gases. The process is additive and dependent upon the concentration of the sulphuric acid produced.

### 3.4.7 Influence of SO<sub>3</sub>: constant O<sub>2</sub> (13%), CO<sub>2</sub> (15%), Cal008-MEA examples

Section 3.4.6 identified that SO<sub>3</sub> is a dominant producer of aerosol during the reaction of NO<sub>2</sub> and SO<sub>2</sub> to form SO<sub>3</sub>. This section directly examined the aerosol-forming-potential of SO<sub>3</sub>. Figure 19 displays the LDA transmission during the addition of SO<sub>3</sub> at 8 ppm with MEA. These data reveal a 9% reduction in transmission even with only small concentrations of SO<sub>3</sub>, consistent with the results of Figure 16.

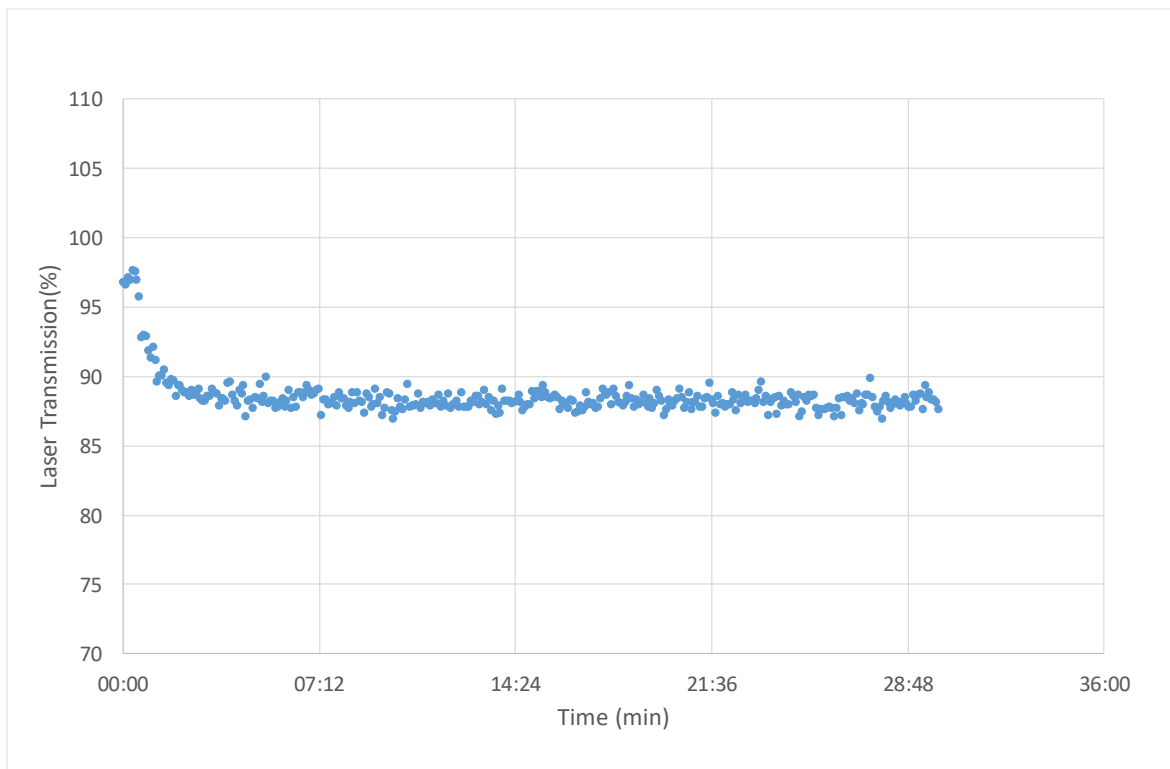


Figure 19 Laser diffraction analyser transmission data 8 ppm SO<sub>3</sub> – MEA

Figure 20 shows the APS particle distribution averaged over the time series of Figure 19. These data are bimodal, showing a very fine mode with diameter <math><0.5 \mu\text{m}</math> (insert) and a second mode at

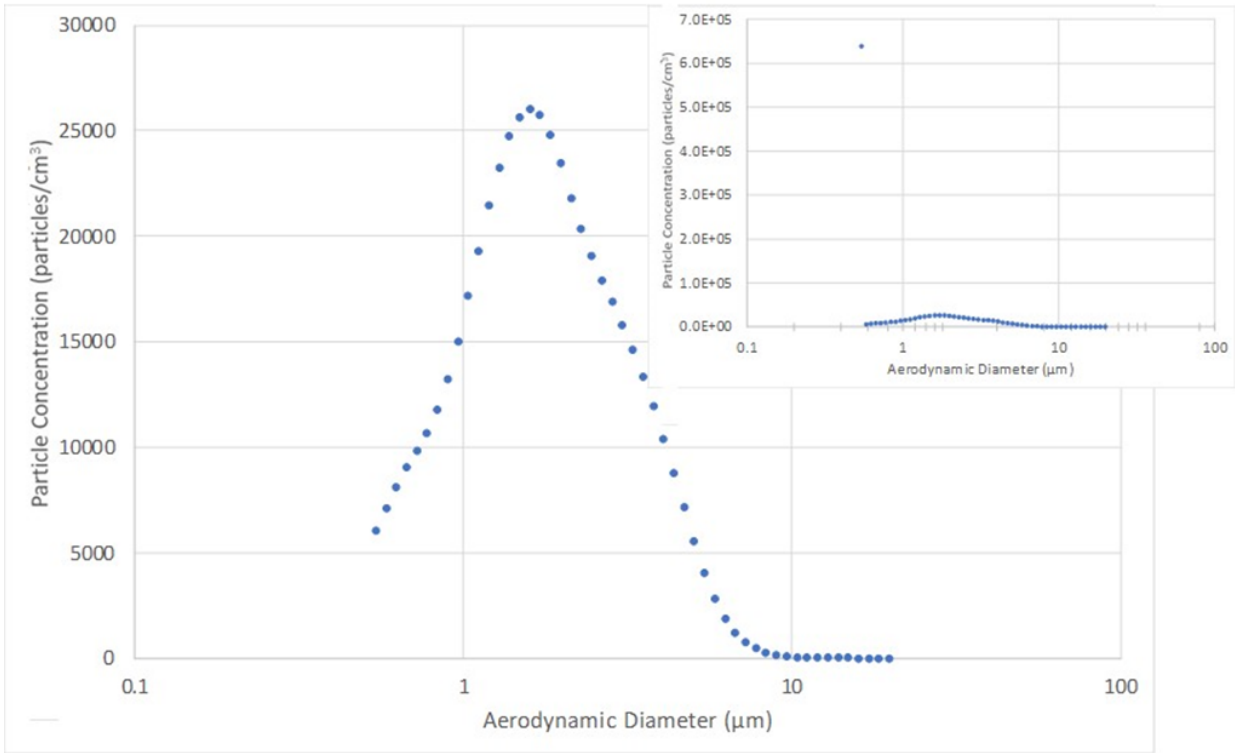


Figure 20 Averaged aerodynamic particle sizer particle size distribution 8 ppm SO<sub>3</sub> – MEA

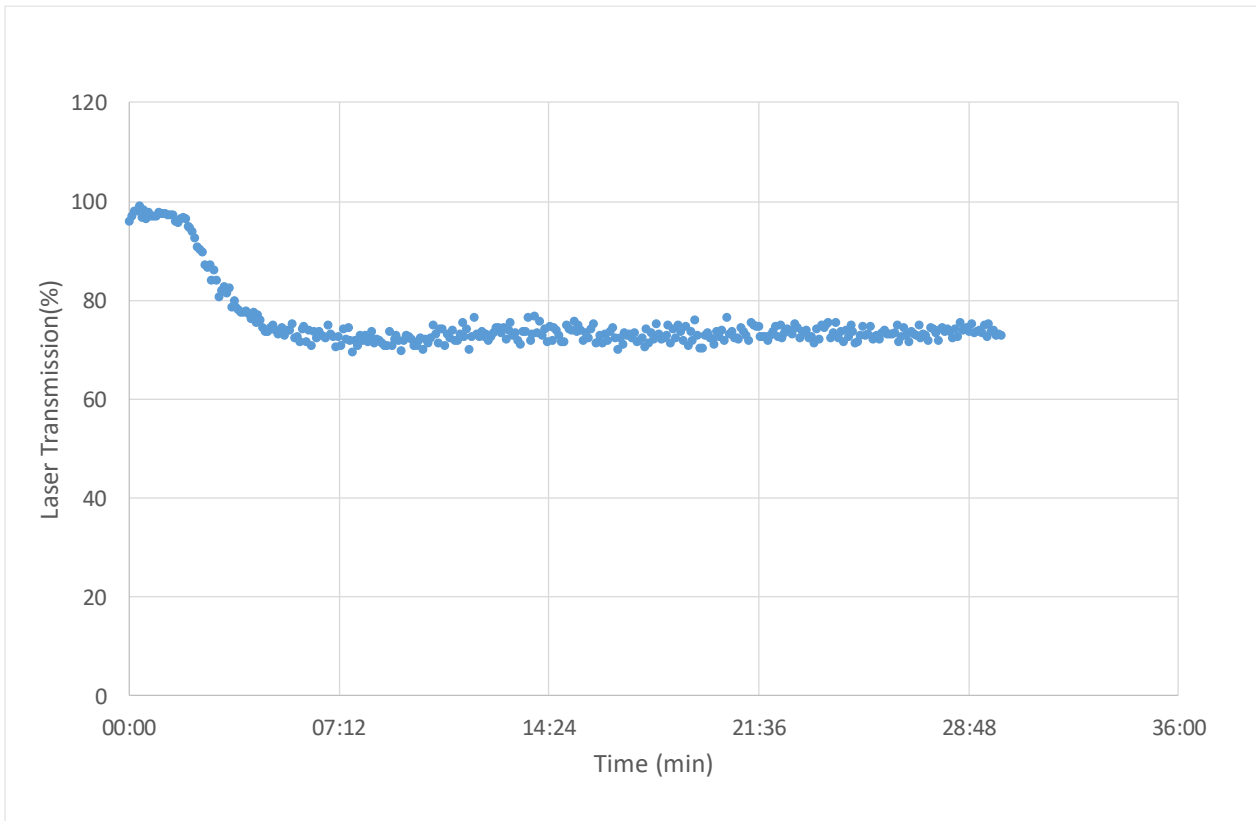


Figure 21 Laser diffraction analyser transmission data 8 ppm SO<sub>3</sub> – CAL008

Figure 21 displays the LDA transmission during the addition of SO<sub>3</sub> at 8 ppm with CAL008. In this case these data indicate a 25% reduction in transmission, suggesting increased aerosol

concentration due to  $\text{SO}_3$  addition. In all experiments involving  $\text{SO}_3$ , large quantities of aerosol were produced, which in many cases exceeded the range of the aerosol instrumentation. Consequently, for future work, increased dilution will be necessary to overcome these limitations. Due to time constraints, a dilution system could not be sourced or developed within the timeframe of the project.

### 3.5 Discussion/conclusion

Approximately 1000 target gas experiments were completed during this study, with a similar number of baseline experiments (excluding preliminary experiments that were undertaken during the development of the apparatus).

Solvent stability was a challenge when using older or more aged solvents, with the solvent requiring many hours of reconditioning to return to the initial conditions. This was especially the case for experiments involving  $\text{SO}_3$ , regardless of whether its presence arose from oxidation of  $\text{SO}_2$  or by direct addition. This ageing effect was significantly greater in MEA than CAL008, with both of these solvents showing a larger residual aerosol than alanine. When new solvent was used at the beginning of each experiments series, the solvent tended to be more stable, with the system returning to baseline generally within 1 hour.

The  $\text{NO}_2$  experiments showed that  $\text{NO}_2$ , in isolation and at concentrations below 160 ppm (the highest used here) has minimal potential to generate aerosols with new CAL008. Similar results were observed for SDR MEA experiments and for experiments at a  $\text{NO}_2$  concentration of 160 ppm at the Vales Point PCC pilot plant. However, at 325 ppm at Vales Point, significant aerosol was produced. These data suggest that a critical concentration exists, above which aerosols are produced, but below which aerosol formation is suppressed. This watershed condition is likely to be a function of the absorption capacity for  $\text{NO}_2$  at the prevailing absorption condition. Given the differences in the aerosol concentrations measured for MEA and CAL008 during these experiments, this potential aerosol suppression capacity is both a function of the solvent chemistry, and most likely a function of the absorber characteristic, such as absorber packing type, since this has an impact on the absorption area available to the  $\text{NO}_2$ . SDR data indicate that MEA has the least capacity to suppress aerosol formation, with the greatest aerosol concentrations observed. CAL008 displayed significantly smaller aerosol formation and greater aerosol suppressing properties compared to MEA. Consequently, these data suggest that aerosol-formation pathways within PCC processes may be limited or reduced by suitable plant design and appropriate solvent chemistry.

The small background aerosol concentrations observed in this study indicate that aerosol formation from the temperature bulge in the absorber may not be as significant as reported in literature. This finding suggests that aerosol genesis may be suppressed by appropriate absorber design. These results suggest that the main pathways of aerosol formation for both the SDR and the Vales Point PCC pilot plant are chemical and originate from sulphuric acid formation through  $\text{SO}_3$  reacting with water. Experiments also suggest that the chemical properties of the solvent can have a large bearing on the amount of aerosol formed during the PCC process and the amount of aerosol nucleation that occurs in the absorber. It is plausible that a critical concentration exists, which is dependent on the chemistry of the solvent, below which little aerosol is formed. It is

plausible that this critical concentration is dependent upon the ability of the solvent to absorb either  $\text{SO}_3$  or  $\text{H}_2\text{SO}_4$ .

It is suspected that the increase in residual aerosol-formation properties of the solvent is a result of increased ammonia in the solvent due to solvent degradation. Ammonia has varying degrees of solubility in amines and can produce ammonium carbonate aerosol. The SDR reported very large quantities of aerosol during ammonia absorption experiments. It is plausible that the large residual aerosol observed for MEA is an ammonium salt produced from the gas-phase reactions of the ammonia formed during solvent degradation. It is possible that the much lower aerosol concentration observed for CAL008 are a function of reduced degradation rates and consequently reduced ammonia formation rates. Differences in  $\text{SO}_3$  (or  $\text{H}_2\text{SO}_4$ ) reactivities and ammonia solubility between each solvent may also have potential impacts on the threshold at which aerosol is formed from acid gases and the resultant increase in residual aerosols formed as the solvent ages.

A range of design changes to the SDR absorber were planned to include instruments with multiple fine thermocouples to measure the temperature profile as determined by internal heating and cooling of various stages of the packing in an effort to artificially influence the shape of the temperature profile. Such experiments would have provided very useful information regarding the significance of the temperature bulge to aerosol formation, as well as determining if critical profiles exist that could minimise supersaturation and thus aerosol genesis. However, such designs were not able to be completed during this study.

Solvent type was shown to have a strong impact on the point of onset and the yield of aerosol during  $\text{SO}_3$  addition. Ammonia was shown to have the strongest propensity to produce aerosol, with large quantities of aerosol being formed at all SDR operating conditions. The aerosol problem was so large that monitoring instruments reached maximum concentrations under all operating conditions. Anecdotal information from pilot plant operation at Vales Point using ammonia as the solvent suggested that this aerosol-formation pathway may not be as significant for pilot-scale measurements than for the SDR. This was indicated because large solvent losses were not generally observed during normal operation with ammonia. The difference between SDR and pilot-scale experiments is likely attributable to different absorber designs.

MEA displayed reduced aerosol-formation propensity compared to ammonia, but a larger propensity compared to both CAL008 and alanine. MEA also displayed increased background aerosol as it was exposed to  $\text{SO}_3$ , with this background phenomenon being much less for CAL008 and alanine. It is hypothesised that these differences are due to variation in the chemical composition of the solvent. It appears that the more sophisticated solvent of CAL008 provided reduced aerosol-forming ability. Alanine also showed greatly smaller aerosol-forming-potential compared to other amines.

$\text{NO}$  addition produced negligible aerosol in the experiments using CAL008, ammonia and alanine. These experimental results add some weight to the hypotheses that the chemical properties, and thus composition, of the solvent can play a large role in the amount of aerosol produced by a solvent. It is plausible that  $\text{NO}$  is influencing an equilibrium reaction that suppresses aerosol formation for species such as  $\text{SO}_3$ , i.e.,  $\text{NO}$  drives the removal reaction further to completion. If such a process exists, this may provide the opportunity to design low-aerosol-forming solvents that contain a chemical pathway to reduce aerosol potential. This may need to be in conjunction

with optimal PCC designs to enhance aerosol suppression. To some degree this is currently the case for CAL008, as this solvent has displayed reduced aerosol concentration for comparable experiments with MEA.

In summary, the core findings of this study are:

1.  $\text{SO}_3$  is the primary driver of aerosol genesis in all solvents examined, whether this gas is added directly or formed from oxidation of  $\text{SO}_2$ .
2. While  $\text{SO}_3$  is the primary driver of aerosol genesis,  $\text{SO}_2$  is a strong initiator of aerosols under suitable conditions.
3.  $\text{NO}_2$  has a negligible influence on aerosol genesis in isolation. However, when combined with  $\text{SO}_2$ , large quantities of aerosol are produced via  $\text{SO}_2$  oxidation to  $\text{SO}_3$ . Aerosols are thus formed from  $\text{SO}_3$  directly and from  $\text{NO}_2$  and  $\text{SO}_2$  mixtures or mixtures from all three gases. The process is additive and dependent upon the cumulative concentration of the sulphuric acid produced.
4.  $\text{NO}$  has a negligible influence on aerosol genesis. However, current work suggests that its presence may suppress aerosol to a small degree in the MEA matrix.
5. A number of differences in results between the SDR data and the Vales Point data have been identified, such as differences in background aerosol concentration, the formation of aerosol with  $\text{NO}_2$  and the formation of aerosol with  $\text{NO}$  and  $\text{SO}_2$  at high  $\text{NO}$  concentrations. These require further investigation at large scale and with real flue gas.

## 4. Vales Point post-combustion capture pilot plant study: Validation of solvent-degradation rig results

### 4.1 Introduction

As described in Section 2.5, the SDR uses an inlet gas mixture consisting of combinations of the main gaseous components present in the flue gas stream of a typical black-coal-fired electricity generating power station. The use of this surrogate flue gas, as well as the small size of the SDR, provides significant advantages in both experimental flexibility and operational efficiency compared to a larger PCC plant using real flue gas from black coal combustion. In addition, gas compositions that are difficult to prepare using real flue gas can be examined experimentally with the SDR system.

While small-scale experimental equipment has the advantages noted above, the results require comparison and validation to comparable experiments at realistic absorber sizes and with real flue gas.

Delays in commencement of the pilot plant operation resulted in these experiments being commenced at the conclusion of the laboratory experimental program and well after the completion of the small-scale experiments for MEA. Delays were a result of a pilot plant equipment failures, power station shutdowns and combinations of these. These delays impeded the completion of the scheduled program, resulting in the following.

1. Pilot plant experiments, that were initially scheduled to coincide with corresponding small-scale SDR experiments, were instead completed at the conclusion of small-scale experiments. The coincidental scheduling would have enabled repeat small-scale SDR experiments as necessary, for the case where the pilot plant showed differing data to the small-scale SDR.
2. No time was available to make modifications or improvements to the experimental program or to make changes to the apparatus to overcome initial design limitations. Consequently, this meant that the experiments had to be completed with the inclusion of any design flaws to the apparatus. The originally conceived pilot plant campaign was of a longer duration and allowed sufficient time for experimental improvements to be completed, and limitations associated with pilot plant systems to be overcome or re-engineered as necessary.
3. Insufficient time was available to explore different pilot plant conditions. The operational window allowed only limited experiments to be completed at a single operational condition. Thus, the additionally planned experiments, such as investigating the impact of the absorber packing heat exchanger upon aerosol genesis and growth, and operation at different temperatures, could not be undertaken.

Delays in establishment of pilot plant operation resulted in pilot plant trials, including installation and shakedown testing of apparatus, being compressed into a very narrow time period, which incidentally included a further unplanned power station shutdown and the 2018–19 Christmas break. Consequently, the results that are shown in this section are the best obtainable from the prevailing operational limitations.

Pilot plant experiments were completed at the Vales Point PCC pilot plant (owned by Delta Electricity) using real flue gas. A black-coal-fired electricity generator ('unit 5' – 660 MW) that included a 'pulse jet' style fabric particle filter provides flue gas for the PCC plant. The PCC plant sub-samples the flue gas after the fabric filter unit. The PCC plant operates in a closed loop with the sampled flue gas re-entrained back into the power station flue gas stream at a distance of several metres downstream of the inlet position and before the inlet to the exhaust stack.

The PCC process conditions selected for this study were chosen to be representative of an efficiently operating MEA PCC capture plant, and these are detailed in Section 4.2.4 .

## 4.2 Equipment and modification to the post-combustion capture pilot plant

The pilot-scale program involved introducing target gas combinations of NO, NO<sub>2</sub>, SO<sub>2</sub> and SO<sub>3</sub> into the flue gas stream before the absorbers, while concurrently monitoring for changes in aerosol concentration and size. To undertake these experiments, sampling ports for both extractive and non-extractive instruments were required to be installed into the inlet and outlet of the absorber.

### 4.2.1 Installation of sampling ports

Extractive and non-extractive sampling ports, compliant to AS 4323.1<sup>2</sup>, were installed into the inlet and outlet flue gas pipe from the absorber. Figure 22 shows both the inlet and outlet flue gas pipes prior to these changes, while Figure 23 provides a schematic view of the PCC plant, including locations of the sampling ports and the location of the target gas introduction port. These sampling ports were installed into a straight section of pipe without obstructions or bends for eight pipe diameters upstream and two pipe diameters downstream of the sampling location. The non-extractive ports were designed to house the LDA and included smooth internal surfaces and features so that the flow of flue gas through the port was unperturbed. Consequently, the LDA sampling port could be located upstream of the respective extractive ports. Extractive sampling ports were designed to allow extractive sampling instruments, such as the APS and other extractive instruments, to concurrently sample the gas stream monitored by the LDA. However, due to the problems associated with these instruments in the MEA system and outlined in the previous sections, these instruments were not operated during this study.

---

<sup>2</sup> AS 4323.1 - Stationary source emissions Selection of sampling positions. Method 1: Selection of sampling positions. 1995 (R2014). Standards Australia

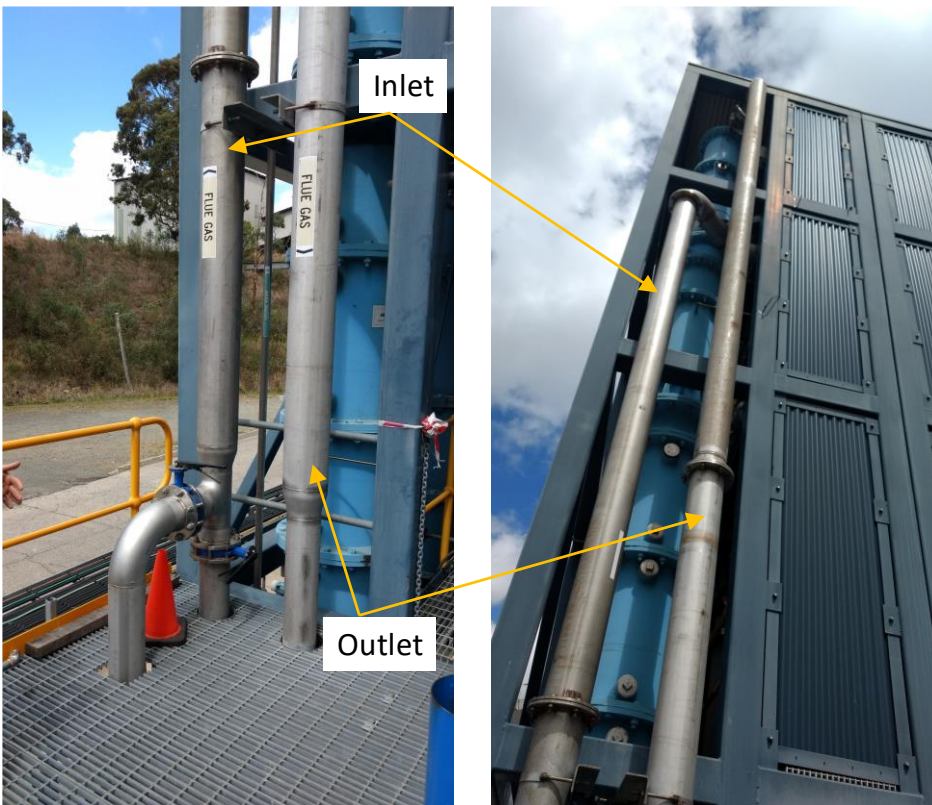


Figure 22 Absorber inlet and outlet flue gas pipes

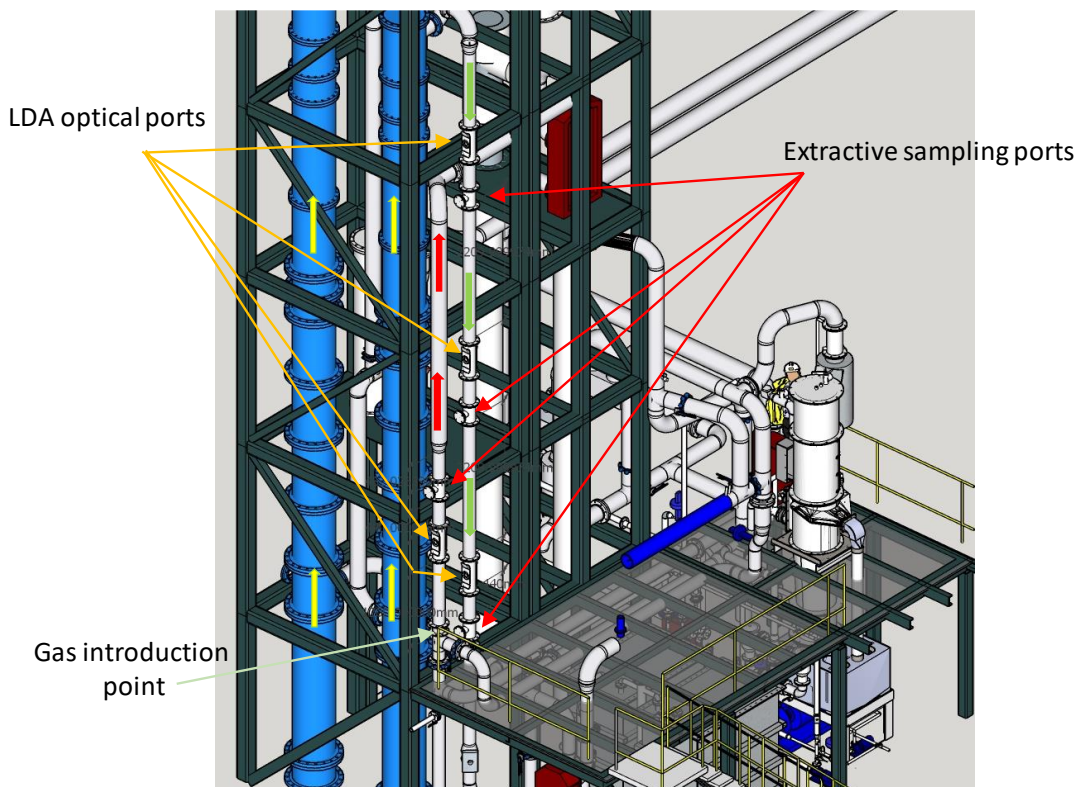


Figure 23 Schematic diagram of sampling ports and locations

The red arrows in Figure 23 show the direction of inlet gas to the absorber, while the green arrows show the direction of outlet gas from the absorber. The yellow arrow shows the direction of gas flow through the absorber.

For correct LDA operation, two opposing optical windows must be precisely maintained at a separation of 150 mm. The LDA manufacturer provides a robust holder assembly to maintain this distance, with this assembly shown in Figure 24. The non-extractive sampling ports were designed to accommodate the LDA manufacturer's assembly as well as maintain a smooth laminar flow of gas through the sampling port. The design utilised a round pipe section (Figure 24, part number 4) into which was welded a recessed steel plate to support the LDA housings and optical windows (Figure 24, part number 2). Gas sealing was achieved by way of a captured O-ring (Figure 24, part number 3). The sampling port includes smooth plates connecting the pipe to the leading and trailing surfaces of LDA support plate with the recessed O-ring and facilitates a smooth gas transition from the cylindrical pipe to the flat optical window surfaces of the LDA. During installation, the housing of the LDA that supports each optical window is clamped against the recessed O-ring to provide a gas-tight seal. When mounted, the protruding surface of the LDA housing/optical window extends through the port aperture to be essentially flush with the internal surface within the sampling port. All internal fabrication welds were ground smooth to minimise surface imperfections to abate gas turbulence within the flue pipe. The design is shown in the form of an exploded view in Figure 24.

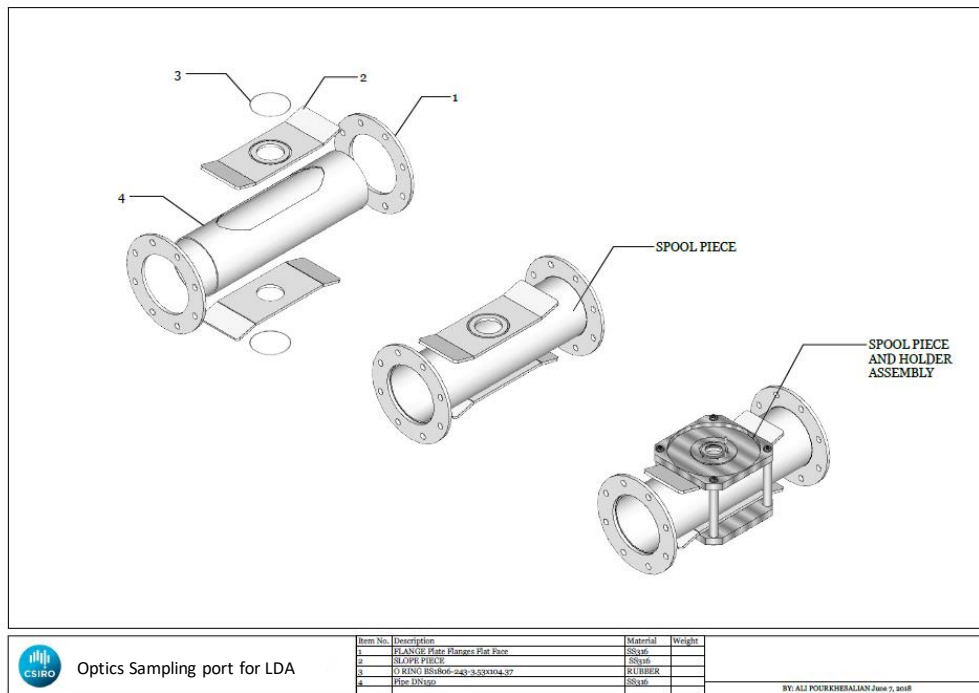


Figure 24 Optics sampling port section for the laser diffraction analyser

The location of the sampling ports during installation is shown in Figure 25.

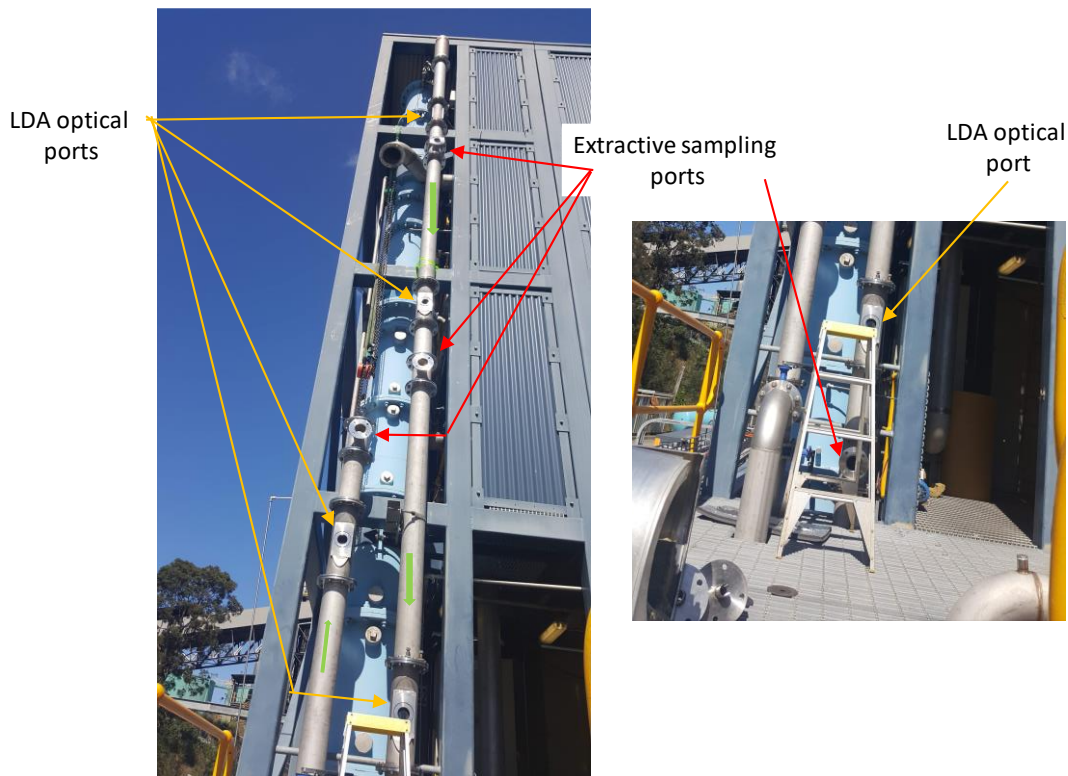


Figure 25 Aerosol sampling ports being installed

#### 4.2.2 Initial experimental plan overview

The initial Vales Point PCC pilot plant experimental plan consisted of an extensive series of experiments to be completed using both the normal pilot plant configuration/operation and a separate series of experiments using non-standard pilot plant operation and delivering the flue gas directly to the absorber and bypassing all acid gas controls. It should be noted that the term ‘real’ flue gas has two definitions. For this work, real flue gas, as opposed to the surrogate flue gas used in the SDR, is a gas derived from coal combustion and included all of the contaminants, such as ultrafine particles, etc., that cannot be replicated in the surrogate gas. For a PCC plant, normal operation using real flue gas is defined as normal operation using all gas precleaning processes but sourcing the gas from the coal-fired power station. In this case the pilot plant is still operating using real flue gas. Non-standard PCC operation involves bypassing gas precleaning processes so that the solvent is exposed directly to the flue gas. This is defined as non-standard operation of the PCC plant using real flue gas. In both cases the pilot plant is operating on real flue gas.

The initial plan consisted of the following parts:

1. Experiments completed using standard pilot plant configuration.

Normal pilot plant operation includes a FPT system to remove acid gases. The inclusion of this process was highly recommended by engineering personnel as MEA ageing significantly increases without this process. Operation without FPT had also not been previously tested with this solvent. Thus, the impact upon pilot plant systems, such as pumps and blowers, etc., was unknown. Consequently, it was recommended that experiments with FPT be completed initially, with those experiments without the use of FPT completed later and as the final experimental component of the program.

It was expected that operating with FPT would provide a low acid gas background concentration and allow the dosing of the cleaned flue gases to occur from lower gas concentrations. This configuration would also provide a lower background particle concentration and be reflective of coal-fired power stations equipped with desulphurisation technologies.

Operation of the pilot plant without FPT provided a higher acid gas background and would require higher dosing rates of target gases. This configuration would also include higher particle concentrations and conversely be reflective of current Australian coal-fired power stations not equipped with desulphurisation technologies. However, as previously noted, such a configuration would age the solvent at an increased rate and thus these experiments were to commence after the experiments using the FPT were completed. The initially planned program consisted of the following:

- a. Define target plant operational conditions for the study. Since MEA had not been previously used as a solvent at the Vales Point PCC pilot plant, it was essential to determine those conditions that would allow the plant to operate reproducibly and at constant operating conditions over the duration of the program. Solvent viscosity, thermodynamic and CO<sub>2</sub> performance as well as maintaining constant solvent composition and constant water-wash efficiency, etc., were assessed during this initial operational period.
  - b. Install and test the aerosol monitoring equipment and gas dosing system.
  - c. Measure background aerosol during target operational conditions.
  - d. Assess aerosol concentrations when PCC absorber is enriched with combinations of NO, NO<sub>2</sub>, SO<sub>2</sub> and SO<sub>3</sub>.
2. Experiments completed using non-standard pilot plant operation.

#### *Absorber heat exchanger*

The absorber included a heat exchanger that allowed some control over the temperature profile of the packing. It was planned to undertake experiments like those of Step 1d, but with the heat exchanger operating. The aim of these experiments was to assess the impact of reducing the size of the normally observed temperature rise within the absorber packing due to CO<sub>2</sub> uptake. The initial experimental plan consisted of the following steps:

- a. Re-commission the heat exchanger system installed within the absorber. This system had not been operated for an extended period and required a period for recommissioning and testing during MEA operation. This heat exchanger cooled the absorber packing, reducing the temperature rise of the packing during normal operation.
- b. Measure background aerosol during target operational conditions.
- c. Assess aerosol concentrations when the PCC absorber is enriched with combinations of NO, NO<sub>2</sub>, SO<sub>2</sub> and SO<sub>3</sub>.

#### *Bypass of the flue gas pre-treatment process*

The planned program consisted of the following:

- a. Define suitable target plant operational conditions that will allow continuous plant operation with the FPT off.
- b. Measure background aerosol during target operational conditions.
- c. Assess aerosol concentrations when PCC absorber is enriched with combinations of NO, NO<sub>2</sub>, SO<sub>2</sub> and SO<sub>3</sub>.

### 4.2.3 Revised experimental plan overview

As noted in Section 4.1, pilot plant operational delays and power station shutdowns necessitated a severely revised experimental program. Consequently, it was clear that insufficient time was available to complete all stages described previously. Experiments from Stage 2 additionally required re-configuration of the inlet to the pilot plant, and again insufficient time was available to undertake plant re-configuration, test pilot plant operation and complete the experiment series. SDR experiments were all completed using a surrogate flue gas with low contaminant concentrations, such as particles. A further consideration to the program was the availability of MEA. All SDR experiments were completed on relatively new MEA with the supply regularly replaced. It seemed logical to complete experiments that required relatively new MEA first, and those experiments that would age the solvent quickly after these. Several aerosol artefacts were also identified during SDR experiments that indicated that it was highly advisable that experiments using normal PCC operation (and that are more representative of the SDR experiments) be completed before the non-standard experiments. Consequently, the available experimental time only allowed a limited number of experiments from step Stage 1 (normal operation) to be undertaken. While this would impinge on the depth of experiment delivered, all experiments would be undertaken on real flue gas. Thus, due to the severe time restriction, all experiments in this section were completed using the FPT.

During the experimental period, additional power station outages arose due to issues that were outside of the control of CSIRO personnel. This further reduced the availability of the PCC facility to operate using flue gas from the power station. This delay occurred towards the end of the allocated experimental time period where there was great urgency to change the solvent to ammonia for competing projects. Consequently, rather than undertaking no experiments at all over this period, experiments using ambient air only were undertaken as an alternative. While this was not considered an ideal situation, it was the only scenario possible for completing the experiment program within the allotted time period. Without CO<sub>2</sub>, it was expected that little solvent heating due to CO<sub>2</sub> uptake would occur over the length of the absorber. These data would provide a baseline measure of aerosol formation under more isothermal absorber conditions and in the absence of the temperature rise that normally occurs over the length of the absorber. Consequently, such data would provide a measure of aerosol under reduced temperature and humidity conditions, and could be considered a compromise for obtaining a measure of aerosol penetration without the strong heating profile normally present along the absorber.

The operational requirement to recommence PCC operation with ammonia solvent at the end of January precluded experiments for this current work after January 2018. Overall, the numerous compounding operational limitations resulted in most experiments targeting primarily SO<sub>3</sub> aerosol formation.

While SO<sub>2</sub> is readily available in Australia from cylinders and the target gases NO<sub>2</sub> and SO<sub>3</sub> could be manufactured onsite from readily available precursors, this is not the case for NO. NO was only available in extremely limited quantities through the directly import of small quantities from China. Consequently, experiments using NO were the most limited in both number and duration. Exhaustion of available NO supplies prior to the completion of individual NO experiments necessitated abandoning individual NO experiments.

The nominated or 'normal' plant-operating conditions were used for all the runs within this campaign, except for those where the use ambient air was unavoidable due to the unavailability of flue gas. Details of normal operating conditions are given in Section 4.2.4.

#### **4.2.4 Summary of process operation details**

##### **Flue gas pre-treatment**

Since amine solvent degradation is a significant cost to PCC operation, to minimise solvent degradation from acid gases in the Vales Point PCC pilot plant, the flue gas entering the absorber normally passes firstly through the FPT system. The power station exhaust stack typically runs a small negative pressure from thermal buoyancy of the hot flue gas. Flue gas inlet temperature from the stack to the FPT is 91°C to 97°C when at stable steady-state conditions. The process contains water dosed with 30% NaOH solution to maintain a stable pH of 7.5 ( $\pm 0.1$ ). The target gas species for removal are SO<sub>x</sub> and NO<sub>x</sub>. Dust and particulates are also removed during the FPT process during the cooling of the flue gas prior to the absorbers. The process uses a liquid circulation rate of 27 L/min with typical liquid temperatures of 44°C at the base of the column and 30°C at the top of column. The FPT system is cooled using plant recirculated cooling water from the plant cooling tower. The system provides >99% capture of SO<sub>x</sub> with negligible CO<sub>2</sub> co-capture. This is measured using differential GASMET SO<sub>x</sub> results before/after the FPT. Other acid gas species are not measured with this gas analyser.

##### **Absorber**

The CO<sub>2</sub> absorbers were operated with a lean solvent return temperature of 40°C  $\pm$  3°C for the first absorber. Steady-state operation yielded absorber temperature peaks of 55°C in the mid-section of the absorbers packing providing a  $\sim$ 15°C cooling of the solvent in the final section of the absorber. Flue gas temperature out of Absorber 2 after the wash section was stable at 23°C. A pressure drop of 1 to 2 kPa was generally observed over the packed section of each of the two absorber units. The solvent temperatures are normally 134°C for the lean hot solvent, 54°C for the lean cool solvent, 44°C for the rich cool solvents and 114°C for the rich hot solvent. The locations of these temperatures are defined in Figure 1.

Flue gas mass flowrate is set to 600 kg/hr  $\pm$ 4% by the air blower, which is operated at fixed speed and manually adjusted to give the target flowrate. The treated flue gas from the FPT enters the gas blower with a pressure of -2.4 kPa at 35°C and leaves at a pressure of 5.5 kPa at 40°C.

Absorbent pumps circulate the lean solvent at a rate of 60 L/min  $\pm$ 1% with the solvent composition or lean/rich ratio = 4.9. This equates to a molar target for [MEA] of  $\sim$ 30wt% MEA. Liquid solvent samples of both rich and lean solvent were taken and analysed regularly during the operation to maintain solvent composition. The CO<sub>2</sub> capture rate is 127 kg/hr CO<sub>2</sub>.

## Stripper section

The stripper was operated by varying steam supply flowrate to achieve 90% capture at a stripper pressure of between 250 and 300 kPa. To achieve this capture efficiency a reboiler steam pressure of  $\sim 325$  kPa  $\pm 30$  kPa was required. The normal stripper solvent temperatures during operation range from  $\sim 134^\circ\text{C}$  at the base up to  $\sim 120^\circ\text{C}$  at the middle section, with  $113^\circ\text{C}$  being observed at the top section while operating at steady-state.  $\text{CO}_2$ -capture efficiency is calculated from GASMET gas-analyser data and confirmed by the magnitude of the product  $\text{CO}_2$  mass flowrate. A  $\text{CO}_2$  concentration drop from 11 to 13 vol/vol% inlet to 0.9 to 1.4 vol/vol% was achieved, delivering 90% process capture  $\pm 5\%$  at steady-state, providing a  $\text{CO}_2$  purity during steady operation of  $> 99\%$ , as confirmed by the GASMET analyser normally installed at this pilot plant.

## Water-wash section

The final water-wash system after the absorber is recirculated at a rate 12 L/min and cooled to a temperature of  $11^\circ\text{C}$ . MEA vapour and other volatile and water-soluble species accumulate in this liquor over time. Since operation time for the experimental program was short, contaminant accumulation would have been small.

### 4.2.5 Supply of target gases and gas introduction to the absorber inlet

The target gases  $\text{NO}$  and  $\text{SO}_2$  were manually metered by a flow rotameter as pure gases through a stainless-steel line directly into the pilot plant inlet gas stream.  $\text{SO}_2$  and  $\text{NO}$  gas was supplied in cylinders. Due to the limited supply of  $\text{NO}$ , only limited  $\text{NO}$  experiments were possible.

$\text{NO}_2$  and  $\text{SO}_3$  were unable to be sourced in Australia in the quantities required for these experiments, and thus these gases were prepared onsite on an as-needed basis.  $\text{NO}_2$  was prepared by thermal decomposition of concentrated nitric acid ( $\text{HNO}_3$ ) within a specially designed reactor. The heated  $\text{NO}_2$  gas mixture, comprised of  $\text{NO}_2$  and steam, was metered directly into the flue gas.  $\text{SO}_3$  was prepared by catalytic thermal oxidation of  $\text{SO}_2$  in the presence of air.  $\text{SO}_3$  gas was also metered directly into the inlet flue gas.

## Gas concentrations

Gas concentration of each target species in the absorber inlet flue gas was calculated according to the flow rate of the target gas entering the inlet the absorber and the mass flow rate of the flue gas at the time of the experiment. Both the thermal dissociation of  $\text{HNO}_3$  and the catalytic oxidation of  $\text{SO}_2$  were assumed to have a 100% conversion efficiency. This assumption was based on initial conversion efficiency measurements undertaken during the initial  $\text{SO}_2/\text{SO}_3$  experiments undertaken using the SDR and while using the ProCeas™  $\text{SO}_2/\text{SO}_3$  analyser (Appendix A). Complete conversion to  $\text{SO}_3$  was observed using this instrument.

### 4.2.6 Instruments

As noted in Appendix A, the MEA environment proved to be a most challenging environment for long-term operation of scientific instruments. At the time of these experiments the APS, EEPs and the  $\text{SO}_2/\text{SO}_3$  analyser were being repaired at their respective manufacturers. In addition, delivery of the alternative multi-gas analyser for  $\text{SO}_2$  was delayed due to manufacturer supply problems.

Due to these instrumental issues and the urgency to finalise this study, the only option for continuation of the experimental program was to complete experiments using the LDA only. As no alternative instruments were available at the time of this campaign, the data presented using LDA data only are the best achieved under the challenging conditions.

Without the SO<sub>2</sub> and SO<sub>3</sub> monitoring instruments, concentrations could only be estimated through calibration of MFCs and correct mixing and without external calibration. The absence of this instrument had a moderate impact on the program, and a significant impact on independent validation of SO<sub>x</sub> concentrations.

## 4.3 Results

Excluding the initial system test experiments undertaken to test the operation of apparatus and instruments, a total of 40 experiments were undertaken at Vales Point PCC pilot plant over December 2018 and January 2019.

### 4.3.1 Background measurements

LDA laser transmission was monitored just prior to the commencement of plant operations. The dataset show transmission values corresponding to essentially 100% laser transmission, indicating that very little laser power is lost through light diffraction. This indicated very small numbers of residual suspended particles present in the stationary environment at the outlet of the absorber. This was surprising, because it was expected that some fly ash particles and some background aerosol would be present in the gas stream and indicate the pre-treatment process is effective in removing acid gases and particles. This also suggests that the temperature rise that normally is produced within the absorber due to the CO<sub>2</sub> removal process has little potential to form aerosol under these operational conditions.

Figure 26 displays the average aerosol size distribution on a number basis from the background measurement (100% laser transmission). These data are presented on a particles per metre basis respective to the path length of the laser and reported as equivalent Stokes particles. These results show very low aerosol concentrations.

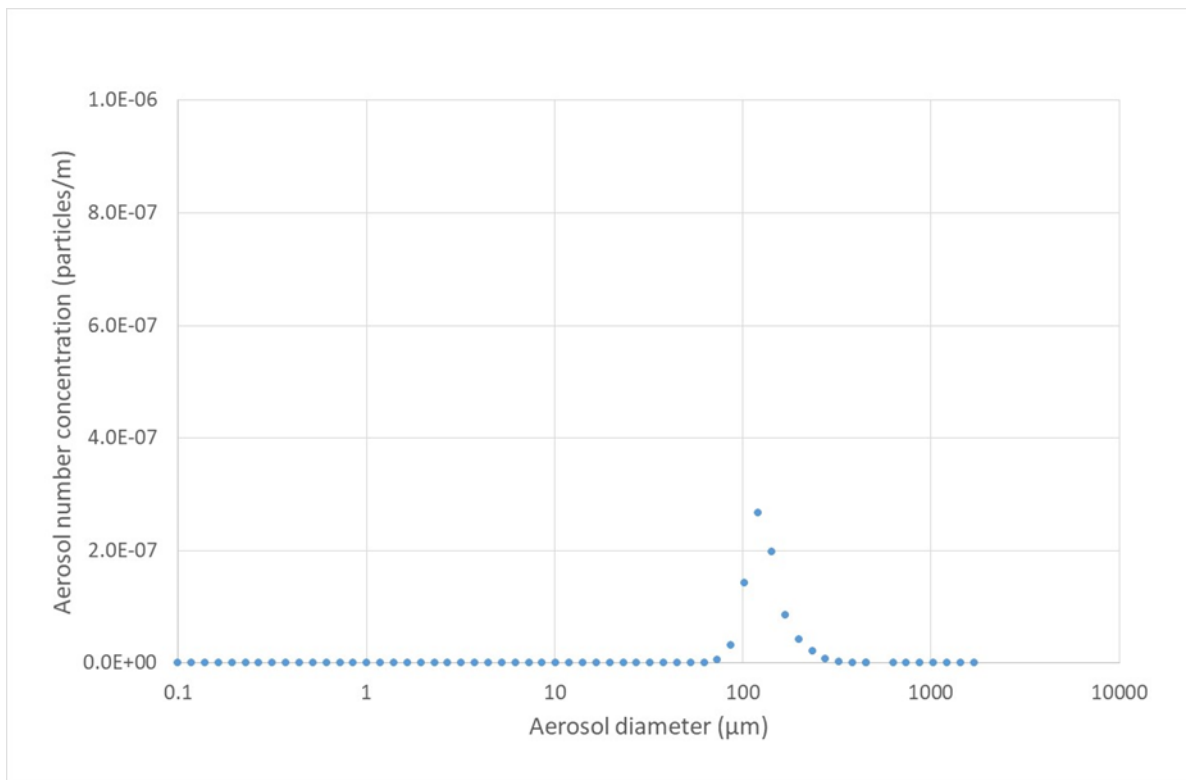


Figure 26 Laser diffraction analyser average aerosol background particle distribution

Figure 26 shows a negligible number of coarse aerosol particles with diameters <100 µm. It is expected that these coarse aerosols are likely a result of liquid effusing from the surfaces of the absorber or surfaces after the absorber. However, these large aerosols can be considered relatively unimportant, as they are small in number and will settle in pipes and ducts or be captured by demister sections due to their larger size. This will especially occur in flow areas with reduced gas velocities. The LDA is also operating with the extremely low numbers of particles and there is a very large uncertainty associated with these data. This would also be the case for other scientific instrument, e.g. the APS, EEPS and electrical low-pressure impactor, which have about 1 to 2 orders of sensitivity less than the LDA depending upon the instrument, particle type and particle size. Other instruments, such as optical particle counters, have significantly reduced sensitivity and would not detect such small particle numbers. It should be noted that the LDA is measuring particles size selectively and not as a total ensemble.

Overall background measurements revealed remarkably little aerosol present in the outlet of the absorber during normal operation. These data suggest that the FPT was highly efficient in removing SO<sub>3</sub> as well as residual suspended fly ash.

### 4.3.2 SO<sub>2</sub> measurements

LDA laser transmission data for SO<sub>2</sub> gas injection into the absorber at a concentration of 60 ppm and for three repeat experiments is shown in Figure 27. This value was selected as a relatively low concentration relative to normal SO<sub>2</sub> stack emissions released from NSW coal-fired power stations. The normal concentration range of SO<sub>2</sub> emissions from NSW coal-fired power stations is generally in the order of 50 to 300 ppm. For this relatively small SO<sub>2</sub> concentration data, little or

no change in transmission was observed following SO<sub>2</sub> addition. A maximum standard deviation of 0.65 was observed for these data.

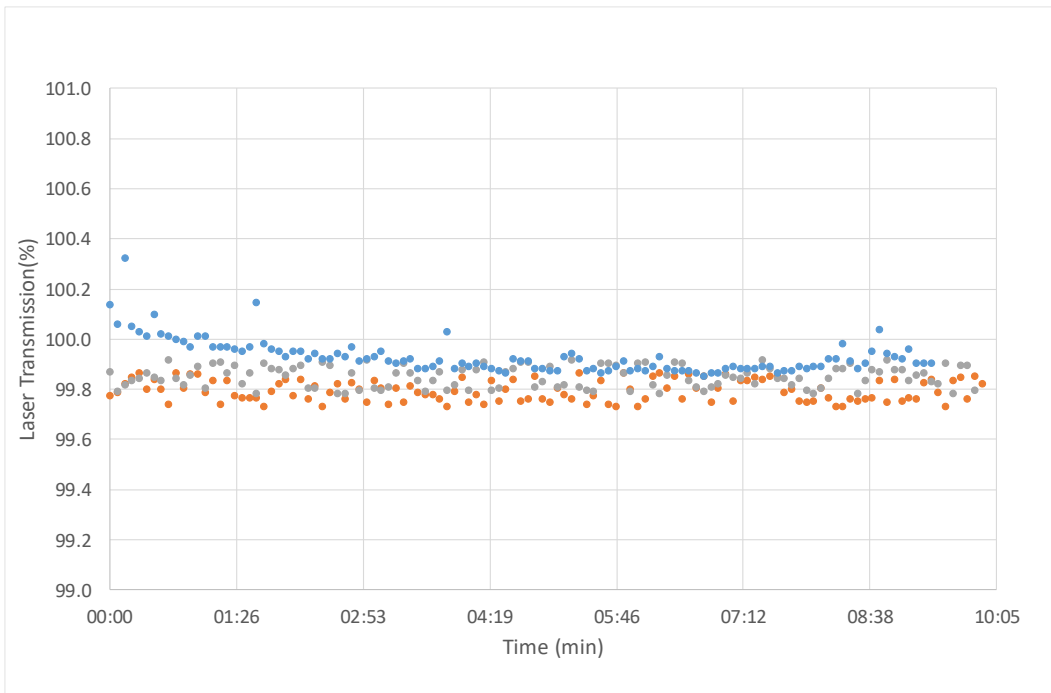


Figure 27 Laser diffraction analyser transmission – 60 ppm SO<sub>2</sub> in flue gas

The corresponding aerosol number concentration is shown in Figure 28, where a small number of ultrafine particles with diameter less than 0.3 μm can be observed.

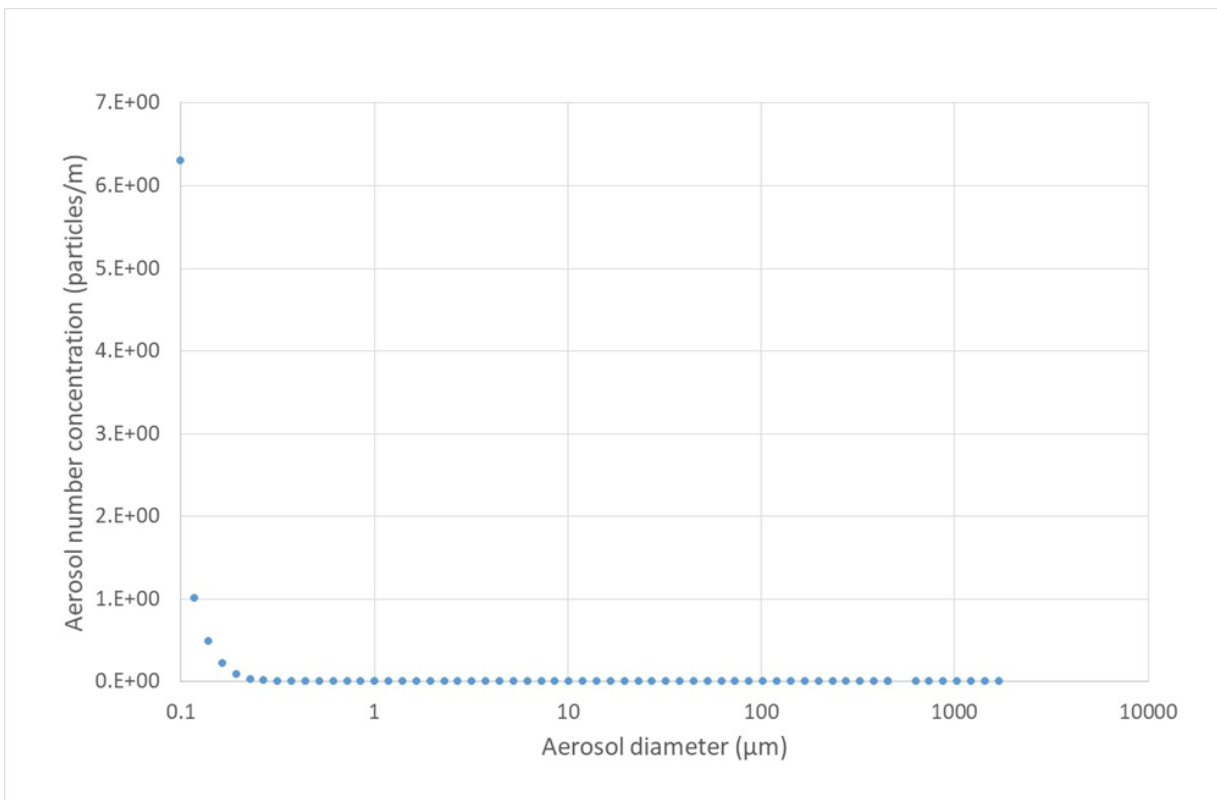


Figure 28 Laser diffraction analyser aerosol distribution – 60 ppm SO<sub>2</sub> in flue gas

Since very small aerosol numbers were observed in Figure 27, the SO<sub>2</sub> dosing was increased to a relatively large value of 1200 ppm in the gas stream. This value is in the order of three or four times greater than the typical range of SO<sub>2</sub> concentrations leaving the Vales Point Power Station and was not selected to coincide with power station SO<sub>2</sub> concentrations. This value was selected as an upper bound value for assessing the small SO<sub>2</sub> derived aerosol. These data are shown in shown in Figure 29 with two experiments displayed. These data exhibit laser transmission vales of ~100%, indicating the presence of little aerosol. This result was also quite unexpected and tends to conflict with the SDR results. However, the instruments gave no evidence of malfunction or errors and thus it is expected that these data are valid. Due to the delays in commencing this pilot plant work, insufficient time was available to undertake follow-up work to investigate this difference in results. This aspect requires further validation and confirmation.

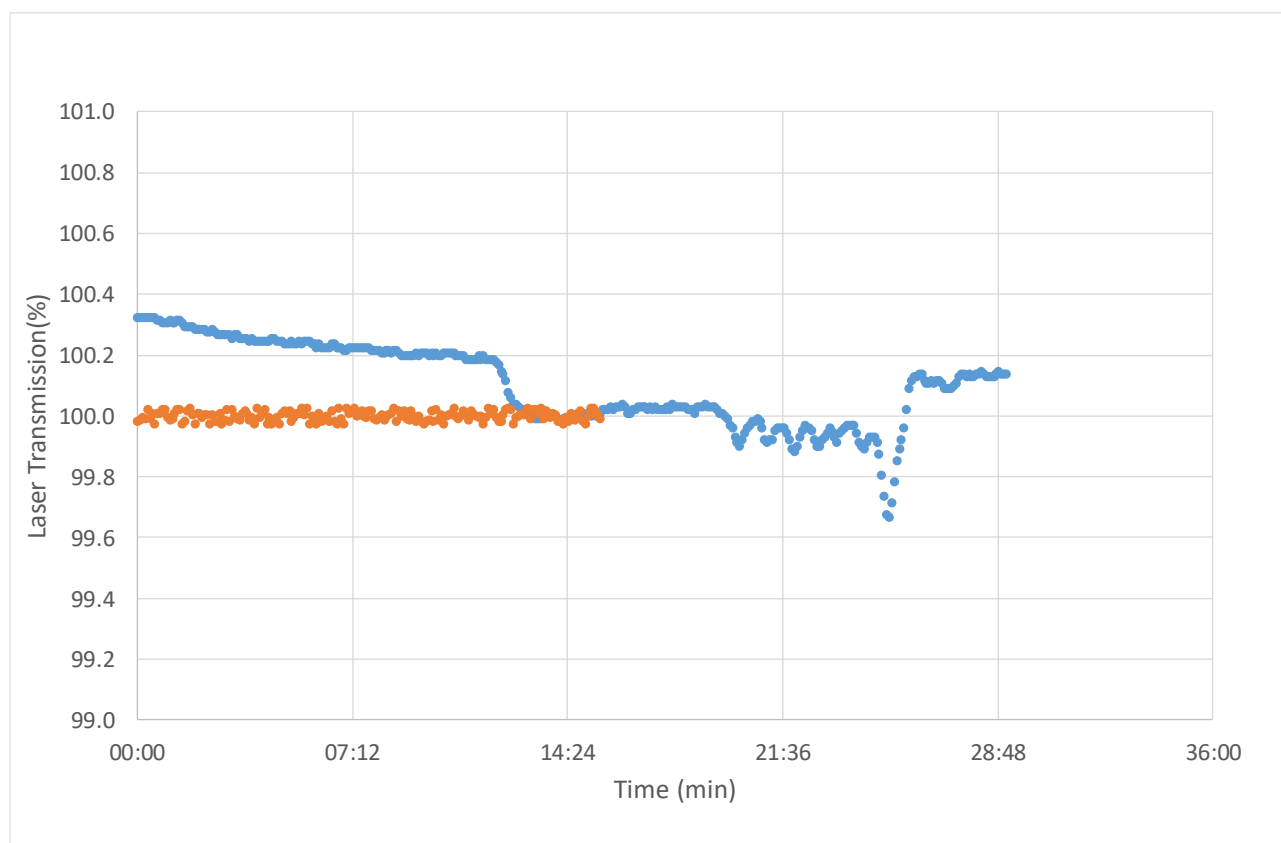


Figure 29 Laser diffraction analyser transmission – 1200 ppm SO<sub>2</sub> in flue gas

### 4.3.3 SO<sub>3</sub> measurements

For the SO<sub>3</sub> formation reaction to proceed, the oxidation catalyst required oxygen. Thus, dry air, at a rate that provides an overall molar excess of oxygen, was added to the SO<sub>2</sub> gas stream. Consequently, the resultant dry gas stream contained dry SO<sub>3</sub> contained in a carrier gas stream primarily composed of dry nitrogen, and a small percentage of oxygen and argon. The small excess in oxygen was necessary to provide complete conversion of the SO<sub>2</sub>. Consequently, SO<sub>3</sub> was added to the absorber within a carrier gas of oxygen-reduced air to produce a concentration of 1200 ppm at the absorber inlet. While several times the concentration of that expected for the Vales Point flue gas, this concentration was used as a high upper bound. The results of this addition are shown in Figure 30. Notice here that the LDA transmission rapidly reduces to zero as the laser is attenuated by the very rapid onset of the high concentration of aerosols.

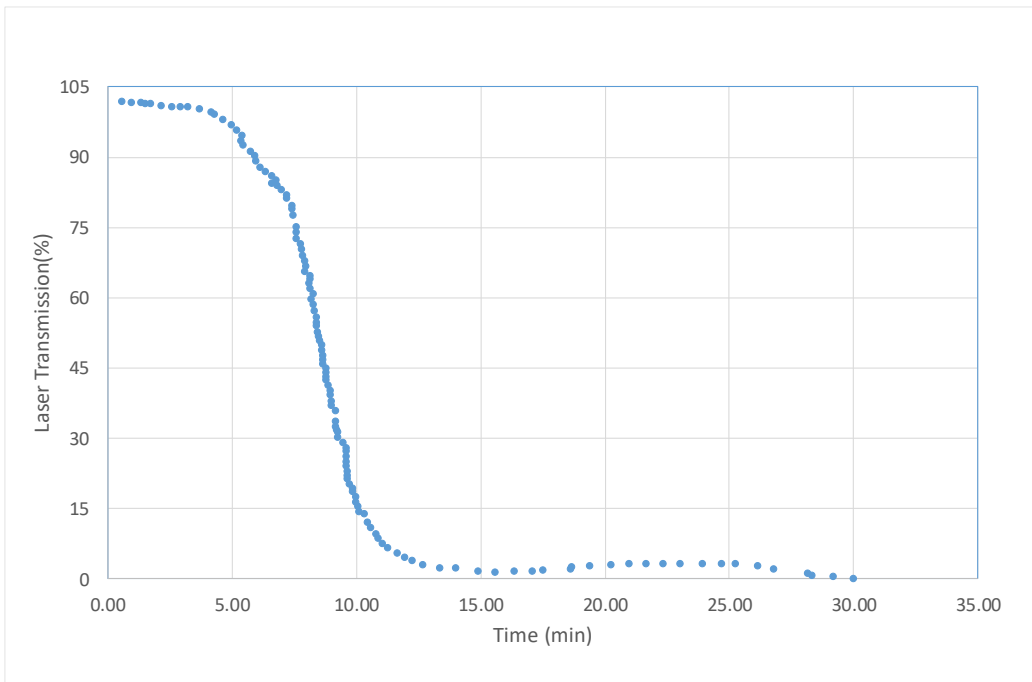


Figure 30 Laser diffraction analyser transmission – 1200 ppm SO<sub>3</sub> in flue gas

The particle size distribution as the laser approaches the limit of transmission in Figure 30 is shown in Figure 31. Following the small aerosol numbers observed in Section 4.3.2 for SO<sub>2</sub>, a relatively high concentration was initially selected for the first SO<sub>3</sub> experiments. As it is expected that SO<sub>3</sub> would provide a strong aerosol-forming environments, this experiment would additionally verify operation for the LDA.

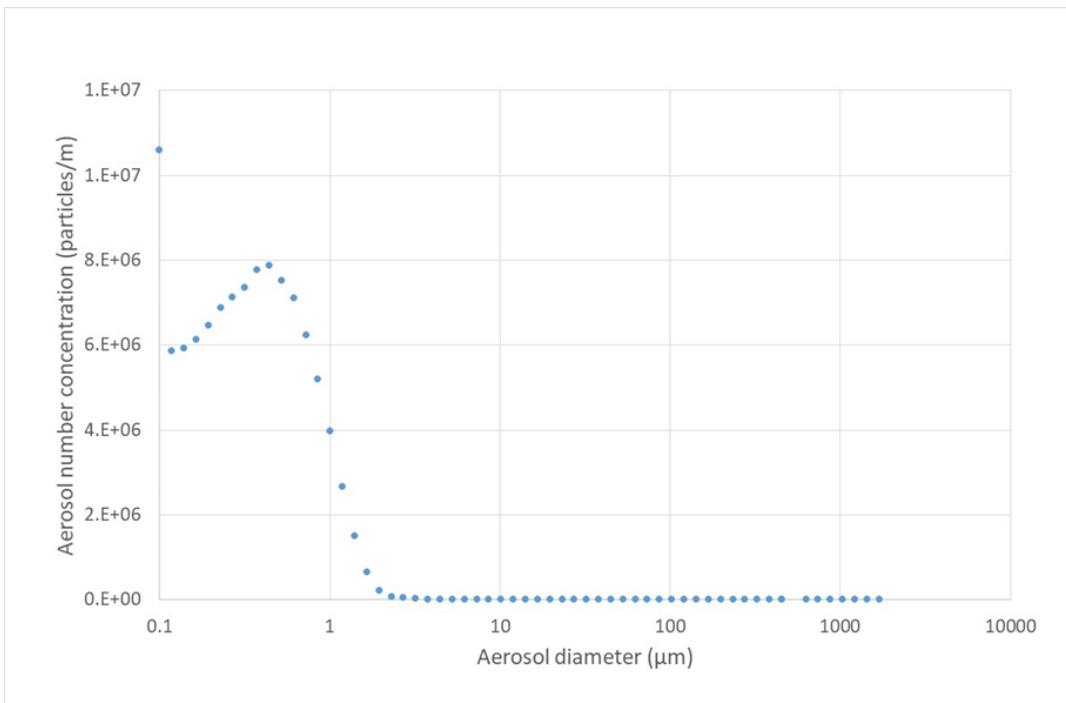


Figure 31 Laser diffraction analyser aerosol distribution – 1200 ppm SO<sub>3</sub> in flue gas

Figure 31 reveals very large numbers of aerosols with a mode centring at ~0.4 µm. At these relatively high aerosol concentrations, the reported data includes increased uncertainty due to low laser transmission. Uncertainties associated with low laser transmission values have not been

investigated prior to this study, as it is preferential to operate the instrument within the normal laser operating range. However, even with these uncertainties, these data clearly confirm that the presence of  $\text{SO}_3$  in MEA flue gas produces large quantities of fine aerosol, with this aerosol penetrating through both the absorber and water-wash systems. Notice that the bin at the lower particle size range of  $0.1 \mu\text{m}$  displays a significantly greater concentration than those data at  $\sim 0.4 \mu\text{m}$ . Particles at this size range have wide diffraction angles and this value may indicate the existence of much finer aerosol fraction.

During this experiment, an extraction port, which allows access to the flue gas after it exits the water wash but before returning to the power station stack, was opened to allow observation of the flue gas. The flue gas pressure is greater than 1 atm at this location and thus the flue gas flows freely from the port. Figure 32 shows an image of the aerosol plume venting from the access port. A black background has been placed behind the aerosol to intensify the image of the aerosol produced. This test was a short-term demonstration completed under controlled conditions for demonstration/recording purposes. Appropriate personal protective equipment was used during this demonstration.

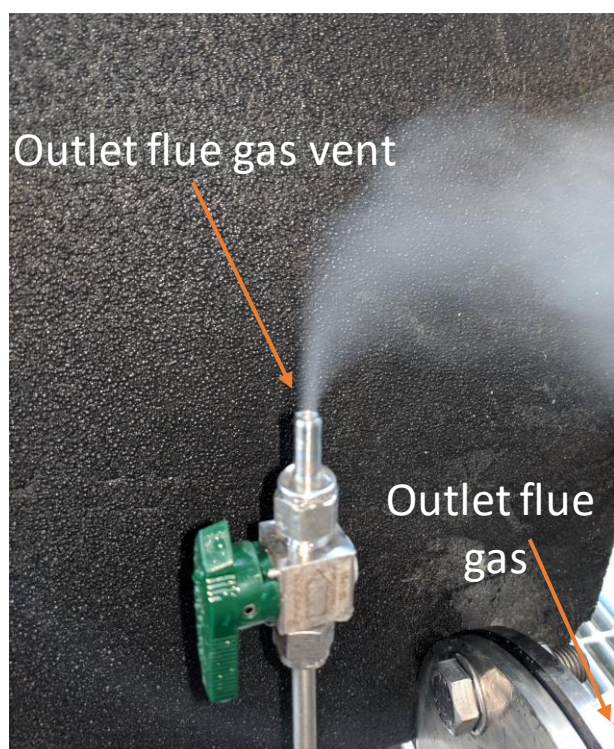


Figure 32 Flue gas venting from the outlet of the absorber during  $\text{SO}_3$  experiments

While this experiment was undertaken at a high concentration, these data clearly reveal that both the absorber and the water-wash systems have little efficiency for removing fine  $\text{SO}_3$ -generated aerosol. These  $\text{SO}_3$  data agree with corresponding SDR experiments and show the  $\text{SO}_3$  is a highly effective pathway for aerosol generation with very little removal in the PCC process other than at the FPT.

#### 4.3.4 $\text{NO}_2$ measurements

LDA measurements demonstrated that  $\text{NO}_2$  is an aerosol nucleator in the presence of  $\text{SO}_2$ , with the redox reaction between these two species forming  $\text{SO}_3$ . Consequently, there exists a potential

pathway for residual SO<sub>2</sub> in the flue gas stream after the FPT to form aerosol. During this experiment, the NO<sub>2</sub> concentration in the inlet gas stream to the absorber was increased to a concentration of 160 ppm. This resulted in no change to the laser transmission of the LDA. The NO<sub>2</sub> concentration was subsequently increased to 325 ppm, after which the LDA transmission slowly reduced over approximately 5 minutes to approach a steady value of 75% transmission. The time series after the gas concentration change is shown in Figure 33.

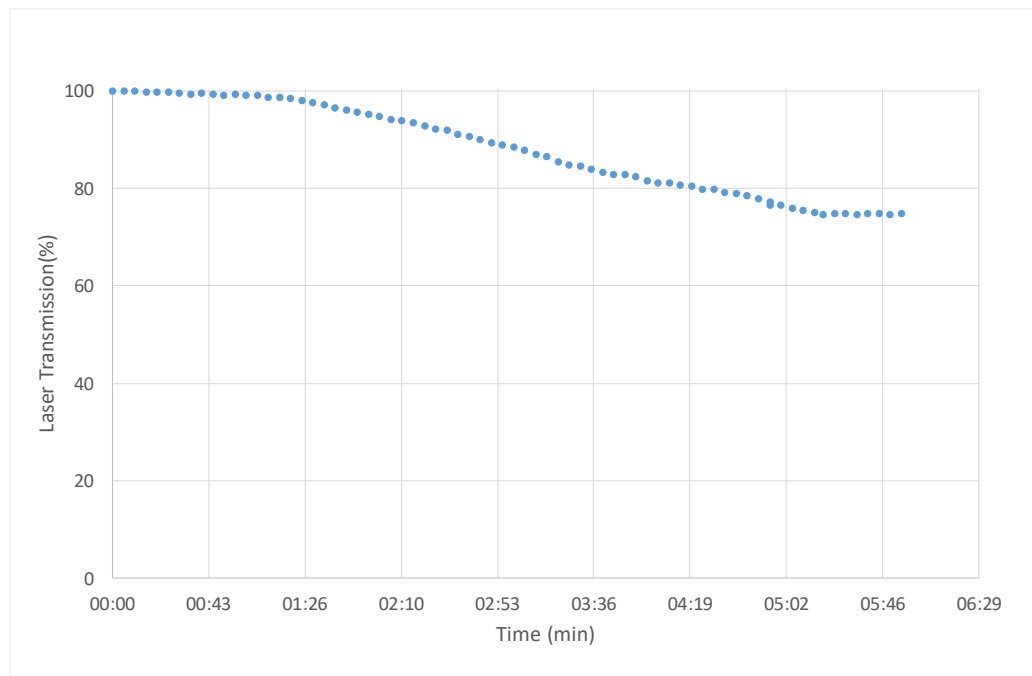


**Figure 33 Laser diffraction analyser transmission with addition of NO<sub>2</sub> to the absorber at a concentration of 325 ppm**

Similar responses were also observed in SDR experiments up to 160 ppm. MEA displayed a similar delayed aerosol increase when exposed to a constant NO<sub>2</sub> atmosphere, as well as a corresponding delayed relaxation to a baseline when the NO<sub>2</sub> flow ceased. This was particularly the case for aged MEA, where the background aerosol concentration varied over the duration of the experiments, as discussed in Section 3.4. This increasing background aerosol was primarily associated with SO<sub>x</sub> and NO<sub>2</sub> and was not observed for NO. A strong hysteresis was also observed between the times taken to reach steady state following exposure to the target gas and termination of the flow. That is, as successive experiments were completed, the rate of recovery to a low aerosol concentration increased to a point where experiments could not be undertaken due to the changing background. The background aerosol concentration appeared to be a function of the acid gas exposure history of solvent, both in concentration and duration, as well as the time not exposed to acid gases. Consequently, to achieve a reproducible background aerosol concentration, regular replacement of the MEA was necessary. This was discussed in Section 3.4. It is likely that the origin of this behaviour is associated with the solubility of SO<sub>x</sub> and NO<sub>2</sub> in MEA. Both acid gases have the potential to form a reversible acid-base reaction with MEA, with the degree of dissolution being dependent upon SO<sub>x</sub> and NO<sub>2</sub> concentrations, similar to CO<sub>2</sub>. It is widely known that acid gases can react irreversibly with MEA to produce heat-stable salt contaminants, such as nitrates and sulphates. Consequently, it is plausible that the acid gas initially forms a reversible equilibrium along the pathway of eventually forming heat-stable salts. It is this initial equilibrium state that produces the observed delayed aerosol response for MEA. This hypothesis also explains why this

problem was not observed for NO. As noted in Section 3.4, experimental time did not allow this phenomenon to be explored further during the SDR program, where experiments at NO<sub>2</sub> concentrations greater than 160 ppm would have provided additional support to the solvent behaviours observed.

Another plausible explanation is that this aerosol is formed as a result of NO<sub>2</sub> forming nitric acid and nucleating aerosol directly. A further possible explanation is that the NO<sub>2</sub> is reacting with residual SO<sub>2</sub> slipping past the pre-treatment absorber to produce SO<sub>3</sub>, and ultimately sulphuric acid mist. It is also possible that the observed behaviour is a combination of these processes or a different phenomenon.

Figure 34 shows the particle distribution at the LDA transmission value of 75% as shown in Figure 33. These data show a generally similar aerosol distribution to those data observed for SO<sub>3</sub> in Figure 31, with a mode in the order of 0.4 μm. While a similar distribution is observed to those SO<sub>3</sub> results discussed in Section 4.3.3, the concentration of aerosol in this current figure is much lower than Figure 31.

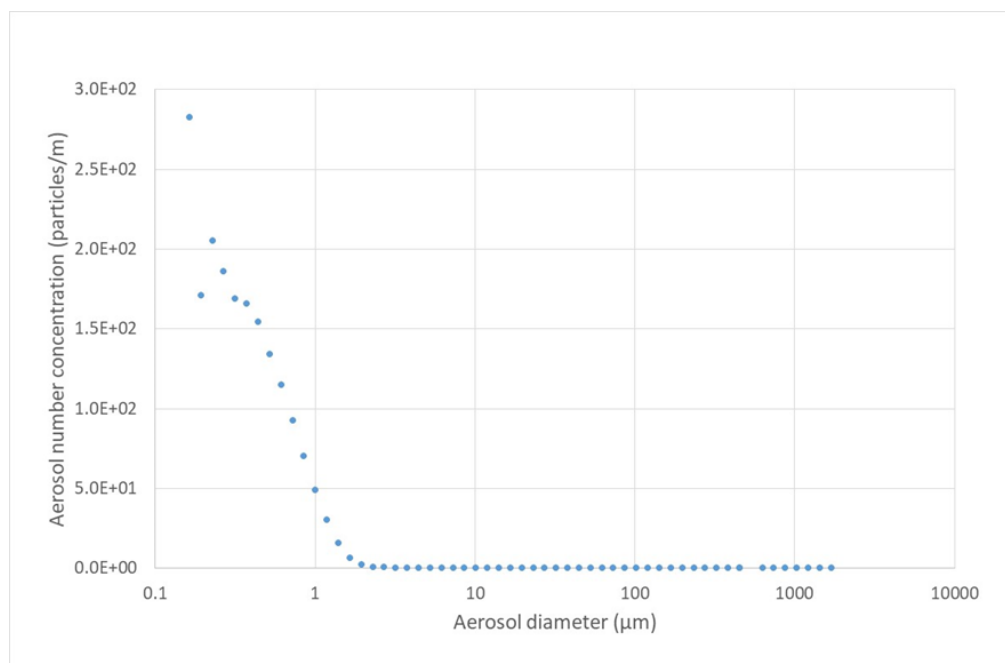


**Figure 34** Laser diffraction analyser particle distribution with addition of NO<sub>2</sub> to the absorber at a concentration of 325 ppm

It is possible that the initial lack of measured aerosol at 160 ppm was due to the either the NO<sub>2</sub> or resultant HNO<sub>3</sub> reacting with another component of the PCC process at this concentration. This possibly indicates non-linear kinetics, with a bifurcation state or critical concentration point above which aerosol formation becomes a problem and below which aerosol is suppressed. Potentially, ammonia from solvent degradation or another solvent component is reacting with NO<sub>2</sub> to suppress aerosols, with aerosol only being observed once NO<sub>2</sub> is at a concentration greater than a watershed value. Thus, the problem of aerosols may diminish below this watershed gas concentration. The corollary here is that aerosols may not be a problem for combustion situations producing concentrations of NO<sub>2</sub> less than the critical value for the process. However, these data clearly reveal that the presence of NO<sub>2</sub> in the inlet gas stream has the potential to produce

moderate quantities of fine aerosol that can penetrate the absorber and water-wash sections of the PCC process.

Assuming that aerosol forms above a critical concentration of  $\text{NO}_2$  (and  $\text{SO}_3$ ) due to a reversible gas-phase equilibrium intermediate with the solvent, then a possible aerosol control process is to enhance the critical concentration value of the process. A plausible solution may be to increase the rate of formation of non-reversible acid gas products in solvent, so these are continuously removed from the equilibrium, possibly through the addition of an additive to the solvent.

An analytical study of acid gas intermediates in solution would provide much information regarding the above hypotheses. Online application of instruments such as selected ion flow tube mass spectrometry, liquid chromatography mass spectrometry and ion chromatography mass spectrometry would be highly suitable to track such chemical reactions in real time, while concurrently monitoring aerosol concentrations.

#### 4.3.5 $\text{SO}_2$ and $\text{NO}_2$ measurements

$\text{SO}_2$  is readily oxidised to  $\text{SO}_3$  in the presence of excess  $\text{NO}_2$ . The concentration of  $\text{SO}_2$  for this example was selected to represent a value towards the lower end of the  $\text{SO}_2$  emissions from the Vales Point PCC pilot plant. Section 4.3.3 clearly indicated that  $\text{SO}_3$  is a strong generator of aerosol at higher concentrations. Figure 35 displays the LDA transmission results when 60 ppm of  $\text{SO}_2$  and 160 ppm of  $\text{NO}_2$  are added to the flue gas inlet. During this addition, laser transmission quickly fell to zero, showing that large quantities of aerosol had been produced that overload the detector.

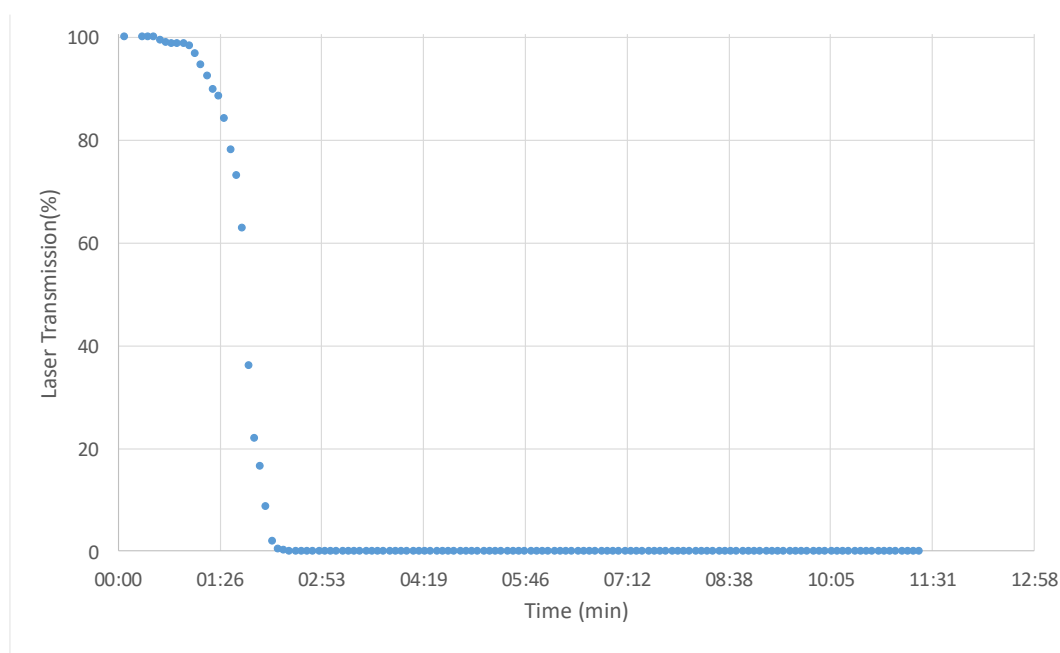


Figure 35 Laser diffraction analyser transmission – 160 ppm  $\text{NO}_2$  with 60 ppm  $\text{SO}_2$  in flue gas

Figure 36 shows the particle distribution just prior to laser obscuration. These data show a generally similar aerosol distribution to those data observed for  $\text{SO}_3$  in Figure 31, but with a mode in the order of  $0.4 \mu\text{m}$  and approximately 20% of the aerosol numbers. It is again noted that at these low laser transmission values, significant uncertainty exists with absolute aerosol concentrations.

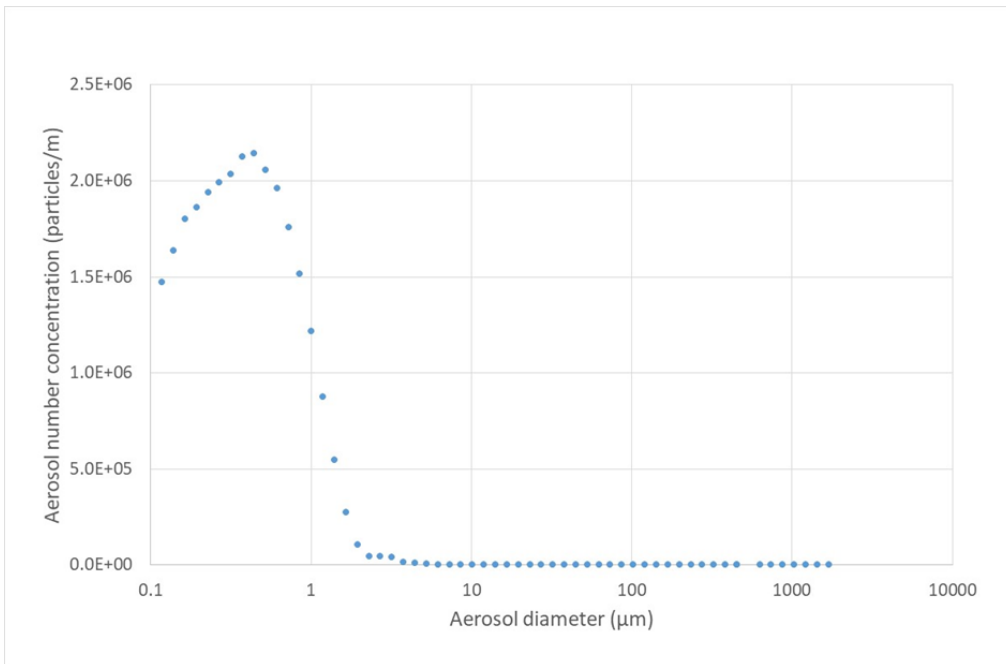


Figure 36 Laser diffraction analyser particle size distribution – 160 ppm NO<sub>2</sub> with 60 ppm SO<sub>2</sub> in flue gas

#### 4.3.6 SO<sub>2</sub> and NO measurements

The MEA at the Vales Point PCC pilot plant was aged by the end of January 2018. At this time, an experiment was completed where NO was added to a SO<sub>2</sub>-enriched inlet gas stream. The time series of the LDA transmission dataset over this experimental period is shown in Figure 37.

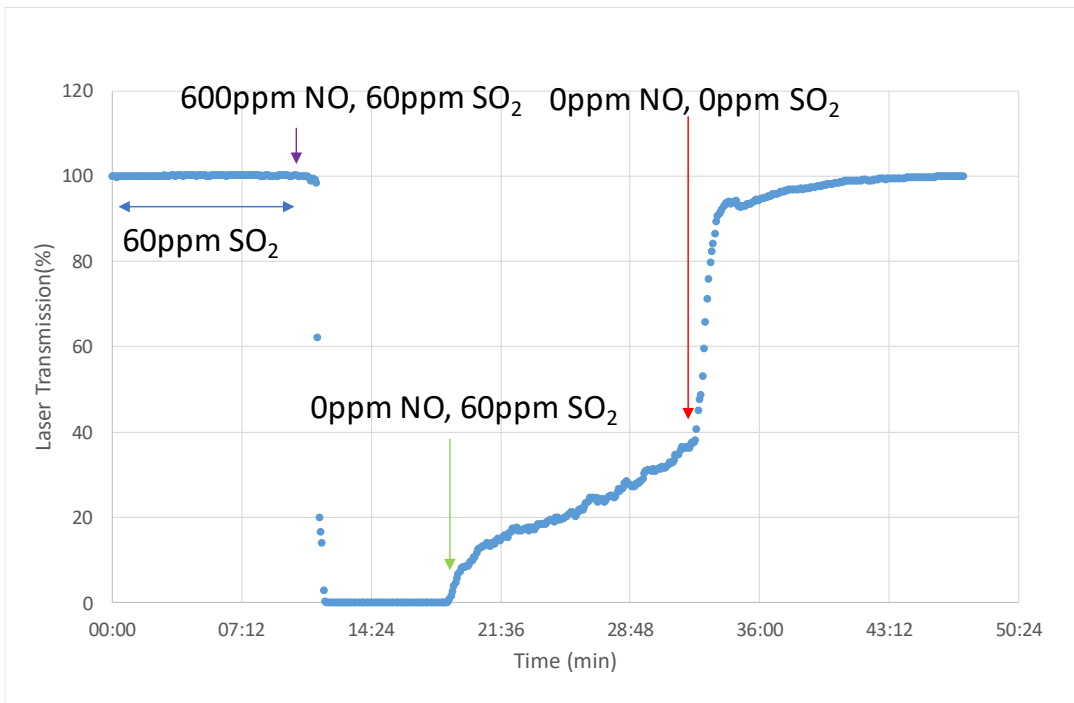


Figure 37 Laser diffraction analyser transmission – 600 ppm NO with 60 ppm SO<sub>2</sub> in flue gas

The blue horizontal arrow indicates the period over which only SO<sub>2</sub> was administered at a flow rate producing 60 ppm in the inlet gas stream and for a period of 11 minutes. Figure 37 data shows that no change in LDA transmission occurs over this time. At a time of 12 minutes, which is

indicated by the purple arrow, NO was added to the inlet gas stream at a concentration of 600 ppm. After this addition, LDA laser transmission quickly reduced to zero, indicating aerosol genesis is occurring. High aerosol concentrations continue until the NO flow is terminated (indicated by the green arrow). Once NO addition stops, laser transmission initially rises quickly, but then slows to constant rise of 1.9%/min after 21 minutes. At a time of 32 minutes the SO<sub>2</sub> flow is also stopped (as indicated by the red arrow). As the SO<sub>2</sub> flow ceases, the LDA laser transmission quickly rises but then slows to approach 100% transmission.

The particle size distributions observed during SO<sub>2</sub> addition have been displayed previously in Figure 28 and similar particle distributions were observed in these corresponding data shown in Figure 37.

Figure 38 displays the LDA particle distribution just before NO flow ceases, as well as just before SO<sub>2</sub> flow ceases. These data show a significant reduction in particles between the respective flow changes, but the aerosol size range remains relatively constant with the mode in each distribution being smaller than 1 μm.

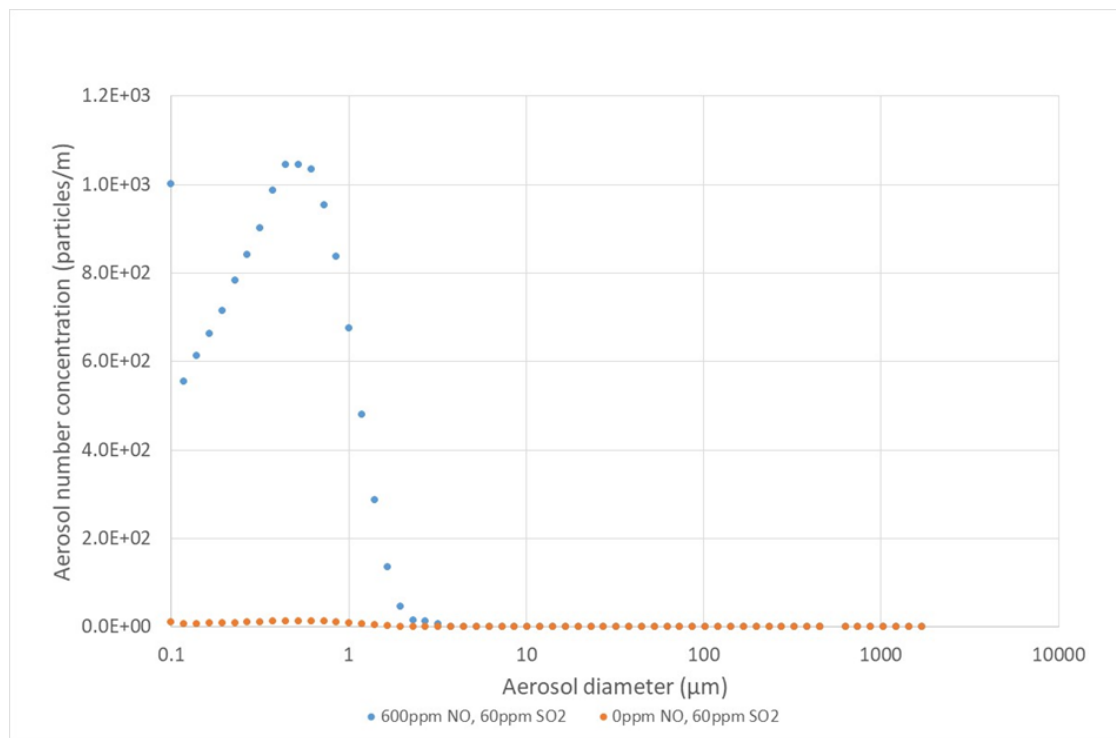


Figure 38 Laser diffraction analyser particle size distribution – 600 ppm NO with 60 ppm SO<sub>2</sub> in flue gas

As noted previously, NO<sub>2</sub> and SO<sub>3</sub> can be thermally or catalytically prepared from more readily available chemicals (nitric acid and readily available SO<sub>2</sub>). However, this was not the case for NO. A very limited amount of NO was able to be sourced either in Australia or internationally. Given the required dosing rate to the absorber, cylinders of NO were rapidly exhausted. Consequently, lower-concentration experiments were completed during apparatus testing and the initial experiments. While it would be preferable to undertake NO experiments at greater NO concentration, NO supplies as well as NO consumption rates prohibited these experiments. SDR results identified that NO did not generate aerosol in the presence of SO<sub>2</sub> and up to a concentration of 60 ppm. While these current data in Figure 37 tend to contrast with the SDR findings, the Vales Point data are at very high concentrations. The SDR data also suggested that SO<sub>2</sub> produced aerosol at moderate concentrations following addition. This was, however, not the

case during this experiment. It is currently unknown why the SDR data and the Vales Point PCC pilot plant data show different results. Clearly additional work is required at larger scale to determine the origin of this anomaly.

## 4.4 Discussion/conclusion

Supersaturation within a gaseous system is the condition where a gaseous species exists at a partial pressure or concentration that is above the equilibrium of maximum partial pressure for the prevailing temperature and pressure conditions. This often occurs atmospherically when a saturated air mass is cooled. As the air mass cools, it can become supersaturated with any species that has vapour pressure greater than the saturation value. Any supersaturated or excess gas species eventually condenses as mist or aerosol. Atmospheric fog formation is a prime example of this phenomenon. The conditions for supersaturation at an amine-based PCC plant can occur within the FPT and absorber. Within the FPT, the flue gas is cooled quickly by the hydroxide wash where the gas passes through the dew point causing both homogeneous and heterogeneous condensation. This condensation produces aerosol of a wide variety of diameters producing a large surface area for gas absorption, as well as washing out suspended solid-phase particles. At the Vales Point PCC pilot plant, the results above revealed extremely small background aerosol concentrations prior to gas addition showing that this process is extremely effective. The data confirm that only negligible concentrations of  $\text{SO}_3$  and  $\text{NO}_2$  penetrated through the process.

At the absorber, conditions for supersaturation occur just past the so-called ‘temperature bulge’, where the temperature reaches a maximum (typically at a distance of two-thirds of the total packing height from the bottom) and further cools at the top of the column. An example of this temperature profile is shown in Figure 39.

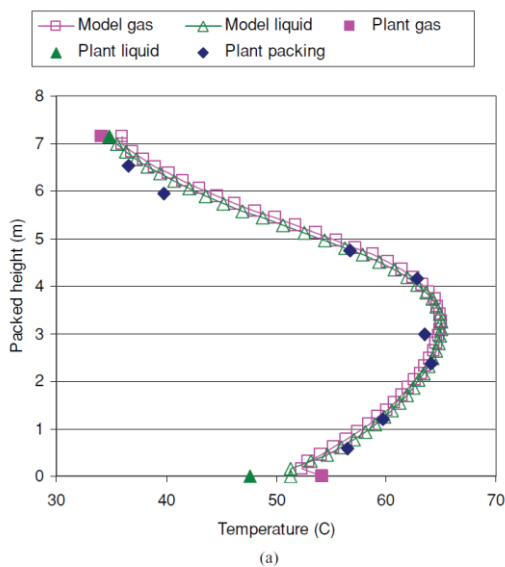


Figure 39 Temperature profile along the packed height of the Tarong post-combustion capture absorber (Cousins, 2012)

Other factors, such as lean absorbent temperature, may also contribute to the near absence of background aerosol. The change in the lean absorbent temperature affects the temperature of the flue gas in the column and thus, higher temperatures would cause less of a temperature gradient

after the hot zone in the absorber, decreasing the supersaturation ratio. The loading of the lean absorbent may also impact on the supersaturation; as the loading of the lean absorbent increases, the transfer of CO<sub>2</sub> to the absorbent shifts lower in the column. Therefore, most of the corresponding heat is also released in the lower sections of the column, resulting in an increase in the supersaturation ratio in the lower section of the column [19].

In this study, little aerosol was observed in the absence of acid gases, which potentially suggests that the degree of super-saturation in the absorber of the Vales Point PCC pilot plant is much less than observed for SDR and other reported studies. SDR experiments showed background aerosol concentrations larger than observed in the pilot plant. It is also plausible that packing material may have an influence upon the heat loss function of the packing and the temperature rise of the flue gas within the absorber. Unfortunately, the temperature control trials for the absorber section were not completed due to pilot plant availability, and the further work planned using the absorber cooler could not be completed. However, even without these temperature-controlled tests, these results demonstrate that it is possible to design suitable absorber operational condition to essentially eliminate aerosol formation from supersaturation processes.

Similarly to Brachert et al., this work has demonstrated the role of SO<sub>3</sub> (H<sub>2</sub>SO<sub>4</sub>) in aerosol emissions of the PCC plant and found a strong delineation between H<sub>2</sub>SO<sub>4</sub> concentrations and aerosol genesis [19, 20]. Similarly, Fulk et al. (2016), who completed laboratory-scale measurements using H<sub>2</sub>SO<sub>4</sub> aerosol injection and pilot-scale experiments, observed similar SO<sub>3</sub> artefacts [1].

Developing predictive models capable of accurately estimating the PM emissions of the PCC plant is a challenging undertaking because of the complexity of the system. The impacts of various process parameters (e.g. the inlet flue gas CO<sub>2</sub> concentration, the temperature of the lean absorbent and the CO<sub>2</sub> loading of the lean absorbent) on the supersaturation profile along the column must be considered, and often not all of these are known. In addition, aerosol formation can be driven by subtle factors that are not captured by simple models.

Khakharia et al. (2014) explained the development of a model that makes a number of assumptions to simplify solution algorithms [16]. These include: constant number concentration at 10<sup>-13</sup> to 10<sup>-14</sup> per cubic metre of gas, spherical aerosols, the whole aerosol phase being modelled as bulk liquid, no nucleation, only growth of pre-existing particles, chemical reactions only in the liquid phase, no direct contact with between the liquid and particulate phase, surface area of the particles being neglected, and Kelvin effect being neglected. During this study it was planned to undertake simple modelling of the aerosol parameter in a similar manner to Khakharia et al. (2014) [16]. Analyses of the absorption conditions in regard to aerosol formation for both the SDR and the Vales Point PCC pilot plant using either Aspen Plus or a custom model would provide significant information about the differences observed between the background aerosol concentrations of each process.

## Challenges

As noted in the introduction to this section, the Vales Point experimental work presented many experimental challenges, which ranged from sourcing sufficient quantities of gases to complete

the initially conceived work program, to gaining adequate operational time at the pilot plant to undertake this work.

Due to time limitations, repeat experiments to evaluate uncertainties associated with these data sets were not possible. This aspect should clearly be addressed in future work. It is also recommended that future work be undertaken into evaluate the aerosol-forming potential of CAL008 at pilot scale, because this solvent exhibited reduced aerosol-forming potential during SDR operation. It is likely that additional work evaluating the more chemically complex CAL008 would provide information regarding the impact of different amine chemistry on aerosol-forming potentials.

Overall, significant value has been generated from this study, including a general validation of the core finding of the SDR-based research. These findings include the following.

1. The Vales Point PCC pilot plant exhibits low aerosol concentrations in the absence of acid gases, and less than those observed in the SDR on a number concentration basis. This indicates that little aerosol has been formed due to supersaturation at the temperature bulge within the absorber. Thus, for this design, and when operating normally with the FPT, loss of solvent and transfer of contaminants to the flue gas is small. Given the lower aerosol numbers observed for CAL008 in SDR experiments, solvent losses from aerosol artefacts are likely to be smaller than those of MEA, with CAL008 potentially able to operate with flue gases with increased acid gas concentrations.
2.  $\text{SO}_3$  is a powerful initiator of aerosol, and once generated, this aerosol penetrates through absorber and water-wash section of a normal PCC process.
3.  $\text{NO}_2$  has a propensity to form aerosols in isolation, and more strongly when in the presence of  $\text{SO}_2$ , since  $\text{NO}_2$  efficiently oxidises  $\text{SO}_2$  to  $\text{SO}_3$ , producing a rapid onset of aerosol. However, the results when  $\text{NO}_2$  is added in isolation tend to contrast with the corresponding SDR results, and thus further work is necessary to identify the origins of this discrepancy.
4.  $\text{NO}$  has a strong propensity to form aerosols in aged MEA in the presence of  $\text{SO}_2$ . The mechanism of this process remains unclear. However, it is possible that this observation is linked to residual contaminants in the solvent that partition from the solvent when in the presence of  $\text{NO}$ . This result contrasts with SDR results, and thus further work is necessary to identify the origins of this discrepancy.

While not new, this study clearly demonstrated the crucial importance of maintaining low  $\text{SO}_x$  and low  $\text{NO}_x$  in the flue gas to the amine PCC absorber if aerosol genesis is to be minimised. The current study demonstrated that even at low concentrations, these gases can easily produce large quantities of aerosol.

The Vales Point PCC pilot plant system includes an additional 'intermediate' cooler that allows the packing in the absorber to be maintained at isothermal conditions. That is, the cooler removes the heat generated during the exothermic absorption process. The increased heat generated in the absorber is potentially another mode for aerosol genesis, and the use of this device may further reduce aerosol formation. This system was not used in this current study, as it was preferential to replicate a more typical temperature profile developed within amine absorbers. Due to time constraints, experiments to investigate the influence of the intermediate cooler on aerosol

formation were not possible. Thus, this is another aspect that should be investigated in future studies.

## 5. Recommendations for future work

A significant finding of this work was that the chemical composition of a solvent has a marked impact upon the amount of aerosol formed within the absorber. The next steps of this work are to compare the aerosol yields for amine solvents with different chemical functionality at pilot scale, or preferably demonstration scale, to compare which chemical features reduce aerosols. CAL008 would be the most practical starting solvent, due to its sophisticated formulation and lower aerosol-forming potential compared with MEA. The inclusion of other commercially available amines with specific chemical functionality would improve the outcomes of such a study, and potentially identify the types of amine structures that suppress aerosol formation. Combining this with a thermodynamic study of the solvent would provide significant additional information.

# Shortened forms

---

<b>AMP</b>	2-amino-2-methyl-1-propanol
<b>APS</b>	aerodynamic particle sizer
<b>BDU</b>	Brownian demister unit
<b>CCS</b>	carbon capture and storage (also known as carbon capture and sequestration)
<b>CINSW</b>	Coal Innovation New South Wales
<b>CRDS</b>	cavity ring down spectroscopy
<b>CSIRO</b>	Commonwealth Scientific and Industrial Research Organisation
<b>EEPS</b>	electrical engine particle spectrometer
<b>ELPI</b>	electrical low pressure impactor
<b>EPRI</b>	Electric Power Research Institute
<b>ESP</b>	electrostatic precipitator
<b>FGD</b>	flue gas desulphurisation
<b>FPT</b>	flue gas pre-treatment
<b>LDA</b>	laser diffraction analyser
<b>MDEA</b>	methyldiethanolamine
<b>MEA</b>	monoethanolamine
<b>MFC</b>	mass flow controller
<b>MHI</b>	Mitsubishi Heavy Industries
<b>NO<sub>x</sub></b>	oxides of nitrogen
<b>NSW</b>	New South Wales
<b>PCC</b>	post-combustion CO <sub>2</sub> capture
<b>PM</b>	particulate matter

---

---

<b>ppm</b>	parts per million
<b>ppmv</b>	parts per million by volume
<b>S</b>	saturation number
<b>SDR</b>	solvent degradation rig
<b>SOx</b>	oxides of sulphur
<b>WESP</b>	wet electrostatic precipitator
<b>WFGD</b>	wet flue gas desulphurisation

---

# Glossary

**Aerosol** A colloidal system in which the dispersed phase comprises either solid or liquid particles, and in which the dispersion medium is a gas, usually air.

**Amine** These are formally derivatives of ammonia, wherein one or more hydrogen atoms have been replaced by a substituent such as an alkyl group (alkylamines) or aryl group (arylamines) or both (alkylarylamines). Amine scrubbing has been used to separate CO<sub>2</sub> from natural gas and hydrogen since 1930. It is a robust technology and is ready to be tested and used on a larger scale for CO<sub>2</sub> capture from coal-fired power plants.

**Amine** Organic chemical compound containing one or more nitrogens in -NH<sub>2</sub>, -NH or -N groups. In carbon capture and storage, the main post-combustion carbon capture technology for separating CO<sub>2</sub> from flue gas or other gas streams is scrubbing the gas stream using an amine. After leaving the scrubber, the amine is heated to release high-purity CO<sub>2</sub> and the CO<sub>2</sub>-free amine is then reused.

**Anthropogenic** The effects, processes, objects or materials (e.g. climate change) derived from human activities, as opposed to those occurring naturally and without human influence.

**Atmosphere** The layer of gases surrounding the planet Earth that is retained by the Earth's gravity. It is where CO<sub>2</sub> and other greenhouse gases are released, and it currently contains about (by molar content/volume) 78.08% nitrogen, 20.95% oxygen, 0.93% argon, 0.038% CO<sub>2</sub>, trace amounts of other gases, and a variable amount of water vapour.

**Capture** The removal of CO<sub>2</sub> from fossil fuels either before or after combustion. Estimates suggest that carbon capture and storage could typically reduce carbon emissions by 80–95% from a power station.

**Capture efficiency** The amount (as a fraction) of CO<sub>2</sub> that is removed or separated from the gas stream of a production source.

**Carbon capture and storage** Also known as carbon capture and sequestration, this is the process of capturing waste CO<sub>2</sub> from large point sources, such as fossil-fuel power

plants, transporting it to a storage site, and depositing it where it will not enter the atmosphere, normally in an underground geological formation.

**Carbon dioxide (CO<sub>2</sub>)** A colourless, odourless gas that is produced when animals (including humans) breathe or when carbon-containing materials (including fossil fuels) are burned. CO<sub>2</sub> is essential to the photosynthesis process that sustains plant and animal life; however, it can accumulate in the air and trap heat near the Earth's surface (the 'greenhouse effect').

**Climate change** The variation in the average global or regional climate as measured by comparators such as average temperature and rainfall. The term is now commonly used to describe climate variation arising from anthropogenic activities.

**Coagulation** Occurs when an aerosol particle collides with another aerosol particle and together they form a new one.

**Condensation** Describes the growth of a particle (droplet or dry solid particle) as a result of gas condensing onto it.

**Deposition** The process by which particles within an aerosol are collected or deposited on a surface.

**Diffusion** The movement and transport of particles caused by Brownian motion, the random movement of particles caused by collision between the particles and surrounding gas molecules.

**Electrical mobility equivalent diameter** The diameter of a sphere with the same migration velocity in a constant electric field as the particle of interest.

**Flue gas** Gases that are produced through the combustion of a fuel. These are gases normally emitted into the atmosphere.

**Greenhouse gas** Greenhouse gases include carbon dioxide (CO<sub>2</sub>), methane (CH<sub>4</sub>), nitrous oxide (N<sub>2</sub>O), hydrofluorocarbons (HFCs), perfluorocarbons (PFCs) and sulphur hexafluoride (SF<sub>6</sub>).

**Impaction** Occurs because large particles, which have more inertia when in motion, tend to maintain their velocity and not follow changes in the direction or speed of the flow. Thus, they may impact and stick to the wall of the exhaust or sampling system.

**Impurities** Substances inside a confined amount of liquid, gas or solid that differ from the chemical composition of the material or compound.

<b>Injection</b>	Using significant pressure to force gases or liquids into wells using pressure.
<b>Mitigation</b>	An anthropogenic intervention to reduce the anthropogenic forcing of the climate system; it includes strategies to reduce greenhouse gas sources and emissions and enhance greenhouse gas sinks.
<b>Nucleation</b>	The process by which particles are formed from a supersaturated vapour.
<b>Particle mass concentration</b>	The mass of particles in unit volume of air; one of the most frequently measured parameters of an aerosol.
<b>Particle number concentration</b>	The number of particles in one unit of volume of air (number/cm <sup>3</sup> ). Particle number concentration within an aerosol is another important characteristic emerging in aerosol science.
<b>Particle size distribution</b>	The amounts of different size particles of solids or liquids that are suspended in the air as an aerosol.
<b>Post-combustion capture</b>	The removal of CO <sub>2</sub> from power station flue gas before its compression, transportation and storage in suitable geological formations, as part of carbon capture and storage.
<b>Saturation</b>	The condition in which vapour pressure is equal to the equilibrium vapour pressure over a plane surface of pure liquid water, or sometimes ice.
<b>Scrubber</b>	A gas–liquid contacting device for the purification of gases or capture of a gaseous component.
<b>Sequester</b>	To store something so that it is no longer available. Carbon sequestration involves the removal or storage of carbon dioxide so that it cannot be released into the atmosphere.
<b>Storage</b>	A process for retaining captured CO <sub>2</sub> so that it does not reach the atmosphere.
<b>Supersaturation</b>	A state of a solution that contains more of the dissolved material than could be dissolved by the absorbent under normal circumstances. It can also refer to a vapour of a compound that has a higher (partial) pressure than the vapour pressure of that compound.
<b>Thermophoresis</b>	A phenomenon observed in mixtures of mobile particles where the different particle types exhibit different responses to the force of a temperature gradient. Thermophoretic force results from a temperature gradient established in the gas medium. An aerosol in that temperature gradient experiences a force in the direction of decreasing temperature; thus,

particles are directed and concentrated around the surfaces with lower temperature, and are eventually deposited on them.

# References

1. Fulk, S.M., *Measuring and modeling aerosols in carbon dioxide capture by aqueous amines*. 2016.
2. Khakharia, P., *Aerosol-based emission, solvent degradation, and corrosion in post combustion CO2 Capture*. 2015, TU Delft, Delft University of Technology.
3. Khakharia, P., et al., *Field study of a Brownian Demister Unit to reduce aerosol based emission from a Post Combustion CO2 Capture plant*. International Journal of Greenhouse Gas Control, 2014. **28**: p. 57-64.
4. Kolderup, H., et al., *Emission Reducing Technologies H&ETQP Amine6*, in Gassnova, SINTEF, Editor. 2014, Gassnova: Gassnova.
5. Agency, S.E.P., *Review of Amine Emissions from Carbon Capture Systems*. 2013. **V1.1**.
6. Fulk, S.M. and G.T. Rochelle, *Modeling Aerosols in Amine-based CO2 Capture*. Energy Procedia, 2013. **37**: p. 1706-1719.
7. Khakharia, P., et al., *Investigation of aerosol based emission of MEA due to sulphuric acid aerosol and soot in a Post Combustion CO2 Capture process*. International Journal of Greenhouse Gas Control, 2013. **19**: p. 138-144.
8. Azzi, M., et al., *Analysis of environmental legislative and regulatory requirements for the use of amine-based CO2 post combustion capture (PCC) in Australian power stations*. Global CCS Institute, 2012.
9. Låg, M., et al., *Health effects of amines and derivatives associated with CO2 capture. Report by the Norwegian Institute of Health*. Norwegian Institute of Air Research, 2011. **NILU Report**.
10. Agency, I.E., *Carbon Capture and Storage Legal and Regulatory Review*. 2010.
11. Veltman, K., B. Singh, and E.G. Hertwich, *Human and environmental impact assessment of postcombustion CO2 capture focusing on emissions from amine-based scrubbing solvents to air*. Environmental science & technology, 2010. **44**(4): p. 1496-1502.
12. Lawal, A., et al., *Dynamic modelling of CO2 absorption for post combustion capture in coal-fired power plants*. Fuel, 2009. **88**(12): p. 2455-2462.
13. Institute, E.P., *Amines for Post-Combustion Capture*. 2011.
14. SaskPower, *Boundary Dam Carbon Capture Project*.
15. US Department of Energy, O.O.F.E., *Petra Nova - W.A. Parish Project*.
16. Khakharia, P., et al., *Predicting Aerosol Based Emissions in a Post Combustion CO2 Capture Process Using an Aspen Plus Model*. Energy Procedia, 2014. **63**: p. 911-925.
17. Mertens, J., et al., *ELPI+ measurements of aerosol growth in an amine absorption column*. International Journal of Greenhouse Gas Control, 2014. **23**: p. 44-50.
18. Khakharia, P., et al., *Understanding aerosol based emissions in a Post Combustion CO2 Capture process: Parameter testing and mechanisms*. International Journal of Greenhouse Gas Control, 2015. **34**: p. 63-74.
19. Brachert, L., et al., *The challenge of measuring sulphuric acid aerosols: Number concentration and size evaluation using a condensation particle counter (CPC) and an electrical low pressure impactor (ELPI+)*. Journal of aerosol science, 2014. **67**: p. 21-27.
20. Brachert, L., T. Kochenburger, and K. Schaber, *Facing the sulphuric acid aerosol problem in flue gas cleaning: pilot plant experiments and simulation*. Aerosol Science and Technology, 2013. **47**(10): p. 1083-1091.

21. Azzi, M., et al., *CO2 Capture Mongstad - Project A – Establishing sampling and analytical procedures for potentially harmful components from post-combustion amine based CO2 capture*. Gassnova, 2010.
22. Ltd, P.c.w.A.s.A.P., 2016 to 2020.

# Appendices

# Appendix A: Instrumentation – Limitations and challenges

## A.1 Introduction

This section provides a brief discussion of instruments used in this study, instrument limitations, and discussion regarding possible modification that will be necessary to complete measurements in a monoethanolamine (MEA) post-combustion capture (PCC) environment. Aerosol monitoring instruments that were considered during the desktop research component of this study are shown in Table.

A range of aerosol and gas monitoring instruments were evaluated according to monitoring effectiveness, long-term reliability and cost of operation, including repairs. These instruments were selected because they were available and had ranges and resolutions that allowed reliable particle and gas concentrations to be determined.

Instruments considered for this study included: laser diffraction analyser (LDA), aerodynamic particle sizer (APS), engine electrical particle spectrometer (EEPS), electrical low-pressure impactor (ELPI), condensation particle counter (CPC), and a SO<sub>2</sub>/SO<sub>3</sub> analyser based on the technique of cavity ringdown. A high-resolution multi-gas analyser (SO<sub>2</sub>, NH<sub>3</sub>, O<sub>2</sub>, CO<sub>2</sub>, CO) was also purchased during the project; however, manufacturing and delivery delays resulted in its delivery after the experimental program ceased. The operating principle of each instrument is briefly discussed below in addition to a brief discussion about the limitation of the instrument and where possible, potential modifications to allow future use with MEA, CAL008, ammonia and amino-acid based PCC processes.

## A.2 Laser diffraction analyser

The LDA (manufactured by Malvern Insitac) uses low-angle forward scattering of light or diffraction to measure particle size. This technique has a number of advantages compared to other light-scattering instruments, such as 90-degree side scattering techniques, since the diffraction technique is independent of the refractive index and reflectivity of the aerosol. The instrument uses proprietary scattering algorithms to calculate particle distributions through an array of 32 detectors used to analyse the diffraction scattering pattern. The instrument has a very wide aerosol size range from ~0.1 µm to 2200 µm with 60 size bins over this diameter range.

Having no surfaces in direct contact with PCC absorbent, this instrument proved to be extremely stable and reliable during both long-term operations while attached to the solvent-degradation rig (SDR) gas stream and while sampling at the Vales Point PCC pilot plant. The instrument proved to be easily transported between monitoring operations with minimal realignment of the laser and detectors being required during the re-installation operation. This instrument proved to be the most reliable of all aerosol monitor instruments trialled and required no further modification for aerosol sampling in PCC systems.

### A.3 Aerodynamic particle sizer

The APS is a high performance research grade instrument that directly counts and sizes particles on the basis of aerodynamic number concentration. The principle of operation uses the time-of-flight of the particle as it moves through a critically defined airflow to assign the aerodynamic diameter of the particle. The timing is measured by a precision nanosecond timer, which is started and stopped when the particle passes between two laser beams mounted orthogonal to the airflow and particle direction. Thus, a direct measure of particle number concentration is completed with a maximum concentration of  $\sim 1 \times 10^7$  particles /cm<sup>3</sup>.

The time-of-flight sizing inherently accounts for different particle shapes, with the instrument reporting particle diameter as the spherical equivalent diameter. The monitoring principle is unaffected by the refractive index of the particle, refractive or Mie scattering properties, and thus is highly suitable for measuring spherical aerosols such as those found in PCC processes. In addition, the monotonic response curve of the time-of-flight measurement ensures high-resolution sizing over the entire particle size range. The TSI model 3321 APS combines time-of-flight measurements with 90-degree side scattering measuring techniques to detect particles less than 0.5  $\mu\text{m}$ , while the time-of-flight counter counts particles from 0.5 to 20  $\mu\text{m}$ . While APS instruments can suffer from particle coincidence at high particle concentrations, by using proprietary algorithms and changing the operation mode at higher concentrations, the TSI software minimises uncertainty associated with coincidence.

While the APS is an extractive instrument, aerosols have a short path length through the instrument before the aerosol is captured by a filter. Filtered sheath air is used to protect laser optics and minimise exposure of internal surfaces to aerosols. The instrument proved to be robust and continued to operate over the larger portion of the study. However, during the latter experimental series of the study, the optics suffered from severe contamination and this manifested at large background number counts during operation. This was noted by the Australian supplier and consequently it was necessary for the instrument to be returned to the manufacturer in the USA. Upon disassembly, the manufacturer noted that extensive repairs were required as the internal optics were severely affected by exposure to amine solvent. As a result, the instrument was unavailable for experiments using ammonia and alanine as well as measurements undertaken at the Vales Point PCC pilot plant.

For future studies, it is recommended that a dynamic dilution system be used. An instrument such as a rotating disc thermophilizer (TSI USA), or similar, would be suitable as this unit preserves the size distribution and concentration of aerosols due to the short time between dilution and measurement. However, the temperature and the humidity of dilution air will need to be controlled as the use of dry air during dilution will have the potential to evaporate moisture from the aerosol droplets and cause bias in particle size distributions.

### A.4 Engine exhaust particle spectrometer

The EEPS was designed to measure particles emitted from combustion engines. It measures particle sizes from 0.0056 to 0.56  $\mu\text{m}$  with a size resolution of 16 channels per decade, providing a total of 32 channels. The instrument uses the electrical mobility of the charged particle to classify the particles according to electrical mobility diameter. Classifying occurs when the particle, which

has a known applied charge, passes through an electric field of known strength. The trajectory of the particle is deflected according to the magnitude of the electrical mobility, with the charged particle impinging onto one of 32 electrometers that intercepts the flight of the particle. Small particles have fast deflection, while larger particles have slower deflections in the electric field. The electrometer infers particle concentration according to the measured charge flow, the standard charge applied to the particle, and the standard trajectory of the equivalent Stokes particle. Consequently, the instrument reports particle diameter on the basis of electrical mobility diameter of the equivalent Stokes particle. This instrument is one of the few that can measure ultrafine particles at 10 Hz. It has an internal heater allowing heating of the instrument to  $\sim 40^{\circ}\text{C}$ , allowing it to operate in humid environments.

The instrument was initially operated during the recommissioning and first stages of the SDR study, but failed due to MEA amine vapour condensing within the control and pump systems after the particle collector. The instrument was not repairable in Australia and was returned to the manufacturer in the USA for repairs. Upon disassembly the manufacturer noted that extensive repairs were required as the control system and pumps as these were severely affected by exposure to amine solvent. The manufacturer observed that the MEA solvent degraded a number of internal plastic and non-stainless-steel metal surfaces and fittings. Due to the extensive repairs that were necessary, delivery times, the complexity of the instrument, and the unavailability of some components and a wide number of other delays, the instrument was only returned after the completion of the Vales Point PCC pilot plant study. Consequently, this instrument was unavailable for essentially the entirety of this study.

## A.5 Electrical low-pressure impactor

At the commencement of this SDR research program, the CSIRO-owned ELPI was found to be non-operational after several years of storage. Due to the age of the instrument, and it being superseded by a newer model, it was classified as obsolete and non-repairable by the manufacturer. Given the price associated with replacement and considering the limitations associated with the instrument discussed as following, upgrade to the newer model was not possible.

When measuring fine liquid phase or volatile aerosols, and especially when measuring at diameters smaller than approximately  $1\ \mu\text{m}$ , the ELPI aerosol classification principle can bias aerosol results. This bias occurs because the design of the instrument relies on reduced pressure to classify finer aerosols. With pressures during aerosol sizing at each of the finer collection stages progressively reducing from 1 atm at the  $1\ \mu\text{m}$  stage to  $\sim 0.1$  atm at the smallest collection stage of  $0.03\ \mu\text{m}$ , water and other volatile species contained in the droplet can evaporate from aerosols, causing droplet shrinkage and underreporting of aerosol diameter. Thus, data for aerosols of  $\sim 0.6\ \mu\text{m}$  and smaller will have additional uncertainties, as particle diameters will be biased towards smaller diameters. Such uncertainties become greater as the size of the aerosol becomes smaller.

The ELPI was selected because it was available at the time of the study and had been used in other studies [17] and thus the limitations of this instrument could be demonstrated by comparing to other particle-measuring instruments.

## A.6 ProCeaas™ SO<sub>2</sub>/SO<sub>3</sub>

A ProCeaas™ SO<sub>2</sub>/SO<sub>3</sub> analyser was purchased to undertake this work. The low-pressure sampling system (100 mbar absolute) was reported by the manufacturer as suitable for the online analysis of these gases in industrial environments such as PCC plants, although it had not been used in such plants previously [22]. However, it was later found that this recommendation was made without experimental testing with MEA. The instrument was reported to provide measurements with a very high spectral resolution, providing accurate measurements of the target gases potentially to concentrations below 1 ppm. The analysis system was promoted as a simplified design with no heated lines, interference-free, providing fast and sensitive analysis, regardless of the matrix of the gas to be analysed. The instrument used the principle of cavity ring down spectroscopy (CRDS) providing an optical path of ~10 km. The CRDS uses two separate and independently tuned lasers (one tuned to an SO<sub>2</sub> absorption band and the other to an SO<sub>3</sub> absorption band) to characterise each gas species with minimal interference. Other instruments using this measuring technique that CSIRO have operated have proven to be very reliable, with very high measurement stability with little to no zero drift and little drift in calibration.

In the MEA PCC environment, the instrument did not operate as promoted and problems in the sampling system were identified with initial use with the SDR [22]. The source of the problem was that the dew point of MEA at 100 mbar was only a few degrees above the sample line temperature. At the inlet port, reduced pressure was regulated using a critical orifice, which is placed just after a sintered stainless-steel filter. During operation, aerosolised solvent collecting on the filter permeated through the filter to the critical orifice. At this orifice, solvent partitioning occurred due to the latent heat of vapourisation cooling MEA below the dew point. This resulted in MEA being drawn into the optics, causing the failure of the instrument. Consequently, it was necessary to return the instrument to the manufacturer for cleaning and repairs. Unfortunately, as was the case with the EEPS, continued delays with the manufacturer resulted in the device only being returned to CSIRO after the conclusion of all experimental work.

Discussion with the manufacturer resulted in the revision of a new design of a new sampling system and increasing the temperature of the heated lines and instrument sensor to 100°C. The revisited sampling system included the use of two stainless-steel filters heated to 200°C. The first of these filters was designed to vapourise all the liquid phase of the solvent with the residual non-volatile components contained in the liquid phase collected on the second heated filter. By using the proposed revised sampling system, it was expected that the issue of MEA condensation in the sampling lines would be eliminated.

Without this instrument SO<sub>2</sub> and SO<sub>3</sub> concentrations could only be estimated through calibration of MFCs and correct mixing and without external calibration. The absence of this instrument has a moderate impact upon the program and a significant impact on independent validation of SO<sub>x</sub> concentrations.

## A.7 Conclusion

Overall, the MEA environment proved to be extremely challenging for both research grade instruments. One noteworthy aspect is that amines, and specifically MEA, tended to degrade several materials. This degradation was observed not only with instruments, but also with polymers, such as electrical connectors, that came into long-term contact with the solvent during SDR operation. While it was known that amines degrade copper and its alloys, the problem of degradation of some polymers was not reported in the open literature.

Only one instrument, the LDA, operated in all conditions without fault. The APS was also relatively reliable and operated without fault over a larger portion of the project period.

As a side note, instrument failures can provide much information regarding how instruments could be potentially modified, or sampling systems revised, to allow future operation in a MEA system. Consequently, an important outcome from this work is the knowledge generated about the shortcomings of the instruments trialled, how such instruments may be modified for operation with future work, and which instruments are unsuitable for PCC monitoring.

### Core findings – Instruments

1. Research instruments such as the APS, EEPS, CPC, ELPI and optical particle counters are unsuitable for the longer-term monitoring of MEA-based PCC generated aerosol. For short-term operation, these instruments will require significant dilution of the aerosol sample to reduce exposure to the MEA absorbent.
2. Amines, and specifically MEA, tended to degrade a range of polymers, and this degradation was observed with instruments as well as fittings and electrical connectors. Amines are corrosive to copper and copper alloys, and thus appropriate precautions are necessary.

# Appendix B: Assessment of solvent-degradation rig operation

## B.1 First experiments

Initially, more than 200 experiments were completed to assess the performance of the solvent-degradation rig (SDR) apparatus and to determine its suitability to successfully undertake the proposed laboratory-scale investigation. The results of these experiments have been previously reported in the March 2018 Annual Report.

As outlined in that report, a range of abnormal and unexpected data sets were observed during these initial experiments. The results tended to display poor repeatability, and this prompted a critical and detailed reassessment and re-evaluation of SDR apparatus overall. A systematic investigation of targeted experiments was undertaken to ascertain the origins of these anomalies. Rather than provide the reader with an in-depth account of the experimental details of these anomalies, they will simply be noted.

Following a detail re-analysis of SDR aerosol data sets, it was identified that:

- Aerosol responses tended to show apparent diurnal and/or irregular fluctuations. Repeat experiments for identical conditions showed differing aerosol behaviours that often changed between morning and afternoon, but not consistently so.
- Condensation particle counter (CPC) aerosol responses, and especially the rate to return to background concentration following exposure to SO<sub>x</sub>, varied according to the time between refresh of the butanol fluid used in the aerosol counting process.
- CPC data sets sometimes showed negative aerosol responses to SO<sub>2</sub> and or CO<sub>2</sub> in the inlet gas stream.
- The presence of O<sub>2</sub> in SO<sub>2</sub> tended to increase aerosol formation rates for constant SO<sub>2</sub> concentrations.
- The monoethanolamine (MEA) solution appeared to 'condition' as it was exposed to SO<sub>3</sub>, resulting in aerosol being formed at a later time when the solution was exposed to CO<sub>2</sub>. Essentially, the CO<sub>2</sub> tended to drive the formation of aerosol depending upon the amount of solvent ageing. It was suspected that this was associated with the formation of ammonia during the degradation process with the CO<sub>2</sub> reacting with NH<sub>3</sub>.

After the in-depth reassessment, the SDR system was found to display a large degree of variability associated with aerosol formation. The investigation indicated that some of the variability of the SDR data sets originated from the chemical ageing process through exposure of MEA solvent over time to NO<sub>2</sub>, SO<sub>2</sub> and SO<sub>3</sub>. Essentially, the aerosol propensity of the MEA solvent at any time was a function of type and the duration of the target gases or the exposure history of the solvent. This appeared to be strongly the case for the gases SO<sub>3</sub> and NO<sub>2</sub>, as exposure to these gases tended to increase what could be considered the residual aerosol-forming potential of the solvent.

Effectively the results indicated that the baseline was constantly changing during the preliminary experiments.

Additionally, it was found that the solvent temperature was not fully regulated in all areas of the SDR system, allowing the solvent temperature to fluctuate according to ambient room temperature.

Following the assessment of the SDR rig, the thermal stability of the rig was further improved. An automated system was developed to replace the MEA solvent after each experimental series, thus maintaining new solvent in the SDR absorber at the commencement of each measurement series.

Further improvements included the complete automation of the rig so it could operate essentially unmanned 24 hours a day. This automation was a significant benefit, as it allowed a large number of experiments to be systematically undertaken. Consequently, background measurements could be made before and after exposure to the target gases of the experiment. In addition, experiments were completed in triplicate to assess reproducibility.

## B.2 Second-phase experiments (following solvent degradation rig modifications)

After the final automation modifications were completed, 550 experiments were undertaken using MEA, 870 experiments completed using Cal008, 132 experiments completed using ammonia and 463 experiments completed using the amino acid alanine.

Experimental conditions were maintained by the newly developed computer software platform, allowing reproducible experimental conditions to be defined and maintained over the duration of the experiment. Experiments were undertaken with NO<sub>2</sub>, SO<sub>2</sub>, NO and SO<sub>3</sub> as separate individual gases and as combination of these gases within a makeup gas of N<sub>2</sub>, Ar, CO<sub>2</sub> and O<sub>2</sub> with concentrations representative of a coal-fired power station.

At the start of the experiment, the initial base composition of the surrogate flue gas was delivered to the absorber. This was then altered by adding the target gas(es) in appropriate combinations and concentrations to achieve a final mixture. The duration of individual experiments was normally assigned to be 1 hour. This time was initially considered as a reasonable compromise between the time necessary for the SDR reaching steady-state conditions and a reasonable time period to demonstrate stable aerosol concentrations. As the study progressed, it became apparent that for some experiments, such as those using NO<sub>2</sub>/SO<sub>2</sub> and SO<sub>3</sub> mixes with aged solvent, the solvent quickly became 'conditioned' during the experiment, resulting in large numbers of residual aerosol being observed after 1 hour. This necessitated longer background times to 're-condition' the solvent to similar conditions to those at the beginning of the experiment. However, for some experiments, and generally those involving higher concentrations of SO<sub>3</sub>, the solvent did not revert to the original conditions even with an extended background run time of 20 hours. Consequently, for these cases, it appeared that the solvent was non-reversibly altered, with this change in solvent behaviour limiting the ultimate concentrations of the target gases.

Each target gas mix was repeated in triplicate with each 'target' gas experiment separated by a baseline experiment of at least a 1-hour. The baseline experiments consisted of passing the mixture of non-target gases through the absorber. Using this protocol, each experimental

combination required a minimum of 6 hours SDR run time. Normally, the SDR required between 2 and 5 minutes to reach steady-state after target gas flow commenced.

# Appendix C: Extracts from State of Knowledge – Review

## C.1 Aerosol characterisation

Aerosols generated by post-combustion capture (PCC) plants can impose a major cost factor on the plant as well as bringing about a number of environmental issues and costs. Aerosol formation and characterisation is highly complex. This section provides a brief introduction to the fundamentals of aerosol science.

### C.1.1 Definition and background

An aerosol is defined as a suspension of liquid droplets or solid particles in a gaseous medium, where the gas is usually air. Atmospheric aerosol particles have a broad size distribution that spans more than four orders of magnitude, including freshly born nuclei particles composed of a few molecules (~1–2 nm) to coarse particles composed of an agglomeration of smaller particles, whose diameter can be more than 10 µm (1, 2, 3). Hence, the chemical and physical properties of atmospheric particles can vary significantly within this wide size distribution.

A range of aerosol terminologies are used by researchers in different fields of science. In general, coarse particles are those with a spherical aerodynamic diameter of more than 1000 nm, fine particles those below 1000 nm, and ultrafine particles below 100 nm (3). Environmental regulatory agencies generally use mass-based terms such as particulate matter (PM)<sub>2.5</sub> or PM<sub>1</sub>, where the subscript indicates the cut-off for spherical particle diameter in micrometres (1). Particles can also be classified in terms of different modes (e.g. nucleation, Aitken, accumulation and coarse modes), each of which has its own formation mechanisms, source, deposition mechanisms, chemical compounds and size range (4, 5).

Aerosol science focuses on the generation, dynamics, transformation and removal of aerosols, and the influence of aerosols on the environment and humans. The following section explores the basic concepts used in aerosol science.

### C.1.2 Formation of particles – Terminology

The mechanisms by which particles are formed influences the properties of particles (6). Particles can be delineated into what is normally classified as primary and secondary particles on the basis of origin. Primary PM is directly emitted into the atmosphere by different anthropogenic and natural sources. These particles can be formed through attrition processes, such as grinding and abrasion of windblown crustal material, e.g. agricultural dust, as well as through combustion processes, e.g. diesel soot. Secondary aerosols form through gas-phase chemical reactions where products with reduced partial vapour pressures are formed, leading to aerosol formation. During some reactions desublimation occurs with the resultant formation of aerosol, which is called a *reaction aerosol* by some authors (7). An example of this reaction that is

of importance for the PCC processes is that of:  $\text{NH}_3(\text{g}) + \text{HCl}(\text{g}) = \text{NH}_4\text{Cl}(\text{s})$ . Aerosols that form as a result of crossing a dew point line are often called *condensation aerosols*.

While atmospheric particles can be formed in several ways, the most important particle formation mechanism in a PCC process is gas-to-particle conversion to produce condensation aerosols. However, once aerosols are formed and released from the PCC process, changes in humidity and vapour pressure may cause further changes in the aerosol, including droplet evaporation. This may lead to the formation of a solid phase of a more concentrated liquid droplets, and aerosol growth in the case of hygroscopic species (4, 5, 8).

## Nucleation

Vapour pressure is fundamental to aerosol formation or disappearance. Vapour pressure is defined as the pressure at which a liquid and a gas phases are in equilibrium (9) and is important for understanding aerosol formation and disappearance. Changes in vapour pressure may occur as a result of physical processes, such as dilution and cooling, or chemical changes, such as direct reaction between precursors and photochemical reactions.

The saturation ratio is a quantity that can be used for predicting aerosol formation or disappearance. This quantity is a measure of the equilibrium partial vapour pressure relative to the equilibrium saturated partial vapour pressure at the equilibrium air temperature (113, 4).

$$S = p_A/p_A^s(T)$$

where  $S$  is the saturation ratio,  $p_A$  is the partial vapour pressure at temperature  $T$ ,  $p_A^s$  is the saturated equilibrium partial vapour pressure at temperature  $T$ .

In simple terms, the saturation ratio provides a measure of aerosol formation or disappearance. When  $S < 1$  the vapour is unsaturated and aerosol formation is generally not favoured. When  $S > 1$  the vapour is defined as supersaturated and aerosol formation is favoured. Supersaturated vapour is always unstable. In a PCC context, temperature, vapour pressure and the saturation vapour pressure will be important for understanding and predicting aerosol formation and aerosol properties. While the saturation ratio indicates the likelihood of aerosol formation, it does not indicate the rate of aerosol formation, as this is determined by a wide range of factors.

Nucleation is the process by which particles are formed from gaseous chemical precursors and usually when the saturation vapour pressure exceeds one. Nucleation generally occurs by one of two main process modes – homogeneous nucleation mode and heterogeneous nucleation mode – each of which can be further delineated into two additional pathways.

- Homogeneous nucleation includes
  - homogeneous homo-molecular nucleation – in which gas molecules of the same chemical composition merge to form a sustainable, quantifiable aerosol
  - homogeneous hetero-molecular nucleation – in which gas molecules with different kinds of chemical composition merge to form a sustainable, quantifiable aerosol
- Heterogeneous nucleation includes
  - heterogeneous homo-molecular nucleation – in which gas molecules of the same chemical composition accumulate on particles with a different chemical composition to form a sustainable, quantifiable aerosol

- heterogeneous hetero-molecular nucleation – in which gas molecules with different kinds of chemical composition accumulate on particles with a different chemical composition to form a sustainable, quantifiable aerosol (4).

Where there exists an abundance of existing particles, heterogeneous nucleation is favoured and thus the initial particle size will be determined by the size of the existing particles. Homogeneous nucleation usually occurs in the absence of enough existing particles to cause heterogeneous nucleation, and the gaseous precursors condense to form stable aerosol. In this case the initial size of the aerosol at the time of nucleation will be very small.

Condensation describes the initial formation and growth of a particle (droplet or dry solid particle) as a result of gas condensing onto it. Such particles can be homogeneous or heterogeneous. The extent to which a particle grows (or potentially disappears) depends on the particle size, saturation ratio, surface tension and particle size relative to the mean free path of the gas. The mean free path is the average distance a gas molecule travels in the gas before it collides with another molecule. Depending on these parameters, different numbers of vapour molecules will collide with the aerosol particle surface; therefore, the growth rates will be different (4, 5).

Although supersaturated vapour is unstable, for modest degrees of supersaturation the rate of aerosol formation is very slow. However, as the degree of supersaturation increases, a critical value is reached where aerosol formation is experimentally observed, and this condition is defined as the critical supersaturation conditions for that species. The formation of an aerosol can be calculated by analysing the critical supersaturation conditions for the aerosol particles or droplets (a common practice when predicting cloud formation). The relationship between equilibrium aerosol size, chemical composition and ambient conditions can be described by the Köhler equation (10). This equation comprises a Kelvin term that describes the extra supersaturation needed to form and maintain a droplet with spherical curvature, rather than a flat surface, and a Raoult term that describes the lowering of the critical supersaturation conditions by solute artefacts. Understanding and being able to predict the critical condition for condensation in a PCC process is essential for understanding aerosol genesis and transport through the process.

### **C.1.3. Growth of particles**

#### **Coagulation**

Coagulation is the process whereby an aerosol particle collides with another aerosol particle to form a new, larger particle. The most common type of coagulation is thermal coagulation, which is a spontaneous reaction that occurs as a result of the Brownian motion of aerosol particles (4). The coagulation rate depends strongly on particle number concentration.

### **C.1.4. Classifying aerosols**

Fundamentally, aerosols can be defined according to their chemical composition and physical properties. However, the chemistry of most aerosols is complex; thus, aerosols are usually described using their physical attributes.

## Physical classification

### Aerosol size

Atmospheric aerosols exhibit a broad range of sizes spanning more than four orders of magnitude. The smallest aerosols comprise ensembles of molecules that are sufficiently large to remain stable; these are often called 'nucleation size particles'. The size of spherical aerosols can be described by a single dimension – diameter – and this greatly simplifies particle analysis. The diameter of spherical particles is often called the Stokes diameter. Coarser particles can be composed of agglomerates and can exhibit simple and complex geometries. Accurately describing size across such a wide range of possible geometries is a complicated mathematical undertaking that requires a multidimensional approach. In some fields (e.g. detailed computational fluid dynamics analysis of multiphase flow systems with highly complex and large particles), the uncertainties associated with equivalent spherical geometry become unacceptable, and thus multidimensional particle size analysis is used (11).

Aerosols of more complex geometric shapes require additional dimensions to accurately describe size. Alternatively, a correction factor or 'shape factor' can be used to account for non-spherical geometry in some cases. However, increased accuracy of shape comes at a cost, usually in terms of computing time and mathematical complexity. Consequently, a simplified approach is generally used that includes the definition of an equivalent spherical particle approach. Terms such as 'equivalent spherical diameter', 'Stokes diameter' and 'Stokes particles' are used to encapsulate the fundamental behaviour of geometrically complex aerosols, enabling them to be described by a single simplified dimension. However, this simplification comes at the cost of additional uncertainties with respect to particle size, especially the visual size (e.g. from microscopy studies). For example, the large and highly complex fractal-like geometries of diesel soot have greatly smaller Stokes diameters than those measured by microscopy. It is thus extremely difficult to deduce Stokes diameters from spectroscopy data sets.

For many cases, the uncertainty associated with the equivalent Stokes particle approach is acceptable, and this approach is widely used scientifically. Fortunately, for the case of the PCC absorber, such arduous analysis of particle size is not necessary, because aerosols are expected to be primarily comprised of liquid water phase.

The Stokes or ideal particle is defined as the spherical particle with unit density; hence, the use of the equivalent Stokes particle approach greatly simplifies particle descriptions. Atmospheric fogs and mists are good examples of Stokes particles.

The strict definitions of the most frequently used equivalent diameters are as follows.

- Aerodynamic equivalent diameter,  $d_a$ , is defined as the diameter of a sphere with standard density that settles at the same terminal velocity as the particle of interest (12).

Instruments that measure aerodynamic diameter include impaction sizing instruments such as the electrical low-pressure impactor (ELPI), micro orifice uniformly deposited impactor, aerodynamic particle sizers and cyclonic sizing devices.

- Electrical mobility equivalent diameter,  $d_m$ , is defined as the diameter of a sphere with the same migration velocity in a constant electric field as the particle of interest (13).

Instruments that measure electrical mobility diameter include the differential mobility analyser, a scanning mobility particle sizer and electrical engine particle spectrometer.

- Vacuum aerodynamic equivalent diameter,  $d_{va}$ , is defined as the aerodynamic diameter in a vacuum when the Knudsen number is much smaller than 1. In such a regime, the air flow is no longer described as a continuum, but rather as discrete collisions between the gas molecules and particles (12). The latter equivalence diameter is frequently measured in instruments that use low pressure (<1.5 Torr or 200 Pa), with aerodynamic lens systems as inlets, such as many aerosol mass spectrometers, including the Aerodyne aerosol mass spectrometer (12).
- Volume equivalent diameter,  $d_{ve}$ , is defined as the diameter of a sphere that has the same volume as the particle (14).

As the shape of a particle becomes more complex and diverges from spherical geometry, the above equivalent diameters also diverge. For example, large diesel soot particles displaying highly complex fractal-like geometry will exhibit different sizes in aerodynamic and electrical mobility diameter as a result of the complex shape.

### **Aerosol mass**

Particle mass concentration of PM is a fundamental measure of how much matter is present in the particle. Particle mass is defined as the mass of particles in one unit volume of air. Measurements of particle mass concentration are important for regulatory agencies, since air pollution and workplace exposure standards are reported on the basis of human exposure to the amount of matter.

Mass concentrations for regulatory purposes are delimited according to Stokes particle size on the basis of penetration into the lung, the most common being:

- $PM_{10}$  – mass of the particles with spherical equivalent aerodynamic diameters of less than  $10\ \mu\text{m}$  (particles  $>10\ \mu\text{m}$  Stokes diameter are considered too large to be inhaled into the human body)
- $PM_{2.5}$  – mass of the particles with spherical equivalent aerodynamic diameters of less than  $2.5\ \mu\text{m}$  (particles  $<10\ \mu\text{m}$  Stokes diameter are considered to be sufficiently small to be inhaled into the human lung)
- $PM_{1.0}$  – mass of the particles with spherical equivalent aerodynamic diameters of less than  $1.0\ \mu\text{m}$  (particles of  $<1.0\ \mu\text{m}$  Stokes diameter are considered to have a high penetration efficiency deep into the human lung).

The amount of total suspended particulates is also used as a measure of the total aerosol mass.

Each of the size-selective PM mass measures is a subset of the larger size particle set. That is,  $PM_{10}$  includes the  $PM_{2.5}$  mass fraction, as well as the fraction with a mass below  $PM_{10}$  but greater than  $PM_{2.5}$ .

The fundamental measure of mass concentration is by gravimetric methods. However, other indirect methods that calculate mass on the basis of another property, such as light scattering, are also in use (15). In addition, different light-scattering instruments can measure different light-scattering properties of the particle. Thus, these instruments can be influenced by different optical

limitations and interferences, and consequently report different mass results from the same particles.

### **Number concentration**

The particle number concentration within an aerosol is defined as the number of particles in the unit of volume of air (number/cm<sup>3</sup>). Recent studies have suggested that health effects caused by PM may be more sensitive to number concentration than to mass concentration (16, 17). However, this conclusion indirectly suggests that the penetration efficiency into the lung is a better measure of human exposure than simple exposure on a mass basis. There is also a growing suggestion in medical fields that the particles that present to the lung wall are those that have the greatest effect on human health.

Counters that monitor particle numbers can be categorised as direct and indirect detection instruments. Direct particle counters determine the particle number concentration by counting individual particles, which may be artificially grown to a larger optically active size. Indirect instruments estimate the particle number concentration by measuring some other qualities of the aerosol, such as light scattering or current flow in the case of charged particles (2). An example is the condensation particle counter (CPC).

### **C.1.5 Deposition and deposition mechanisms**

In aerosol science, deposition is the process by which particles within an aerosol are collected or deposited on a surface. Particles have different deposition mechanisms depending on their size (4), as explained below.

#### **Diffusion**

Brownian motion is the random movement of particles caused by collision between the particles and surrounding gas molecules. The movement and transport of particles caused by Brownian motion is called diffusion, and is described by the Stokes–Einstein equation. Brownian diffusion is the most effective deposition mechanism for particles smaller than 0.1 μm (18).

#### **Gravitational settling**

Deposition by gravitational settling is caused by the influence of Earth's gravity on particles suspended in the air. As the terminal velocity of particles is directly proportional to the size of the particles, this deposition mechanism is more effective on larger, coarse particles (19).

#### **Electrostatic attraction**

When a charged particle is exposed to an electric field, it will migrate at a velocity that is determined by a balance between the resisting electrostatic force and the aerodynamic drag that resists its motion (14). Thus, larger particles deposit more slowly than smaller particles due to electrostatic forces (2). The latter principle is used in many sizing instruments in order to classify the particles in a poly-disperse aerosol (14).

## Thermophoresis

Thermophoresis is a phenomenon observed in mixtures of mobile particles, in which the different particle types exhibit different responses to the force of a temperature gradient. Thermophoretic force results from a temperature gradient established in the gas medium. An aerosol in that temperature gradient experiences a force in the direction of decreasing temperature. Therefore, particles are directed and concentrated around the surfaces with lower temperature and are eventually deposited on them (5).

## Impaction

Larger particles have more inertia when in motion. Hence, they tend to maintain their velocity and not follow changes in the direction or speed of the flow, so they may impact and stick to the wall of the exhaust or sampling system. It is clear that impaction is the dominant deposition mechanism for larger particles in a flow, particularly for coarse mode particles larger than  $0.5\ \mu\text{m}$  (14, 2, 20). Impaction is a critical process for aerosol removal and is critical for understanding aerosol removal in demisters.

## C.2 Particulate matter emissions from a post-combustion capture plant

The stack emission from a PCC plant can be in the form of vapours or gases, and aerosols. Emission in the form of vapours or gases is well understood, and there are extensive standards to guide representative sampling and quantify the wide array of volatile, semi-volatile and solid-phase species released by industry. New analytical methods are being developed to quantify the concentrations of both new and existing absorbents and their decomposition products. Nevertheless, analytical methods development is a mature and well-developed science. In addition, new analytical instruments are greatly improving the sensitivity of analytical methods. Conversely, understanding the issues associated with aerosols in PCC plants is less mature, because it has not been widely or comprehensively studied (21, 22, 23, 24), including the influence that the flue gas supplied to the PCC plant has on the final pollutant makeup, especially the influence of  $\text{H}_2\text{SO}_4$  precursors (21,25, 26, 22, 27, 28, 29).

Rao and Rubin (30) were one of the first to examine amine-based carbon capture for flue gas clean-up, and reported that the presence of acid gas impurities in power plant flue gas adversely affects the performance and cost. More recently, it has become evident that these impurities may lead to increased degradation of the amines, and thus produce emissions of organic components together with the flue gas (30). Environmental concerns associated with PCC aerosol emissions were first raised during the Electric Power Research Institute amine workshop (31). Kamijo (MHI) noted difficulties in amine mist control using conventional demister technologies and highlighted the need for a special (MHI proprietary) demister. In addition, Kamijo raised concerns regarding the high sensitivity of aerosols to  $\text{SO}_3$  concentrations in the flue gas.

Mertens et al. (32) reported that both the number concentration of fine PM in the flue gas and the concentration of nuclei-forming volatile species are most likely to be important drivers for the formation of larger amine aerosols. This is an important observation, because submicron ( $<1\ \mu\text{m}$ )

PM serve as condensation nuclei and thus facilitate heterogeneous nucleation pathways (32). Consequently, accurate characterisation of the inlet flue gas phase of a PCC facility is critical. Mertens et al. (32) concluded that it is crucial to understand aerosol formation in the PCC process, and vital to use real flue gas to understand complex aerosol formation chemistry. A common consensus on this aspect is reported in the scientific literature (32).

Flue gas that contains sufficient aerosol nuclei ( $>10^6$  particles/cm<sup>3</sup>) may result in economically and environmentally unacceptable amine emissions from liquid aerosol (smaller than 2.5 µm droplets) (33). The wide range of aerosol nuclei reported in the literature indicates that the chemical form of the aerosol nuclei is not critical, and H<sub>2</sub>SO<sub>4</sub> (1–10 ppmv), low volatility or condensing species, fly ash of sufficient small size and entrained salts can act equally well as nucleation drivers under suitable conditions. An important note is that several PCC pilot plants attached to coal-fired power stations release abnormally high pollutant levels and have observed concentrations of amine carryover that are about five times the expected value. In one example, amine emissions exceeded 10 ppm from the water-wash systems where the emissions were expected to be about 20% of this value (33). One explanation is that the aqueous nuclei have an amine concentration that is rich in CO<sub>2</sub> and thus the CO<sub>2</sub> absorption equilibrium remains closer to the carbamate form. Consequently, in this case the bulk amine solution has a lower CO<sub>2</sub> loading. Depending on aerosol size, for most amines, the amine vapour pressure of the bulk solution will be greater than that of the aerosol, and thus the amine transfers to the aerosol, taking with it CO<sub>2</sub> and additional water. If these nuclei grow but stay smaller in size than about 2.5 µm, then they are not captured within conventional water-wash systems (34). If aerosol nuclei grow to sizes larger than 2.5 µm then these droplets may be captured in the water wash.

Khakharia et al. (34) suggested that this ineffectiveness arose from these smaller aerosols following the trajectories of the gas flow lines and not being captured by impaction with the demister structure (34). Such information is consistent with and underpinned by conventional multiphase flow physics. This physics is critical for understanding aerosol dynamics and capture processes, as it positively shows the importance of quantifying the concentration of aerosol nuclei, and the growth rates of the aerosol once it has formed. In addition, the residence time of the aerosol before passing to the water-wash section of the PCC plant will be critically important. This aspect has been further highlighted by Branchert, Kochenburger and Schaber (22), who reported that due to the small sizes of formed particles, even after coagulation and considering the residence time of around 10 seconds, it may be difficult to precipitate aerosols using common methods (22). Consequently, this information suggests that mechanisms that accelerate aerosol growth kinetics to sizes of greater than 2.5 µm in the period before the aerosol enters the water wash may increase aerosol removal efficiencies of the demister. Conversely, as also highlighted by Branchert, Kochenburger and Schaber (22), species that increase the critical saturation temperature of aerosols or increase aerosol surface tension according to the Kelvin effect, may increase aerosol instability, inhibit aerosol growth or stimulate aerosol disappearance (22). With this complicated mechanism, results should be expected to vary with the type of amine solution, process and flue gas source (33). Technology suppliers such as Mitsubishi Heavy Industries (MHI), Aker and BASF have all reported successful testing of countermeasures to minimise amine aerosol emissions. BASF discussed use of a dry bed of packing between the absorber and water wash with some success (35).

A common observation from both pilot plant research and more general PCC emission studies is that resolving the problem of aerosol formation is a key part of reducing possible atmospheric releases from amine-based CO<sub>2</sub> capture plants. This idea is now gaining a significant voice internationally and is a key issue in the conclusions of more recent PCC aerosol studies. The failure of conventional wash columns, and the potential financial impact of improving the efficiency of particle collectors, necessitates further targeted fundamental research to identify efficient processes for controlling emissions for large-scale processes. Understanding interconnectivities between the operating conditions of the bulk CO<sub>2</sub> removal process and aerosol dynamics will provide the necessary insight required to either design new systems or enhance existing systems for suppressing droplet growth or, conversely, to condition aerosols for easier removal (36, 28). The influence of the oxides of sulphur on aerosol formation is also likely to be critical.

Although MEA is a common and widely researched PCC absorbent, the link between particle number concentrations of the inlet flue gas and aerosol emissions from the PCC plant has only recently been experimentally confirmed (21). This work has also shown that operating parameters, and especially the presence of CO<sub>2</sub>, influence the extent of aerosol genesis. Increasing the temperature of the lean absorbent results in a lowering of the amine emissions. Aerosol-based emissions are observed only at a relatively high lean pH. As the CO<sub>2</sub> content of the flue gas is reduced from 12.7 to 0.7 vol.%, a maximum in the emissions is normally observed at 6 vol.% CO<sub>2</sub>. Several authors have found that particle number concentration, the degree of supersaturation, and the reactivity of the amine are important for understanding aerosol-based emissions in a CO<sub>2</sub> capture absorber (37, 7). These observations add to the existing understanding of aerosol formation and growth by incorporating the theory of heterogeneous nucleation into the analysis of counter-current gas–liquid absorption processes (21).

The economic costs associated with loss of amine due to thermal and oxidative degradation has been the main historical driver for the development of new and more stable amines. However, pilot plant studies have increasingly shown that aerosol emissions can dominate the amine losses from the process (34,26). These economic drivers are focusing new efforts towards vapour emissions control and minimising aerosol formation.

In March 2017, the importance of the genesis and fate of aerosols in the PCC process was validated within the Norwegian national program for research, development, piloting and demonstration of CCS technologies (CLIMIT). This program affirmed the importance of the problem that aerosols present to the wider deployments of PCC technology (38, 39). A new 12-month study to provide ‘results pertaining to urgent issues in full-scale CO<sub>2</sub> capture projects’ has been awarded, with a primary focus on understanding the problems of aerosol genesis and transport pathways through a PCC plant (38). This watershed research program demonstrates the critical importance placed on PCC aerosol science by European research organisations, as it includes many European stakeholders that are both commercial stakeholders and government bodies.

While findings from that study may apply to the Australian PCC deployment plan, Australia has many unique aspects associated with both flue gas composition and coal-fired power plant operations. Consequently, the unique challenges that are likely to confront Australian coal-fired power operators in the wider deployment of PCC will potentially limit the direct application of European and US findings to the Australian scenario. The importance and sensitivity of aerosol

formation to multiple factors has been clearly demonstrated by international research. Since Australian power generators do not currently use acid gas clean-up technologies, it is likely that the influence of SO<sub>x</sub> and NO<sub>x</sub> will be significant in determining the pollutants from the Australian approach to clean coal, as well as the other flue gas clean-up techniques that will be necessary to meet regulatory guidelines. Pollution clean-up technologies, such as different fabric filter technologies, are also likely to affect the inlet flue gas particle size composition, and thus the nucleation potential for a retrofitted PCC plant.

The presence of sulphur in coal leads to aerosol generation. SO<sub>3</sub> is also formed from the catalytic oxidation of SO<sub>2</sub> inside a selective catalytic reduction system during the reduction of the NO<sub>x</sub>. In wet flue gas desulphurisation (WFGD), the quenching of flue gas temperatures rapidly initiating supersaturation of the flue gas assists in converting incoming gaseous H<sub>2</sub>SO<sub>4</sub> precursors to homogeneously nucleated aerosol droplets. Therefore, designing countermeasures for aerosol emissions is crucial for cost-effective and environmentally benign commercial applications of PCC technology (25, 40, 7). The ramification of SO<sub>x</sub> gases for PCC and the complexity of the chemistry of these oxides are detailed in Section 3.1.

In one of the most important reported PCC aerosol studies, a consortium of European researchers conducted detailed experiments on a pilot PCC plant and concluded that aerosol emissions of the plant depend on several factors, as outlined below (25).

- Change of temperature of the mixture in the absorber column: In the absorber column, the temperature of the gas increases as the gas moves up the column due to the exothermic reaction between CO<sub>2</sub> and monoethanolamine (MEA). The temperature of the flue gas reached its maximum typically at two-thirds of the column. The temperature decreases as it reaches the upper section of the column, causing a drastic rise in the saturation of the mixture. Hence, there is a potential for heterogeneous nucleation and growth of particles due to condensation of water and MEA. Figure 39 in Section 4.4 showed an example of the temperature profile along the absorber, including the 'temperature bulge' at about 3 m height for this example. Such temperature changes can have significant influence on the supersaturation ratio and thus aerosol-formation potential.
- Effect of inlet flue gas CO<sub>2</sub> concentration: The concentration of CO<sub>2</sub> in the flue gas can vary from 2 to 13%. The supersaturation ratio along the column increases as the CO<sub>2</sub> content in the flue gas is reduced.
- Effect of lean absorbent temperature: The change in the lean absorbent temperature affects the temperature of the flue gas in the column. Thus, higher temperatures would cause less of a temperature gradient after the hot zone in the absorber, decreasing the supersaturation ratio.
- Loading of the lean absorbent: As the loading of the lean absorbent increases, the transfer of CO<sub>2</sub> to the absorbent shifts lower in the column. Therefore, most of the corresponding heat is also released in the lower sections of the column, resulting in an increase in the supersaturation ratio in the lower section of the column (21).

It is clear that emissions of organic components must not only be monitored but also minimised, since their release to the atmosphere may cause environmental concerns (51). There will be a continued need for research into these emissions, particularly for new and increased efficiency absorbents whose environmental impacts may not have been investigated. The current scientific

literature describes the volatility and degradation of amines, but generally under controlled laboratory conditions, with fewer pilot plant scale studies (41, 42, 43, 44).

Although amine-based PCC is a promising technology, amine emissions in the form of aerosols must be controlled for this technology to be commercially successful (45). In addition, there are conflicting findings in the details from some studies. Thus, research is needed to crystallise the primary drivers of aerosol formation and stability so that control measures can be applied.

### C.2.1 Role of SO<sub>2</sub> and SO<sub>3</sub> in new particle formation

It has been extensively reported that SO<sub>3</sub> present in the flue gas from coal-fired power stations can cause aerosol formation. For example, for many years, coal-fired power operators have used electrostatic precipitator (ESP) technologies to control fly ash emissions. To improve capture efficiencies for some fly ash types, oxidised sulphur is injected into the flue gas stream upstream of the ESP to precipitate fly ash. Due to the strong reaction of water vapour and SO<sub>3</sub> in flue gas, H<sub>2</sub>SO<sub>4</sub> is formed after injection to the flue gas, precipitating additional (and finer) fly ash particles. This injection also changes the resistivity of the formed particles, which helps to improve particle capture efficiencies of ESP units.

The phenomenon of aerosols for PCC, however, has only more recently been reported (46). SO<sub>3</sub> will be present in the flue gas as H<sub>2</sub>SO<sub>4</sub> due to the water vapour and abundance of liquid water present in the gas phase. MHI reported work identifying aerosol problems from SO<sub>3</sub> in the flue gas, and resolved the problem with SO<sub>3</sub> countermeasures, such as the development of a new multistage water-wash section and a simulator that predicts SO<sub>3</sub>-derived mist (46).

WFGD is a common technology to remove SO<sub>x</sub> from the gas phase before release from an emissions stack. However, the gas-phase H<sub>2</sub>SO<sub>4</sub> condenses in an FGD system as it crosses its dew point, and thus leads to formation of H<sub>2</sub>SO<sub>4</sub> aerosols. Moreover, coal-derived flue gas contains other PM such as soot, fly ash and salts. These pollutants, in addition to H<sub>2</sub>SO<sub>4</sub> aerosols, can act as nuclei for further aerosol formation and growth in the absorber column of a PCC plant. Mertens et al. showed that the appropriate use of a gas/gas heat exchanger before the FGD system would minimise H<sub>2</sub>SO<sub>4</sub> nuclei before the amine scrubber and therefore reduce amine aerosol emissions (47). The Netherlands Organisation for Applied Scientific Research demonstrated the use of a Brownian diffusion filter to remove the aerosol after the water wash. Despite some success with these measures, many problems remain because the mechanisms and countermeasures are not yet completely understood.

Brachert et al. investigated the role of H<sub>2</sub>SO<sub>4</sub> in aerosol emissions of the PCC plant and found a strong delineation between H<sub>2</sub>SO<sub>4</sub> concentrations and nucleation mode aerosols (25, 22). During thermal quenching in absorption processes, the gas phase may become supersaturated due to simultaneous heat and mass transfer. Subsequently, nucleation and aerosol formation will occur. For most strong acids, heterogeneous nucleation on pre-existing foreign nuclei is the dominating mechanism of nucleation in flue gas absorption processes. If H<sub>2</sub>SO<sub>4</sub> is present in the flue gas, the dominating mechanism is homogeneous nucleation only, in the form of H<sub>2</sub>SO<sub>4</sub> and water itself, without the need for foreign nuclei. This phenomenon is predicted theoretically.

Fulk et al. (2016) completed laboratory-scale measurements using H<sub>2</sub>SO<sub>4</sub> aerosol injection and pilot-scale experiments to SO<sub>2</sub> and SO<sub>3</sub> artefacts (48). They observed that total amine emissions

are a function of the inlet SO<sub>3</sub> content in the flue gas, the location and magnitude of the temperature bulge in the absorption section, the use of absorbent intercooling and the amine content in the water wash (48). This US work is ongoing, and the findings are consistent with similar research findings from European agencies.

The formation of aerosols can lead to further problems, because the absorbent and other harmful components may absorb onto those forming aerosol droplets and be carried through the process with the H<sub>2</sub>SO<sub>4</sub> aerosol (25). The submicron-sized droplets are difficult to precipitate and may pass through spray towers, packed bed scrubbers and venturi scrubbers (22).

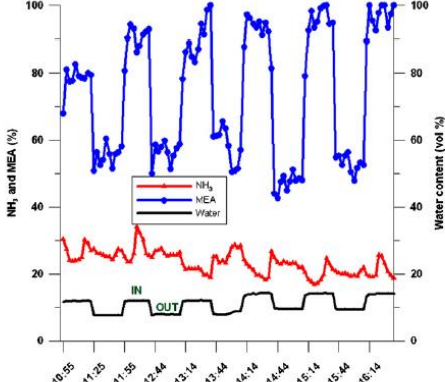
Published literature has shown that the efficiency of WFGD decreases according to the degree of formation of submicron particles of H<sub>2</sub>SO<sub>4</sub>. Also, the formation of H<sub>2</sub>SO<sub>4</sub> particles in the column reduces the SO<sub>2</sub> absorption rate considerably (34). The presence of deNO<sub>x</sub> systems with catalytic convertors tends to escalate the issue because the operation of catalytic convertors leads to higher conversion rates of SO<sub>2</sub> to SO<sub>3</sub>. The oxidation of SO<sub>2</sub> to SO<sub>3</sub> could also occur as a result of ozone formation in the electric high-voltage fields of the ESP (25). Thus, the efficiency of wet electrostatic precipitators (WESP) can vary depending upon the aerosol size, with WESP reported to produce aerosol in high H<sub>2</sub>SO<sub>4</sub> conditions (25).

There have been contradictory findings with respect to the impacts of number concentration of particles and the correlation to the concentration of H<sub>2</sub>SO<sub>4</sub> in the flue gas. Brachert et al. (21) reported that these H<sub>2</sub>SO<sub>4</sub> particles are due to homogenous nucleation, because the injection of foreign seed particles does not affect the concentration of the PM (25, 22). The authors concluded that owing to the small sizes of the formed particles and the residence time in the process, it may be difficult to precipitate aerosols using common methods (25, 22). Contradictory results were found by Moser et al. (49) based on several testing campaigns at the PCC pilot plant at the RWE power plant in Niederaussem, Germany. The authors concluded that ultrafine solid Na<sub>2</sub>SO<sub>4</sub> particles in the flue gas flow act as nuclei for aerosol formation, and that these particles are important for predicting the level of aerosol emissions. They also found that aerosol emissions from organic compounds are likely when the number concentration of aerosol droplets exceeds about 1 x 10<sup>5</sup> cm<sup>-3</sup> in the flue gas upstream of the CO<sub>2</sub> absorber (49). This study suggests that amine-based PCC at coal-fired power stations will be more involved than simply removing SO<sub>3</sub> from the flue gas to avoid H<sub>2</sub>SO<sub>4</sub> droplet formation. A simple SO<sub>3</sub>/H<sub>2</sub>SO<sub>4</sub>-dependent, homogeneous nucleation mechanism cannot explain that solid nanoparticles – mainly comprising Na<sub>2</sub>SO<sub>4</sub> – are found to be decisive for the aerosol-based emissions. This is an important finding and indicates that solid-phase particulates should be investigated for aerosol genesis in addition to SO<sub>2</sub> and SO<sub>3</sub>.

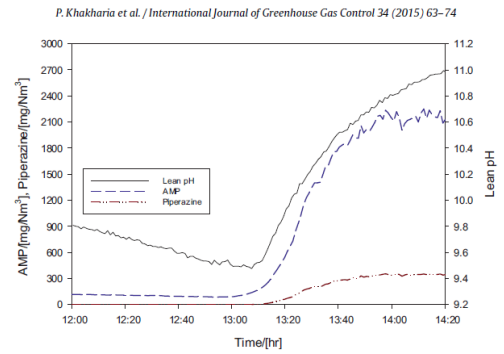
There has been experimental work done in which various parameters are altered to investigate the effect on solvent (MEA) emissions. Table C.1 maps the experimental parameter space and briefly presents results.

**Table C.1 Summary of experimental investigations of the significance of SO<sub>3</sub> for aerosol formation and findings**

Author	Experiment	Result
Brachert et al., 2014 (25)	Varies dilution of sample gas stream for measurements with condensation particle counter (CPC) and electrical low-pressure impactor (ELPI) while varying	CPC & ELPI are viable options for measuring sulphuric acid particles/fog in post-combustion capture (PCC) processes and both gave number concentrations in the order of 10 <sup>8</sup> particles/cm <sup>-3</sup>

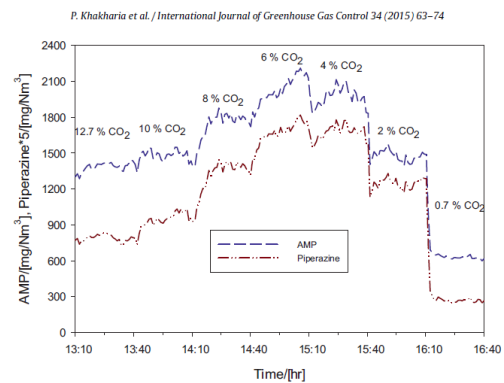
	SO <sub>3</sub> concentration in surrogate flue gas stream	
Kamijo et al., 2013 (46)	Varies low SO <sub>3</sub> concentrations and investigates the effects on the solvent emissions	Significant increase on solvent emissions with increase in SO <sub>3</sub> in flue gas. Even at concentrations as low as 1 ppm SO <sub>3</sub> monoethanolamine (MEA) emissions increased from 0.8 to 29.8 ppm
Mertens et al., 2013 (50)	Running long-term experiment (~3600 h) with real flue gas at fixed operating conditions	MEA emissions are sporadic in nature. Hypothesised that this variability is due to changes in flue gas composition, but suggested it could also be due to changes in solvent chemistry over time
	Non-isokinetic sampling for MEA	Found that the solvent contained mist particles that are very small as isokinetic and non-isokinetic sampling methods gave the same results in MEA concentrations
	Looked at the effect of water washing the gas leaving the plant	 <p>Fig. 6. Single stage water wash shows no effect on the NH<sub>3</sub> emissions and reduces the MEA emissions up to 50% (water concentration is plotted to show the sampling location: lower water contents are found behind the water wash due to the lower flue gas temperature).</p>
Khakharia et al., 2015 (21)	Varying temperature in absorber column (& therefore supersaturation level)	<p>Showed a decrease in particulate MEA from 1900 mg.Nm<sup>-3</sup> as temperatures rose from 40°C to 60°C at 1200 mg.Nm<sup>-3</sup></p> <p>As temperatures in absorber were increased further an expected rise in gaseous MEA was emitted</p>
	Change of solvent from MEA to 2-amino-2-methyl-1-propanol (AMP) and piperazine	The emissions followed a similar pattern as MEA when SO <sub>3</sub> , and therefore homogeneous mist particles were varied

Varying the stripper temperature and therefore changing the lean solvent loading and therefore changing the lean pH



As the pH of the lean solvent increases (i.e <math>CO\_2</math> loading) the temperature in the absorber increases as more  $CO_2$  is absorbed in the solvent during the process. The emissions of solvent are correlated to one or both of these functions. i.e temperature or  $CO_2$  take up

Varying  $CO_2$  concentration in flue gas from 0.7 to 12.7 vol%



Emissions hit a maximum at 6%  $CO_2$

Using AMP-Ktau (amino acid) and alternating  $SO_3$  in flue gas and no  $SO_3$  in flue gas

AMP emissions basically not affected by the presence or lack of  $H_2SO_4$  aerosols in the flue gas, suggesting emissions are in the vapour phase only. However, this is not behaviour noted in the AMP-piperazine experiment where emissions were indeed correlating to changes in  $SO_3$

Khakharia et al., 2013 (51)

Adding soot produced by incomplete combustion of natural gas into the gas stream

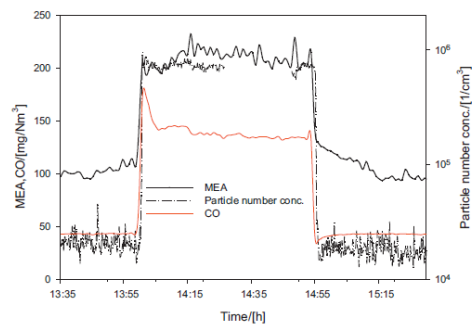


Fig. 5. Effect of particle number concentration of soot on MEA emissions. CPC which measures the particle number concentration was not connected for short intervals and thus, there are no measurement data points for this time interval. The horizontal axis represents the time of the day in hours during which the experiment was performed.

MEA emissions double when the particle number concentration increases by 2 orders of magnitude

Varying SO<sub>3</sub> in flue gas

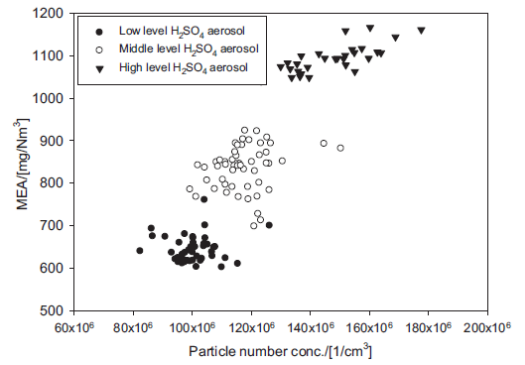


Fig. 8. Effect of different H<sub>2</sub>SO<sub>4</sub> aerosol number concentrations in flue gas on MEA emissions. (●) represents the low level H<sub>2</sub>SO<sub>4</sub> aerosol concentration with average particle number concentration of  $1.02 \times 10^8$  per cm<sup>3</sup>, (○) represents the middle level H<sub>2</sub>SO<sub>4</sub> aerosol concentration with average particle number concentration of  $1.18 \times 10^8$  per cm<sup>3</sup> and (▼) represents the high level H<sub>2</sub>SO<sub>4</sub> aerosol concentration with average particle number concentration of  $1.42 \times 10^8$  per cm<sup>3</sup>.

MEA emissions are also increased with an increase in number concentration of H<sub>2</sub>SO<sub>4</sub>

A range of experimental and theoretical work as displayed in Table has been completed over recent years to gain some understanding of the effects that SO<sub>3</sub> in flue gas has on PCC processes emissions. While the production of homogeneous and heterogeneous particles in absorbers seems to be well understood, there are gaps in the knowledge as to how real flue gas will influence the emissions of solvent. Khakharia et al. (51) has done some work to map out the effects of various parameters including the influence of SO<sub>3</sub>. However, there is still much experimental work and understanding to be gained from undergoing a systematic experimental campaign.

### C.2.2 Supersaturation and particle emission

Aerosol formation and growth in gas–liquid contact devices such as absorption columns has been extensively studied for the quenching of acid gases (22, 37, 23, 24,7). Aerosol formation by heterogeneous nucleation in a counter-current absorption of HCl in water has been studied by Wix et al. (52) and similar mechanisms are expected to occur in a counter-current absorption of CO<sub>2</sub> in an absorbent (52).

Conditions for supersaturation to occur in an amine absorption plant lie just past the so-called ‘temperature bulge’, where the temperature reaches a maximum (typically at a distance of two-thirds of the total packing height from the bottom) and further cools at the top of the column. This thermal quenching can lead to a significant temperature difference between the gas and liquid phases, resulting in the supersaturated environment.

Khakharia et al. (15) investigated the degree of saturation along a CO<sub>2</sub> capture absorber column using a rate-based approach in Aspen Plus. They showed that the maximum saturation occurs at the top of the column and in the range of 1.05–1.2 depending on the operating parameters. In the presence of nuclei and supersaturation in the flue gas, the volatile components can condense on these nuclei, leading to a growth of aerosol droplets (34). Mertens et al. measured a slightly lower particle number concentration at the outlet of the absorber than at the inlet, and attributed this to possible coagulation in the absorber column. However, the growth of particles by means of condensation is expected to be the dominant mechanism (53). Moreover, amine-CO<sub>2</sub> reactivity is

essential for aerosol growth from volatile amine species (21). Similar results have been reported by Fulk et al. (48).

### C.2.3 Predicting particulate matter emissions from post-combustion capture plants

Developing predictive models capable of accurately estimating the PM emissions of the PCC plant is a challenging undertaking because of the complexity of the system. The impacts of various process parameters (e.g. the inlet flue gas CO<sub>2</sub> concentration, the temperature of the lean absorbent and the CO<sub>2</sub> loading of the lean absorbent) on the supersaturation profile along the column must be considered, and often not all of these are known. In addition, aerosol formation can be driven by subtle factors that are not captured by simple models.

However, aerosol-based emissions of absorbent and its components from a PCC plant will need to be understood in detail from both an experimental and theoretical perspective for any broad-scale industrial deployment, because of its impact on the environment and the operating costs. As Khakharia et al. state in (34), 'It is important to understand the mechanism of aerosol formation and growth so that appropriate countermeasures can be applied in reducing the total emissions'.

So far, only simplified methods are proposed for predicting aerosol-based emissions from a CO<sub>2</sub> capture column of a PCC process. The basis of these methods is to split the counter-current gas–liquid interaction from the counter-current gas–aerosol interaction. The absorption column is discretised into multiple alternating gas–liquid and gas–aerosol sections in Aspen Plus, with an assumption that aerosols behave as a continuous phase rather droplets. The degree of supersaturation, which is important for aerosol formation and growth, is calculated along the column. The effect of the changes in parameters of the PCC plant are investigated; parameters include the CO<sub>2</sub> content of the inlet flue gas, the lean absorbent temperature and the lean absorbent loading on aerosol-based emissions.

In general, the aerosol-based emissions follow the trend of the supersaturation ratio at the top of the absorber column. Khakharia et al. (34) propose an approach for predicting aerosol-based emissions with absorbents other than MEA and in reactive absorption processes (34). The authors conclude that more in-depth research is needed and that research on this topic be directed towards comparing the model results with experiments to validate the model (34).

Khakharia et al. explain the development of a model that makes a number of assumptions to simplify solution algorithms (34). These include:

- constant number concentration at  $10^{13}$  to  $10^{14}$  per cubic metre of gas
- spherical aerosols
- the whole aerosol phase being modelled as bulk liquid
- no nucleation, only growth of pre-existing particles
- chemical reactions only in the liquid phase
- no direct contact with between the liquid and particulate phase
- the surface area of the particles being neglected
- the Kelvin effect being neglected.

The model is then used to predict the PM emissions of the PCC plant and the related size distribution. The authors conclude that more efficient models are needed, and more experimental works should be carried out to validate the model (34). However, model development cannot occur in isolation, and thus significant experimental aerosol data are required to both validate and provide empirical input data to model algorithms (34).

#### C.2.4 Absorbent management

The flue gas in Australian coal-fired power stations typically contains 100–600 ppm SO<sub>2</sub> and trace levels of SO<sub>3</sub> (54, 55). Unlike most developed countries, Australian power stations are not required to remove SO<sub>x</sub> from flue gas (55). As SO<sub>2</sub> is very water-soluble, it rapidly oxidises to sulphate in the presence of dissolved oxygen. Sulphate is a much stronger acid than CO<sub>2</sub> and forms heat-stable salts with amines such as MEA, reducing the CO<sub>2</sub> absorption capacity of the PCC absorbent (56, 54).

A number of processes have been used in the natural gas sweetening industry to manage corrosion and absorbent purity by separating heat-stable salts and other degradation products from MEA (and other amine absorbents). These purification techniques include distillation, electrodialysis, and ion exchange or activated carbon filters, and are described in detail by Kohl and Nielsen (57).

Amine losses to the stack present environmental problems. The amine can participate in atmospheric reactions to produce ozone and other toxic compounds. The makeup cost of amine lost through stack emissions will be economically significant, especially with more expensive amines. Higher amine volatility will also increase the capital cost of the water-wash system (41).

The volatility of an amine in a given loaded system can be adequately represented by its apparent activity coefficient. As loading is increased, the amine volatility or its apparent activity coefficient decreases accordingly, as there is less free amine present in the solution due to greater CO<sub>2</sub> consumption (41).

It appears that the less volatile systems have higher amine (apparent) partial molar excess enthalpies. There is no apparent correlation between amine volatility and the amine heat of vapourisation (41). Aerosols were found to be the major contributor to overall emissions. A Brownian demister unit (BDU) was also tested as an emission-reducing technology and found to be efficient in reducing aerosol emissions. The emission levels of MEA at the capture plant were higher than initially anticipated; however, there are several factors that may account for this. The exhaust gas may have a high content of condensation nuclei. In combination with temperature gradients in the absorber, this can result in high absorbent concentration in mist (27).

There is abundant scientific evidence showing that one of the main mechanisms of PCC absorbent loss is aerosols. Aerosol-driven emissions can easily exceed vapour pressure driven absorbent loss by two orders of magnitude (58). Three ways of dealing with aerosol emissions and MEA migration (59) are:

- minimising PM formation
- minimising particle loading with amine
- growing the particles so they can be collected using conventional methods.

Moser et al. identified five different process configurations to mitigate emissions and their interaction, tested in individual operations or coupled operations (59):

- water-wash temperature
- acid wash
- dry bed
- flue gas pretreatment
- WESP.

It was demonstrated over many thousands of plant-operating hours that emissions caused by both vapour pressure and aerosol formation could be reduced up to an order of magnitude by three different mitigation measures as follows.

- Aerosol formation can be minimised as far as possible when the solid, inorganic particles that trigger the emissions are removed before they enter the CO<sub>2</sub> capture process. This can be reached by a pretreatment of the flue gas; for example, oversaturating of the flue gas by cooling or steam injection (to initiate the growth of the solid particles by condensation to a size that is sufficient for their separation) or by special prescrubbing techniques and ESP before the flue gas enters the CO<sub>2</sub> absorber.
- The WESP can decrease the number concentration of particles larger than 50 nm. The WESP has two opposing effects. It supports the proprietary pretreatment technique by removing solid particles, especially from the second, larger fraction of the bimodal size distribution of particles and droplets around 100 nm. However, it also produces especially small aerosol droplets or particles of the first mode of the bimodal size distribution.
- Using counter-current multistage dry bed configuration reduces the concentration of the absorbent components in the gas phase.

It is also concluded that solid particles of below about 250 nm seem to be responsible for aerosol formation and absorbent loss in PCC plants (59).

## C.2.5 Environmental effects

It is essential that the commercial-scale deployment of PCC achieves a net positive environmental impact. Consequently, the substitution of the enormous anthropogenic CO<sub>2</sub> emissions from coal-fired power stations with low-level emissions of ammonia and volatile organic compounds, as well as aqueous and solid waste streams, must be carefully considered. Preliminary environmental assessments from PCC pilot and full-scale plants have suggested that human and environmental impacts will be mild, but fresh water ecotoxicity is expected to increase (60).

Absorbent reclamation is an integral part of the natural gas sweetening industry, but this has received modest attention during the development of aqueous amine absorption for PCC. While several technologies that have been developed within the natural gas industry may be suitable for PCC absorbent reclamation, adapting and developing technologies to new degradation products will require further research. However, absorbent reclamation also generates additional aqueous or solid waste streams; thus, appropriate methods of treating, reusing and disposing of these wastes need to be investigated (32, 57).

Current PCC pilot plant programs provide excellent opportunities for validation of laboratory simulations of absorbent degradation and volatile emissions. This is also an opportunity to develop and validate absorbent reclamation and absorbent monitoring technology for PCC as well as understanding absorbent loss modes. Extended waste monitoring and management practices, including liquid and solid wastes and absorbent management practices, will ultimately ensure that PCC of CO<sub>2</sub> from coal-fired power stations has a net positive human and environmental benefit (61).

Nitrosamines are assumed to be formed from reactions between secondary and tertiary amines and NO<sub>x</sub>, both in the absorber and in the atmosphere. There are several major uncertainties in the selected nitrosamine assumptions, such as formation time and conditions, stability and resulting concentration levels in the plant and surroundings. Formation of nitrosamines has been experimentally observed in laboratory experiments (4).

Secondary amines react with the nitrite ions at stripper conditions to make carcinogenic nitrosamines, which may create significant secondary environmental impacts if released into the atmosphere. Fine (2015) has completed a comprehensive dissertation on the formation and fate of nitrosamines in amine scrubbing (62). Nitrogen dioxide contained in the flue gas as 2–5% of the total NO<sub>x</sub> is partially removed in a typical SO<sub>2</sub> polishing scrubber. With the addition of thiosulphate and ethylenediaminetetraacetic acid to inhibit oxidation, or the addition of triethanolamine or other cheap tertiary amines, it should be possible to remove 70–95% of the NO<sub>2</sub> in the polishing scrubber. Residual NO<sub>2</sub> will be removed in the amine absorber by reaction with the amine in the liquid to produce oxidised amine and nitrite. Secondary and tertiary amines will remove 90–99% of the NO<sub>2</sub>. Primary amines react more slowly and may remove as little as 50%. Side reactions to produce nitrosamine in the absorber are minor, converting less than 20% of the absorbed NO. A minor amount of NO will be absorbed with the NO<sub>2</sub>. In the absence of NO<sub>2</sub>, NO is removed and the primary source of nitrite is oxidation of the amine, with a yield less than 10% of the oxidation rate. At the temperature and residence time of the stripper, practically all of the nitrite reacts with the amine. The reaction with secondary amine produces stoichiometric nitrosamine. However, the reaction with primary and tertiary amine is slower and produces oxidation products and N<sub>2</sub>. Because absorption liquids comprising tertiary or primary amines will have secondary amines that are products of degradation, nitrosamines will still be produced at the stripper conditions. At the temperature of the stripper the nitrosamine thermally degrades to oxidation products and probably N<sub>2</sub>O. The nitrosamine will accumulate to a steady-state concentration in equilibrium with the rate of production from NO<sub>2</sub>. The temperature and liquid holdup in the stripper bottoms is one determinant of the steady-state concentration. Fine (62) estimates values of steady-state nitrosamine with 120 °C stripping that vary from 0.9 mM in MEA to 20.5 mM in MDEA/piperazine.

Thermal reclaiming will also destroy nitrosamine. The thermal decomposition is catalysed by high pH, so thermal reclaiming at 150 °C with the addition of NaOH will provide the conditions to eliminate nitrosamine in the reclaimer waste. Therefore, nitrosamine accumulation can be managed by the amine selection, high-temperature stripping, NO<sub>2</sub> removal in the polishing scrubber, and upstream NO controls. With minimal accumulation there should be little risk of nitrosamine emissions through the water wash. Specific amines may have insurmountable problems with gas emissions if they yield degradation products that are volatile secondary amines. Otherwise, the most significant issue related to the formation of nitrosamines will be the risk of spilling liquid inventory containing nitrosamine (62).

## C.2.6 Aerosol emission management

One significant problem of MEA-based processes is the relatively high energy demand, which reduces the efficiency of the power plant (68). Along with the increased energy demand, other aspects – such as emissions, especially of the absorbent – are of growing concern (28, 50). Emissions not only occur in the form of gaseous components, but also in the form of aerosol droplets (28). Recent pilot plant test data indicate that amine and its degradation produce emissions in the form of aerosols, which must be controlled for commercial success of this technology (45).

The loss of absorbent and its degradation products leads to higher operating costs as well as negative effects on the environment in and around the area of the PCC plant (32). Many of these compounds are carcinogenic in nature; thus, their emissions must be limited (60). There is no information available for measured gas-phase nitrosamine and nitramine concentrations from CO<sub>2</sub>-capture pilot plants. Typically, countermeasures such as a water wash and standard demisters are employed for emission reduction as they are capable of reducing emissions to acceptable levels (~ppm) (34). Previously mentioned countermeasures such as a water wash and a demister are not effective in removing aerosol-based emissions, as the aerosol droplets are typically much less than 10 µm (0.04–4 µm). These aerosol droplets follow the trajectory of the gas molecules and are not effectively captured by the water wash or standard demisters (34). Conventional countermeasures such as a water wash and a demister are highly effective in reducing vapour-based absorbent emissions (less than 5 ppmv) but are ineffective against aerosol-based emissions (34). Khakharia et al. tested the application of a BDU as a countermeasure against aerosol-based emissions (25). They concluded that while the BDU is a suitable countermeasure for removal of aerosol-based emissions, based on a rough estimate, the BDU would lead to an increase of 26–52% in the electricity consumption and €1/tonne of CO<sub>2</sub> in operating costs for a full-scale CO<sub>2</sub> capture plant (34).

Moser et al. investigated causes and prevention techniques of PCC plant aerosol-based emissions (49). Two effective methods were studied:

- pretreatment of the flue gas to remove solid aerosol nuclei from the flue gas before they enter the absorber
- dry bed configuration, which has the capability to remove aerosol-based mist from the flue gas behind the CO<sub>2</sub> absorber.

In another study by Moser et al., efficiency of using a WESP was investigated (58). It was shown that the WESP can cause aerosol formation by increasing the number concentration of ultrafine particles/droplets in the flue gas. The results also indicate that this highly negative, voltage-dependent effect cannot be explained by a measurable increase of the SO<sub>3</sub> concentration downstream of the WESP at the entrance of the CO<sub>2</sub> absorber. Varying concentrations of SO<sub>2</sub> in the flue gas – which can react to SO<sub>3</sub> by ozone that is generated in the high-voltage field of the WESP – does not verifiably influence the entrainment. Oxidation of gaseous pollutants – as SO<sub>2</sub>, NO and Hg – can occur as a result of ozone formation in electric high-voltage fields such as that of WESP. One major focus of the investigations was to determine possible effects of the WESP operation on SO<sub>2</sub>/SO<sub>3</sub> and NO/NO<sub>2</sub> concentrations, which are known to trigger aerosol-based emissions from PCC (17). In another study on a single tube WESP, Anderlohr et al. show that for

higher levels of residual SO<sub>2</sub> in the flue gas, WESP collection efficiencies were greatly reduced due to aerosol formation inside the WESP (10). It is suspected that the reactive species produced in the non-thermal plasma of the corona discharge oxidise the SO<sub>2</sub> to SO<sub>3</sub>, which forms H<sub>2</sub>SO<sub>4</sub>. This causes supersaturation with subsequent homogeneous nucleation and thus aerosol formation (64).

Five different process configurations to mitigate emissions were operated individually or in coupled mode of operation (water-wash section, acid wash, dry bed, flue gas pretreatment, WESP). Low emission levels can be achieved by a special pretreatment of the flue gas and by the so-called dry bed configuration (58).

It is shown that the aerosol is bimodal: the larger particle mode is responsible for migration of MEA and the smaller mode is able to escape common mitigation measures. While use of WESP can effectively remove the larger diameter particles, it can also promote formation of very small PM within the size range 7–50 nm. It is concluded that heterogeneous nucleation on pre-existing Na<sub>2</sub>SO<sub>4</sub> is the dominant particle formation mechanism, and under normal operating conditions the number concentration of solid nanoparticles will determine the level of aerosol-based emissions (49).

Linking the operational data of the plant with the online emission data identified two important operational settings that control the amine emissions from a PCC plant to a large extent: flue gas temperature at the top of the absorber (downstream of the water-wash section), and flue gas temperature difference over the water-wash section. A positive correlation between NH<sub>3</sub> emissions and the O<sub>2</sub> content entering the pilot plant suggests that oxidative degradation occurs. Studies emphasise the importance of a well-designed water-wash section (if necessary, multistage) that will be able to reduce emissions to very low levels; however, it is necessary to keep in mind the lessons learned in this study with respect to its operational settings (32).

Absorbent is lost during the process due to degradation, entrainment, vapourisation and mechanical losses. Amine degradation has been studied for decades, especially for MEA, which is still considered the benchmark absorbent for CO<sub>2</sub> capture in post-combustion (65). However, in a real-life CO<sub>2</sub>-capture plant facility, the process is more complicated, because the gaseous feedstock consists of a mixture of CO<sub>2</sub>, O<sub>2</sub>, CO, SO<sub>x</sub>, NO<sub>x</sub>, HCl and PM (95). Acid gases such as SO<sub>2</sub>, HCl and NO<sub>2</sub> react with the amine to form heat-stable salts that reduce the CO<sub>2</sub> absorption capacity of the absorbent or degradation products, which may be volatile and thus leave the process along with the flue gas. Oxygen is known to be the main driver for the oxidative degradation of amines (44).

In recent years, governments and regulators have begun to examine amine emissions from amine-based CO<sub>2</sub>-capture facilities, and the associated potential impacts to the environment and human health. It is envisaged that in the near future, amine emission reduction will become a critical requirement for all amine-based CO<sub>2</sub>-capture plants (46).

Through testing and commercial experience, MHI has proven that CO<sub>2</sub>-recovery plants that process flue gas containing SO<sub>3</sub> can experience higher amine emissions, specifically as amine mist. As a countermeasure, MHI has developed a special type of multistage water-wash system to drastically reduce SO<sub>3</sub>-related amine emissions, and a simulator that can predict SO<sub>3</sub> and mist-phase behaviour in the absorber. The simulator identified that most of the amine emitted from an absorber exists as 'mist' phase, while representing the actual conditions in the absorber. MHI

continues to improve amine emission-reduction technology by improving engineering controls and the simulator, thus helping to facilitate the safe, environmentally friendly, widescale deployment of CO<sub>2</sub>-capture technology as an effective countermeasure against climate change (46).

The results of the investigation program at the pilot plant at Niederaussem demonstrated that, in addition to the well-known emission formation by SO<sub>3</sub> via aerosols, primarily very small particles in the flue gas are nuclei for aerosol formation and loss of the absorbent (58). It is shown that particles larger than about 255 nm will grow to droplets by condensation along the flue gas treatment process. The droplets are then removed from the gas stream by impaction in the FGD, in the direct contact cooler/prescrubber unit, in the CO<sub>2</sub> absorber or finally in the emission-mitigation system of the capture plant. If the particle size is smaller than about 255 nm, aerosol formation is most likely when the particle number concentration in the flue gas that enters the absorber exceeds  $6 \times 10^4$  to  $10^5$  particles per cm<sup>3</sup>, and when no suitable countermeasures are taken, such as using the dry bed configuration. The particles function as mist condensation nuclei and as carriers of physically and chemically absorbed organic compounds (58).

The correlation between the diameter of an aerosol droplet and the necessary oversaturation ( $S$ , saturation number) of the gas phase with the condensing compound is  $S \sim e^{1/d}$  (115). Thus, for particles with a diameter much smaller than 1 μm, a high oversaturation is needed to form droplets or to stabilise them. Two effects are changing this correlation significantly: heterogeneous nucleation at the wettable surface of small, solid nuclei reduces the need for oversaturation as long as the surface is not fully covered, and soluble compounds in the nucleus are lowering the vapour pressure strongly (5). As a consequence, even small fly ash particles with a size smaller than 100 nm can already start to grow at a relative humidity of about 0.8.

The particle size distribution determined for the flue gas at the absorber entrance of the PCC pilot plant at Niederaussem is normally bimodal, with two modes (7–50 nm and 50–255 nm). Aerosol formation can be minimised as far as possible when the solid, inorganic particles that trigger the emissions are removed before they enter the CO<sub>2</sub>-capture process. Which of the two modes is responsible for the absorbent entrainment in the CO<sub>2</sub>-capture plant depends on the process configuration. The number concentration of smaller particles should be reduced from the normally occurring level to less than  $10^5$  particles per cm<sup>3</sup> and preferably to less than  $4 \cdot 10^4$  particles per cm<sup>3</sup>. This can be reached by a pretreatment of the flue gas; for example, oversaturating of the flue gas by cooling or steam injection (to initiate the growth of the solid particles by condensation to a size that is sufficient for their separation) or by special prescrubbing techniques and by electrostatic precipitation before the flue gas enters the CO<sub>2</sub> absorber. Moser et al. showed that when the flue gas supply to the PCC pilot plant is switched from the conventional FGD to the proprietary pretreatment technique developed, the emissions of the CO<sub>2</sub>-capture process are instantaneously reduced by more than one order of magnitude (58).

When the operational settings of the pretreatment technique are shifted to a less effective mode, the negative effect of the WESP can become overwhelming. Apparently, the precipitator generates a high number of droplets/particles with a size smaller than 50 nm under these conditions, causing high emission rates in the CO<sub>2</sub>-capture process (66).

In parallel to the decrease of absorbent emissions, the particle number concentrations with a size less than 50 nm drops. The WESP has two opposing effects. It supports the proprietary pretreatment technique by removing solid particles especially from the second, larger fraction of

the bimodal size distribution of particles and droplets around 100 nm. However, it also produces especially small aerosol droplets/particles of the first mode of the bimodal size distribution. When the proprietary pretreatment technique is operated solely – that is, when the WESP is switched off – the emissions of the capture plant can be minimised. The smaller fraction of aerosol droplets/particles disappears (21). A very plausible explanation for this effect is the atomisation of small droplets in the high-voltage electric field of the precipitator by Rayleigh instability (also referred to as Coulomb instability). While the electrostatic energy of the charged droplet seeks to increase the droplet's surface (when a droplet passes the electric field the transferred charge carriers reside on the droplet's surface, seeking to increase it by repulsion), the surface energy works to reduce the surface. The Rayleigh limit occurs when the pressure difference maintaining the spherical shape of the droplet is equal in magnitude to the surface stress due to repulsion of the electrostatic charges. When the maximum charge capable of being stored on the droplet of a given diameter is exceeded, or alternatively the radius is decreasing at a given charge, the droplet becomes unstable. The droplet becomes more and more spindle-shaped and emits at the Rayleigh limit, where it undergoes fission: a jet of small charged droplets. The mass loss is small compared to the charge loss (67).

Based on these results, the benefit of a WESP as a measure to reduce emissions of PCC plants is unclear and strongly depends on the composition of the entering flue gas and the boundary conditions of the plant. Also, it is necessary to avoid the generation of aerosol nuclei in large quantities, because these entrain the absorbent out of the absorber (58).

Even if emission-triggering aerosol particles or droplets enter the absorber, this does not necessarily mean that they will leave the capture plant entraining the absorbent components. A powerful measure to reduce emissions is the proprietary dry bed configuration. This counter-current, multistage device can reduce the concentration of the absorbent components in the gas phase. Another important effect for emission mitigation is the slight temperature reduction of the flue gas, particles and droplets in the dry bed. Due to the saturation or oversaturation, water instead of organic compounds will condense on the particles and droplets in the water-wash section downstream. Even though the growing droplets will not be removed from the flue gas flow by inertial separation, on the following flue gas path entrainment of organic compounds is reduced by an order of magnitude. Although dry bed significantly reduces the emissions out of the capture process, it can also cause a very high number of ultrafine aerosol droplets (58).

## References (for Appendix C)

1. Kumar P., Robins A., Vardoulakis S., Britter R. A review of the characteristics of nanoparticles in the urban atmosphere and the prospects for developing regulatory controls. *Atmospheric Environment*. 2010; 44(39): 5035-5052.
2. McMurry P. H. A review of atmospheric aerosol measurements. *Atmospheric Environment*. 2000; 34(12-14): 1959-1999.
3. Kittelson D. B. Engines and nanoparticles: A review. *Journal of Aerosol Science*. 1998; 29(5-6): 575-588.
3. Lee S., Jang M., Kamens R. M. SOA formation from the photooxidation of  $\alpha$ -pinene in the presence of freshly emitted diesel soot exhaust. *Atmospheric Environment*. 2004; 38(16): 2597-2605.
4. Seinfeld J. H., Pandis S. N. *Atmospheric Chemistry and Physics From air pollution to climate change*. Atmospheric Chemistry and Physics, John Wiley & Sons, New York. 1998; 1326.

5. Hinds W. C. *Aerosol technology: properties, modelling, and measurement of airborne particles*. 1982
6. Shipman D. *Basic Concepts in Environmental Sciences* EPA; 2010. Available from: <http://www.epa.gov/apti/bces/index.htm> (Accessed: 30/01/2010).
7. Schaber K. Aerosol formation in absorption processes. *Chemical Engineering Science*. 1995; 50(8): 1347-1360.
8. Friedlander S. K. *Smoke, dust and haze: Fundamentals of aerosol modelling*. New York, Wiley-Interscience, 1977 333 p. 1977.
9. Begat P., Young P. M., Edge S., Kaerger J. S., Price R. The effect of mechanical processing on surface stability of pharmaceutical powders: Visualization by atomic force microscopy. *Journal of pharmaceutical sciences*. 2003; 92(3): 611-620.
10. Köhler H. The nucleus in and the growth of hygroscopic droplets. *Transactions of the Faraday Society*. 1936; 32: 1152-1161.
11. Rosendahl L. Using a multi-parameter particle shape description to predict the motion of non-spherical particle shapes in swirling flow. *Applied Mathematical Modelling*. 2000; 24: 11-25.  
10.1016/S0307-904X(99)00023-2
12. DeCarlo P. F., Slowik J. G., Worsnop D. R., Davidovits P., Jimenez J. L. Particle morphology and density characterization by combined mobility and aerodynamic diameter measurements. Part 1: Theory. *Aerosol Science and Technology*. 2004; 38(12): 1185-1205.
13. Flagan R. Electrical techniques. *Aerosol Measurement: Principles, Techniques, and Applications*. 2001: 537-568.
14. Kulkarni P., Baron P. A., Willeke K. *Aerosol measurement: principles, techniques, and applications*: John Wiley & Sons; 2011.
15. Maricq M. M. Chemical characterization of particulate emissions from diesel engines: A review. *Journal of Aerosol Science*. 2007; 38(11): 1079-1118.
16. Oberdörster G., Celein R. M., Ferin J., Weiss B. Association of particulate air pollution and acute mortality: involvement of ultrafine particles? *Inhalation Toxicology*. 1995; 7(1): 111-124.
17. Seaton A., Godden D., MacNee W., Donaldson K. Particulate air pollution and acute health effects. *The Lancet*. 1995; 345(8943): 176-178.
18. Giechaskiel B., Alfoldy B., Drossinos Y. A metric for health effects studies of diesel exhaust particles. *Journal of Aerosol Science*. 2009; 40(8): 639-651.
19. Rhodes M. *Front Matter*: Wiley Online Library; 2008.
20. Hering S. V. *Impactors, cyclones, and other inertial and gravitational collectors. Air sampling instruments for evaluation of atmospheric contaminants* 8<sup>th</sup> ed Cohen and Hering, editors Cincinnati (OH): ACGIH. 1995.
21. Khakharia P., Brachert L., Mertens J., Anderlohr C., Huizinga A., Fernandez E. S., Schallert B., Schaber K., Vlugt T. J. H., Goetheer E. Understanding aerosol based emissions in a Post Combustion CO<sub>2</sub> Capture process: Parameter testing and mechanisms. *International Journal of Greenhouse Gas Control*. 2015; 34: 63-74.
22. Brachert L., Kochenburger T., Schaber K. Facing the sulphuric acid aerosol problem in flue gas cleaning: pilot plant experiments and simulation. *Aerosol Science and Technology*. 2013; 47(10): 1083-1091.
23. Ehrig R., Ofenloch O., Schaber K., Deuflhard P. Modelling and simulation of aerosol formation by heterogeneous nucleation in gas-liquid contact devices. *Chemical Engineering Science*. 2002; 57(7): 1151-1163.

24. Gretscher H., Schaber K. Aerosol formation by heterogeneous nucleation in wet scrubbing processes. *Chemical Engineering and Processing: Process Intensification*. 1999; 38(4): 541-548.
25. Brachert L., Mertens J., Khakharia P., Schaber K. The challenge of measuring sulphuric acid aerosols: Number concentration and size evaluation using a condensation particle counter (CPC) and an electrical low pressure impactor (ELPI+). *Journal of Aerosol Science*. 2014; 67: 21-27.
26. Mertens J., Anderlohr C., Rogiers P., Brachert L., Khakharia P., Goetheer E., Schaber K. A wet electrostatic precipitator (WESP) as countermeasure to mist formation in amine based carbon capture. *International Journal of Greenhouse Gas Control*. 2014; 31: 175-181.
27. da Silva E. F., Kolderup H., Goetheer E., Hjarbo K. W., Huizinga A., Khakharia P., Tuinman I., Mejdell T., Zahlsen K., Vernstad K., Hyldbakk A., Holten T., Kvamsdal H. M., van Os P., Einbu A. Emission studies from a CO<sub>2</sub> capture pilot plant. *Energy Procedia*. 2013; 37: 778-783.
28. Khakharia P., Brachert L., Mertens J., Huizinga A., Schallert B., Schaber K., Vlugt T. J. H., Goetheer E. Investigation of aerosol based emission of MEA due to sulphuric acid aerosol and soot in a Post Combustion CO<sub>2</sub> Capture process. *International Journal of Greenhouse Gas Control*. 2013; 19: 138-144.
29. da Silva E. F., Lepaumier H. I. n., Grimstvedt A., Vevelstad S. J., Einbu A., Vernstad K., Svendsen H. F., Zahlsen K. Understanding 2-ethanolamine degradation in postcombustion CO<sub>2</sub> capture. *Industrial & Engineering Chemistry Research*. 2012; 51(41): 13329-13338.
30. Rao. A., Rubin E. S. A Technical, Economic, and Environmental Assessment of Amine-Based CO<sub>2</sub> Capture Technology for Power Plant Greenhouse Gas Control. *Environmental Science & Technology* 2002 36 (20), 4467-4475 DOI: 10.1021/es0158861
31. Kamijo T. Amines for Post-Combustion Capture. Electric Power Research Institute (EPRI) amine workshop, 16 August, 2011. Paper number E236637.
32. Mertens J., Knudsen J., Thielens M.-L., Andersen J. On-line monitoring and controlling emissions in amine post combustion carbon capture: a field test. *International Journal of Greenhouse Gas Control*. 2012; 6: 2-11.
33. Feron P. *Absorption-Based Post-Combustion Capture of Carbon Dioxide*: Woodhead Publishing; 2016.
34. Khakharia P., Mertens J., Vlugt T. J. H., Goetheer E. Predicting Aerosol Based Emissions in a Post Combustion CO<sub>2</sub> Capture Process Using an Aspen Plus Model. *Energy Procedia*. 2014; 63: 911-925.
35. Moser P., Schmidt S., Stahl K. Investigation of trace elements in the inlet and outlet streams of a MEA-based post-combustion capture process results from the test programme at the Niederaussem pilot plant. *Energy Procedia*. 2011; 4: 473-479.
36. Fulk S. M., Rochelle G. T. Modeling Aerosols in Amine-based CO<sub>2</sub> Capture. *Energy Procedia*. 2013; 37: 1706-1719.
37. Wix A., Brachert L., Sinanis S., Schaber K. A simulation tool for aerosol formation during sulphuric acid absorption in a gas cleaning process. *Journal of Aerosol Science*. 2010; 41(12): 1066-1079.
38. Mongstad T. C. *European collaboration projects to improve CCS*. Technology Centre Mongstad; 2017.
39. Mongstad T. C. Industrial collaboration to solve aerosol emission from CO<sub>2</sub> capture. *Carbon Capture Journal*. 2017(56).
40. Srivastava R., Miller C., Erickson C., Jambhekar R. Emissions of sulphur trioxide from coal-fired power plants. *Journal of the Air & Waste Management Association*. 2004; 54(6): 750-762.
41. Nguyen T., Hilliard M., Rochelle G. T. Amine volatility in CO<sub>2</sub> capture. *International Journal of Greenhouse Gas Control*. 2010; 4(5): 707-715.
42. Sexton A. J., Rochelle G. T. Catalysts and inhibitors for oxidative degradation of monoethanolamine. *International Journal of Greenhouse Gas Control*. 2009; 3(6): 704-711.

43. Goff G. S., Rochelle G. T. Oxidation inhibitors for copper and iron catalyzed degradation of monoethanolamine in CO<sub>2</sub> capture processes. *Industrial & Engineering Chemistry Research*. 2006; 45(8): 2513-2521.
44. Chi S., Rochelle G. T. Oxidative degradation of monoethanolamine. *Industrial & Engineering Chemistry Research*. 2002; 41(17): 4178-4186.
45. Saha C., Irvin J. H. Real-time aerosol measurements in pilot scale coal fired post-combustion CO<sub>2</sub> capture. *Journal of Aerosol Science*. 2017; 104: 43-57.
46. Kamijo T., Kajiya Y., Endo T., Nagayasu H., Tanaka H., Hirata T., Yonekawa T., Tsujiuchi T. SO<sub>3</sub> Impact on Amine Emission and Emission Reduction Technology. *Energy Procedia*. 2013; 37: 1793-1796.
47. Mertens J., Bruns R., Schallert B., Faniel N., Khakharia P., Albrecht W., Goetheer E., Blondeau J., Schaber K. Effect of a gas-gas-heater on H<sub>2</sub>SO<sub>4</sub> aerosol formation: Implications for mist formation in amine based carbon capture. *International Journal of Greenhouse Gas Control*. 2015; 39: 470-477.
48. Fulk S. M. Measuring and modelling aerosols in carbon dioxide capture by aqueous amines 2016
49. Moser P., Wiechers G., Schmidt S., Stahl K., Vorberg G., Lozano G. A., Stoffregen T. Cause and prevention of aerosol-based emissions –Results from the post-combustion capture pilot plant at Niederaussem. *Post Combustion Capture Conference 3; Ludwigshafen, Germany; 2016*.
50. Mertens J., Lepaumier H., Desagher D., Thielens M.-L. Understanding ethanolamine (MEA) and ammonia emissions from amine based post combustion carbon capture: Lessons learned from field tests. *International Journal of Greenhouse Gas Control*. 2013; 13: 72-77.
51. Khakharia P., Brachert L., Schaber K., Huizinga A., Vlugt T., Mertens J., Schallert B., Goetheer E. Effect of number concentration of soot and H<sub>2</sub>SO<sub>4</sub> on aerosol based emissions from a post combustion capture plant. 2013.
52. Wix A., Schaber K., Ofenloch O., Ehrig R., Deuffhard P. Simulation of aerosol formation in gas-liquid contact devices. *Chemical Engineering Communications*. 2007; 194(4): 565-577.
53. Mertens J., Brachert L., Desagher D., Thielens M. L., Khakharia P., Goetheer E., Schaber K. ELPI+ measurements of aerosol growth in an amine absorption column. *International Journal of Greenhouse Gas Control*. 2014; 23: 44-50.
54. Miller B. G. *Emissions Control Strategies for Power Plants-9*. 2010.
55. Cottrell A., McGregor J., Jansen J., Artanto Y., Dave N., Morgan S., Pearson P., Attalla M., Wardhaugh L., Yu H. Post-combustion capture R&D and pilot plant operation in Australia. *Energy Procedia*. 2009; 1(1): 1003-1010.
56. Heldebrant D. J., Koech P. K., Rainbolt J. E., Zheng F. R. CO<sub>2</sub>-binding organic liquids, an integrated acid gas capture system. *Energy Procedia*. 2011; 4: 216-223.
57. Kohl A. L., Nielsen R. *Gas purification: Gulf Professional Publishing; 1997*.
58. Moser P., Schmidt S., Stahl K., Vorberg G., Lozano G. A., Stoffregen T., Richter T. The wet electrostatic precipitator as a cause of mist formation—Results from the amine-based post-combustion capture pilot plant at Niederaussem. *International Journal of Greenhouse Gas Control*. 2015; 41: 229-238.
59. Moser P., Schmidt S., Stahl K., Vorberg G., Lozano G. A., Stoffregen T., Richter T. The wet electrostatic precipitator as a cause of mist formation—Results from the amine-based post-combustion capture pilot plant at Niederaussem. *International Journal of Greenhouse Gas Control*. 2015; 41: 229-238.
60. Nielsen C. J., D'Anna B., Karl M., Aursnes M., Boreave A., Bossi R., Bunkan A. J. C., Glasius M., Hallquist M., Hansen A. M. K., Kristensen K., Mikoviny T., Maguta M. M., Müller M., Nguyen Q., Westerlund J., Salo K., Skov H., Stenstrøm Y., Wisthaler A. *Atmospheric Degradation of Amines (ADA). Summary Report: Photo-Oxidation of Methylamine, Dimethylamine and Trimethylamine; 2011*.

61. Reynolds A. J., Verheyen T. V., Adeloju S. B., Meuleman E., Feron P. Towards commercial scale postcombustion capture of CO<sub>2</sub> with monoethanolamine solvent: key considerations for solvent management and environmental impacts. *Environmental Science & Technology*. 2012; 46(7): 3643-3654.
62. Fine N. Nitrosamine Management in Aqueous Amines for Post-combustion Carbon Capture: Ph. D. Dissertation, The University of Texas at Austin, Austin, TX, USA; 2015.
63. Cooney R., Hatch-Pigott V., Ross P., Ramseyer J. Carcinogenic N-nitrosamine formation: A requirement for nitric oxide. *Journal of Environmental Science & Health Part A*. 1992; 27(3): 789-801.
64. Anderlohr C., Brachert L., Mertens J., Schaber K. Collection and generation of sulphuric acid aerosols in a wet electrostatic precipitator. *Aerosol Science and Technology*. 2015; 49(3): 144-151
65. Davis J., Rochelle G. Thermal degradation of monoethanolamine at stripper conditions. *Energy Procedia*. 2009; 1(1): 327-333.
66. Herzog H., Drake E. Carbon dioxide recovery and disposal from large energy systems. *Annual review of energy and the environment*. 1996; 21(1): 145-166.
67. Rayleigh L. XX. On the equilibrium of liquid conducting masses charged with electricity. *The London, Edinburgh, and Dublin Philosophical Magazine and Journal of Science*. 1882; 14(87): 184-186.

## Appendix D: List of Key Personnel

Name	Qualifications	Affiliations	Role
Dr Brendan W Halliburton	Ph.D, BSc (Hons)	Royal Australian Chemical Institute	Lead Researcher
Adrian Element	B.Sc (Chemistry)		Technical Officer SDR/Vales Point experiments
Dan Maher	B Chem Eng, BSc (Chemistry)		Lead Engineer Vales Point PCC pilot plant
Phillip Green	Assoc Dip Chemistry		Technical Officer Vales Point PCC pilot plant
Ali Pourkhesalian	Ph.D, BSc		Research projects officer Literature review and engineering support Vales Point PCC pilot plant

SIGN OFF

I, the undersigned, being a person duly authorised by the Grantee, certify that:

(a) the above information is true and complete;

(b) the expenditure of the Funding received to date has been solely on the Project;

(c) there is no matter or circumstances of which I am aware, that would constitute a breach by NSW Department of Industry, Skills and Regional Development or, if applicable the End Recipient, of any term of the Funding Agreement between NSW Department of Industry, Skills and Regional Development and the Grantee dated [insert date] that has not been notified by the Grantee.

Signature:



Position: Project Leader

Name: Dr Brendan Halliburton

Date: 13/11/2020

**Contact us**

1300 363 400  
+61 3 9545 2176  
[csiroenquiries@csiro.au](mailto:csiroenquiries@csiro.au)  
[csiro.au](http://csiro.au)

**For further information**

**CSIRO Energy**  
Brendan Halliburton  
+61 2 49606060  
[Brendan.halliburton@csiro.au](mailto:Brendan.halliburton@csiro.au)  
[csiro.au/energy](http://csiro.au/energy)